GEOLOGICAL SURVEY OF CANADA

OPEN FILE 3498

Flooding from the July 18-21, 1996 rainstorm in the Saguenay area, Quebec: fluvial geomorphic effects and slope stability along selected major river reaches

G.R. Brooks, D.E. Lawrence
Terrain Sciences Division,
Geological Survey of Canada

K. Fung
Canada Centre for Remote Sensing

C. Bégin, D. Perret
Quebec Geoscience Centre,
Geological Survey of Canada

Report prepared for Emergency Preparedness Canada

Emergency Preparedness Canada / Protection civile Canada

1997

ABSTRACT

A major storm system stalled over the mouth of the St. Lawrence River from July 18-21, 1996 and dropped record amounts of rain causing widespread flooding in southern Quebec. Flooding was particularly severe along river systems south of the Saguenay-Lac Saint Jean area, where rainfall in excess of 200 mm fell within a 36 hour period.

The flooding caused severe geomorphic effects along five rivers in the area. These effects varied considerably both between rivers and from reach to reach along the same river. Along the Rivière aux Sables and Chicoutimi Rivière, the flooding caused dramatic, yet localized, lateral bank erosion and incision adjacent to a number of small dams creating deep channels which carried the post-flood flow around the dams. Elsewhere, negligible to moderate bank erosion and sedimentation occurred along the river banks and floodplains. Major lateral channel erosion and avulsions occurred along the lower 10 km of Rivière à Mars causing extensive destruction of the floodplain and erosion of terraces along the valley bottom. Negligible to minor geomorphic changes occurred along the lower 17 km of Rivière du Moulin; there being little evidence of the recent flood along long reaches of the river valley.

The worst flooding in the region occurred along Rivière des Ha!Ha! where the overtopping and erosion of an earthfill dyke caused the drainage of Lac Ha!Ha! reservoir. The geomorphic effects of the flooding varied downstream along the alluvial sections of the river. In general, wide, relatively gently-sloped reaches of valley bottom experienced considerable accretion of sand and silt (up to several metres) and negligible to minor erosion. Major channel incision and moderate channel widening occurred along confined, relatively steeply-sloped sections of valley. Along similarly sloped, but much wider reaches of valley, major channel widening with minor to negligible incision occurred, resulting in the reworking of large areas of the floodplain and the erosion of the valleysides.

Associated with the flooding, a number of landslides occurred along the five study rivers. Most failures were shallow and of limited extent, although two retrogressive slides caused damage to infrastructure and buildings. Triggering mechanisms for the landslides included bank erosion, saturation of the ground from the rainfall, drawdown of reservoirs and recession of flood waves; or a combination of the above. Overall, landsliding along the river banks was a relative minor part of the flood impacts.

PREFACE

This manuscript is a contracted report prepared for Emergency Preparedness Canada. It provides a summary of the fluvial geomorphic effects of the flooding along severely impacted sections of five rivers in the Saguenay area caused by the July 18-21, 1996 rainstorm, and a general assessment of slope stability problems along the river banks. The text is primarily descriptive and supplemented by maps and a large number of photographs. It is intended that a more detailed and quantitative analysis of the geomorphic effects of the flooding will be released in subsequent report(s). This work represents a contribution from the Eastern Canadian Geological Processes and Hazards Project, Terrain Sciences Division, done in cooperation with Canada Centre for Remote Sensing and GSC Québec.

TABLE OF CONTENTS

ABSTRACT 2
PREFACE 3
TABLE OF CONTENTS 4
1. INTRODUCTION 6
Acknowledgments 7
2. BACKGROUND 9
Study area 9
Landsliding and the Laflamme Sea marine sediments 10
3. METHODOLOGY 13
4. METEOROLOGY 16
5. HYDROLOGY 18
Discharge regimes 18
Flood levels along Rivière aux Sables and Rivière Chicoutimi 19
Flood level along Rivière des Ha!Ha! 20
Drainage of Lac Ha!Ha! reservoir 20
Discharge estimates 22
Empirical relationship between peak discharge and drained lake volume 22
Drawdown of reservoir 23
Slope-area method 23
Discussion 24
6. RIVIÈRE AUX SABLES 31
General 31
Geomorphic effects of the flood 31
7. RIVIÈRE CHICOUTIMI 36
General 36
Geomorphic effects of the flood 36
8. RIVIÈRE À MARS 42
General 42
Geomorphic effects of the flood 42
9. RIVIÈRE DES HA!HA! 48
General 48
Geomorphic effects of the flood 48
km 35-27 segment 48
Pre-flood 48
Post-flood 49
km 10.5 to 4.5 segment 50
Pre-flood 50
Post-flood 50
km 4.5 to the river mouth segment 52
Pre-flood 52
Post-flood 52
10. RIVIÈRE DU MOULIN 57
General 57
Geomorphic effects of the flood 58
11. LANDSLIDING AND BANK INSTABILITY 62

Introduction 62
Bank erosion and oversteepening 62
Saturation of soils 62
Drawdown and flood wave recession 63
Landsliding and bank instability 63
Rivière aux Sables 64
Rivière Chicoutimi 66
Rivière à Mars 67
Rivière des Ha!Ha! 68
Rivière du Moulin 70
12. SUMMARY 75
ADDENDUM 77
REFERENCES 78

1. INTRODUCTION

A major rainstorm between July 18-21, 1996 caused widespread flooding along the northshore of the Saint Lawrence River, southern Québec, extending from approximately Trois-Rivières eastward to Sept-Îles (Fig. 1.1). The worst flooding occurred in the Lac Saint-Jean/Saguenay region (study area in Fig. 1.1) which experienced the highest rainfall. Here, in addition to inundation problems, extensive erosion along some river reaches caused major damage, including major channel widening and bank erosion, the breaching of dams and dykes, and damage to bridges and roads. Many commercial and industrial areas located along or dependent upon the rivers were severely affected. The flooding resulted in the evacuation of 14 500 people and the destruction or damage of approximately 970 homes (Progrès-dimanche, 1996). Miraculously, only two people were killed locally (and this was by a small landslide triggered by the rainfall rather than by flood waters) out of a total of ten killed in southern Québec during the storm. The overall damage in southern Québec caused by the July flooding is estimated to be roughly 800 million dollars (Emergency Preparedness Digest, 1997), making this one of Canada's most costly natural disasters.

The extensive fluvial erosion that occurred along the major rivers is particularly important from the perspective of secondary hazards related to the flooding because of the widespread occurrence of sensitive fine-grained marine sediments in the Saguenay area. These deposits are prone to large retrogressive failure and several large landslides have occurred locally this century (see for example, La Rochelle et al., 1970; Brzezinski, 1971; Tavenas et al., 1971). The possibility of similar large landslides being triggered directly or indirectly by the flooding exists due to the unloading of the base of slopes by river bank erosion, and drawdown from the recession of the flood waves along the rivers and the draining of reservoirs.

The purpose of this report is to: 1) summarize the fluvial geomorphic effects (erosion and deposition) of the flooding along the Rivière aux Sables and Rivière Chicoutimi and selected sections of Rivière du Moulin, Rivière à Mars and Rivière des Ha!Ha! (Fig. 1.2); 2) identify the location and cause of landslide activity along these rivers that was triggered directly by the flooding; and 3) assess the potential for future instability along the eroded banks of the rivers.

This report provides an overview of the surficial geology and landslide hazard in the Saguenay area, meteorology of the storm and flood hydrology. For each of the five rivers studies, the pre-flood morphology is briefly summarized and descriptions are provided of the fluvial geomorphic effects of the flooding within separate chapters. The issue of landslides and eroded bank stability along the five studied rivers is addressed in penultimate chapter. The final chapter summarizes the general findings of the study.

Acknowledgments

Financial support for this study was provided by the Geological Survey of Canada and Emergency Preparedness Canada which allowed us to undertake field work in the Saguenay area in the critical period immediately after the flood. Helicopter support was ably provided by Murray Cheslock, Huisson Aviation 1989 Ltd. Helpful discussions with Raimo Kallio, Environment Canada about the hydrological data are appreciated. Terry Pultz (Canada Centre for Remote Sensing) kindly provided post-flood satellite images of Lac Ha!Ha!, Rivière des Ha!Ha!, and Rivière à Mars which aided our interpretations. Sharon Smith assisted with the surficial geology and river maps.

Fig. 1.1 Map of southern Québec showing the location of the Saguenay area.

Fig. 1.2 Map showing the drainage basins of the five rivers discussed in this report. The shaded areas the study reaches examined in this report.

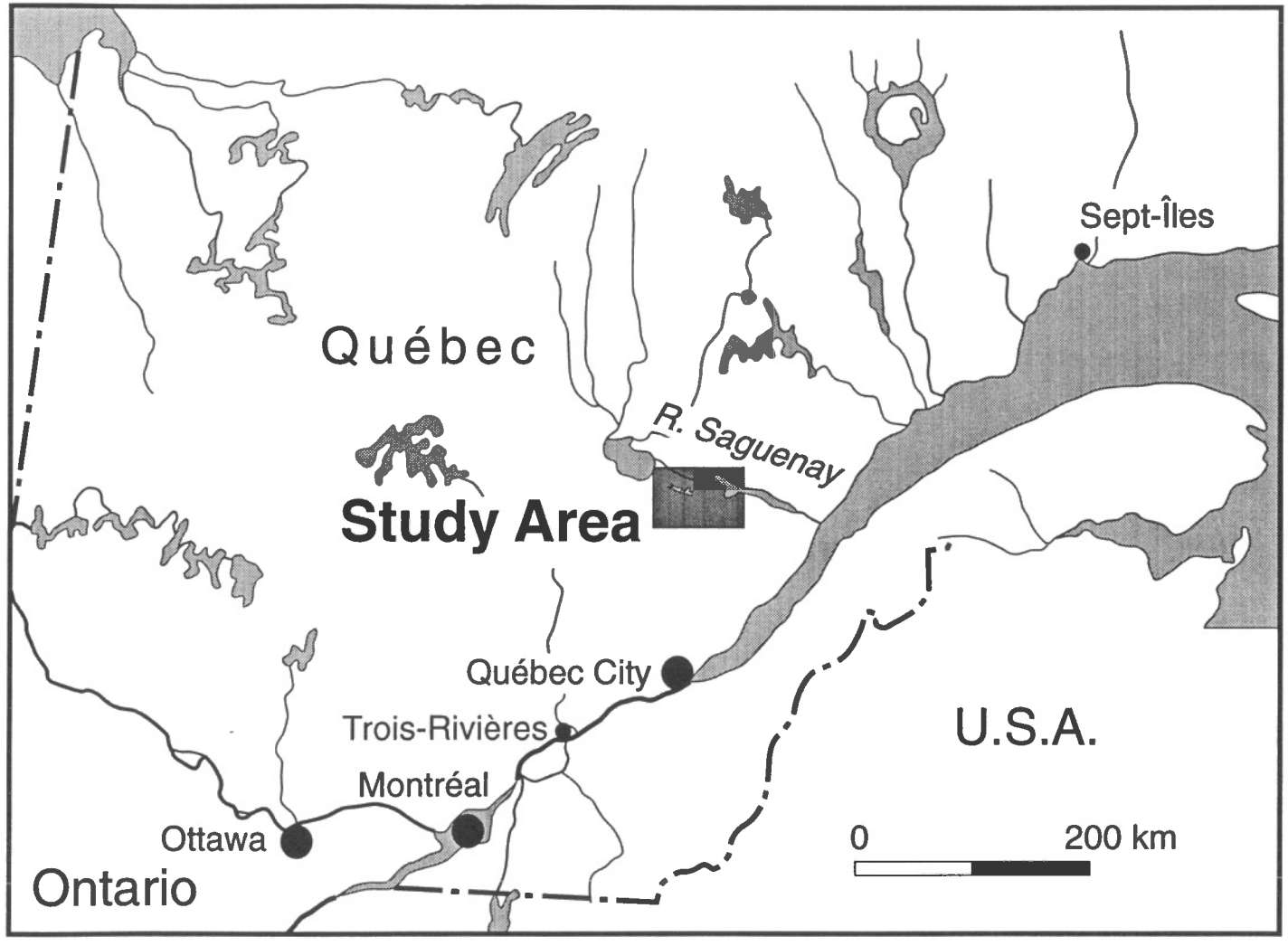
Québec
Study Area
R. Saguenay
Sept-Îles
Québec City
Trois-Rivières
Montréal
Ottawa
Ontario
U.S.A.
0
200 km

Fig. 1.1

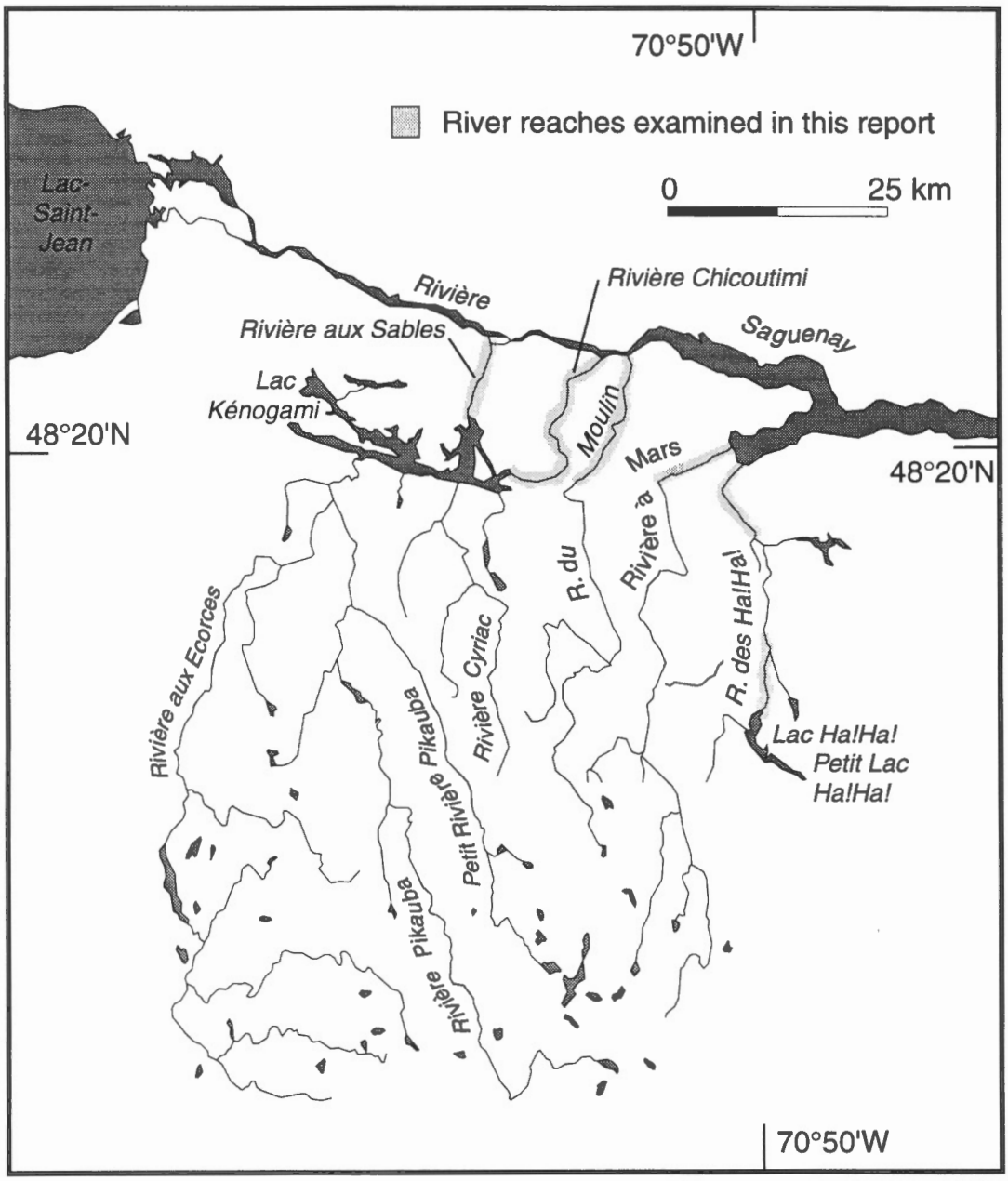
70°50'W
River reaches examined in this report
0
25 km
Lac-Saint-Jean
Rivière
Rivière Chicoutimi
Rivière aux Sables
Saguenay
Lac Kénogami
48°20'N
Moulin
Mars
48°20'N
Rivière à
R. du
R. des Ha!Ha!
Rivière aux Ecorces
Rivière Cyriac
Rivière Pikauba
Petit Rivière Pikauba
Lac Ha!Ha!
Petit Lac Ha!Ha!
70°50'W

Fig. 1.2

2. BACKGROUND

Study area

Rivière aux Sables, Rivière Chicoutimi, Rivière du Moulin, Rivière à Mars and Rivière des Ha!Ha! are part of the 88 100 km^2 drainage basin of Rivière Saguenay (Fisheries and Environment Canada, 1978) and form a small portion of this large watershed. All five rivers originate in the southern part of the Saguenay watershed and flow northwards, eventually crossing the Saguenay Valley and joining Rivière Saguenay (Figs. 1.2 and 2.1). The five watersheds lie almost entirely within the Laurentian Highlands where the drainage networks exhibit a crude parallel stream pattern. This highland area is a rugged, heavily dissected region of the Canadian Shield and elevations in the headwater areas of the watersheds reach up to 1100 m. The vegetated, hummocky bedrock surfaces of the highlands generally outcrop or are covered with a thin, discontinuous veneer of drift (Fulton, 1995). The drift cover thickens and becomes more continuous in the valley bottoms and also towards the Saguenay Valley (Fulton, 1995). Numerous small lakes and wetlands are present within bedrock basins and lowlying and poorly drained areas of the highlands.

The lower portions of the watersheds cross the Saguenay Valley, a broad raised lowland of relatively moderate relief, which is the surface expression of the west-northwest trending Saguenay Graben. Here, large areas of bedrock are covered with a thick layer of Quaternary deposits, predominately fine-grained marine sediments (silt, silty clay, clay) deposited in the Laflamme Sea during the late Pleistocene (Fig. 2.1; LaSalle and Tremblay, 1978). Extensive glaciofluvial and fluvial sand and gravel deposits forming several raised deltas are present along the margin of the lowland and overlie the marine sediment (Fig. 2.1). The deltas prograded into the Laflamme Sea from the mouths of rivers that originated within the Laurentian Highlands. The Laflamme Sea reached a maximum marine limit of about 165 m a.s.l. at about 10 250±150 yrs BP in the La Baie-Jonquière area (LaSalle and Tremblay, 1978; Vincent, 1989). After recession of the sea prior to 8000 yrs BP (Parent et al., 1985), the river networks developed on and gradually incised into the deltaic and marine sediments that form the lowland surface. The present day river network is entrenched into the surficial materials and, in places, has incised down to and thus flows directly upon bedrock. Several large peat bogs are present within poorly drained areas of the lowland (Fig. 2.1).

Communities in the Saguenay region commonly are located along the rivers and streams reflecting a historic linkage to the waterways for transportation, resource exploitation and energy. The cities of Jonquière and Chicoutimi are located along Rivière aux Sables and Rivière Chicoutimi, respectively. Rivière du Moulin flows through Laterrière and Rivière-du-Moulin (a suburb of Chicoutimi) while La Baie (consisting of the communities of Bagotville, Port-Alfred and Grande-Baie) is situated at the mouth of both Rivière à Mars and Rivière des Ha!Ha!. Near Lac Ha!Ha!, Rivière des Ha!Ha! flows adjacent to the hamlet of Boilleau. All of the communities are located upon the lowland, except Boilleau which is located within the Laurentian Highlands. Along the study rivers, the waterways

are exploited by a number of dams which provide water and power for communities and, forest products and aluminum industries.

Landsliding and the Laflamme Sea marine sediments

The fine-grained marine sediments in the Lac Saint-Jean/Saquenay region, also known as Laflamme Sea marine sediments (or clay) and often referred to as Leda Clay, are subject to settlement and instability that cause a variety of engineering problems. At some locations these sediments pose a risk due to their susceptibility for failure and landsliding. A variety of landslide types are common, from relatively small slumps, flows and slides which involve near surface sediments, to large deep-seated rotational failures. However, the sediments are also subject to largescale retrogressive slides and earthflows, like the Champlain Sea marine sediments along the St. Lawrence and Ottawa valleys and the glaciomarine sediments of Scandinavia and Alaska.

The geotechnical behaviour of Laflamme Sea marine sediment is primarily related to its geologic history. The mineral particles making up these deposits are largely feldspars, quartz and micas which have been ground to a rock flour by the abrasive action of the glacier and deposited in marine or brackish water of the Laflamme Sea during the late Pleistocene or early Holocene (Occhietti, 1989). Use of the term clay when referring to these deposits refers to their particle size not their mineralogy, as true clay minerals typically make up only a small portion of the soil constituents (Bentley and Smalley, 1979). Although generally called clays, particle size analysis shows that such marine sediments are largely composed of very fine silt and would be called more appropriately fine silt or clayey silt (Gadd, 1986).

Fine-grained marine sediment generally lacks the strong attractive forces of mineral clays and are arranged in a loose, flocculated structure. The deposits commonly are 30-50 m thick, but locally may be in excess of 100 m (Occhietti, 1989). They accumulated within a 2000 years period prior to isostatic uplift of the land and the draining of the inland sea (Occhietti, 1989). Generally, there was little consolidation of the sediments.

Salt originating from the marine or brackish waters is present within the flocculated soil structure. The cohesive strength of the soil can be reduced where groundwater has leached this salt from the sediments (Bjerrum et al., 1969). When leached sediments fail, a dramatic loss in strength occurs, whereby, the remolded shear strength is much less than the *in situ* shear strength. Sediments which exhibit this dramatic loss of strength are termed sensitive, and commonly are transformed upon failure into a viscous mud.

Landslides in sensitive marine sediments are often initiated or exacerbated by the activities of man, however, for the most part such failures occur due to changes in soil and hydrological conditions in response to natural phenomena. The landslides commonly occur in spring or early summer when snowmelt combines with rainfall to saturate the soils. The combination of early snowfall (which prevents deep frost penetration), heavy winter snowfall, and rapid spring snowmelt and heavy rainfall, contribute to ground

saturation and increased pore water pressures in slopes (Tavenas, 1984). Fluvial erosion at the toe of a slope often triggers the initial failure. Most often these failures are small slumps or slides, however, they may develop into retrogressive flow slides. Under certain conditions (e.g., soils with a sensitivity) retrogression can produce earthflows of enormous size (e.g., see LaSalle and Chagnon, 1968).

Laflamme Sea marine sediments are widespread in the Lac Saint-Jean/Saguenay region (Fig. 2.1). The presence of numerous pre-historic landslide scars, some extremely large, attests to the general problem of slope instability throughout the region (Fig. 2.1). The May 4, 1971 landslide at St. Jean Vianney northwest of Jonquière, (32 ha. in area, 31 people killed; Tavenas et al., 1971) and the October 1, 1924 Kénogami landslide along the lower reaches of the Rivière aux Sables (25 ha in area, one person killed; Brzezinski, 1971), are examples of major historic landslides in the area.

Fig. 2.1 (see POCKET) Map showing the generalized distribution of surficial material and major landslide scars in the Jonquière-Chicoutimi-La Baie area (after Dion, 1986a). Also shown are the thickness of fine-grained marine sediments and boreholes sites showing the subsurface presence or absence of fine-grained marine sediment (after Dion, 1986b).

Fig. 2.1 see POCKET

3. METHODOLOGY

The geomorphic information contained within this report is based on post-flood aerial reconnoitering of the flood damage supplemented by limited ground work at some sites. Meteorological and most of the hydrological information of the storm and flooding, respectively, is based upon reports and data obtained from other government agencies, as noted in the text. Much of this information is preliminary and/or unpublished and may be superseded by later reports. In particular, readers interested in such data should consult the report of the Scientific and Technical Commission on Dam Management (Nicolet Commission) which presents the findings of the Québec government inquiry into the disaster. The findings of this commission were announced in January 1997 as our report was being written, but published copies of the Commission report were not widely available before March 1997.

Field work was conducted between July 27-30, 1996, along the trunk channels of Rivière aux Sables and Rivière Chicoutimi, and selected sections of Rivière du Moulin, Rivière à Mars and Rivière des Ha!Ha! where there were direct effects on communities. Follow-up field work was done between November 13-15, 1996, at selected sites along Rivière aux Sables, Rivière Chicoutimi, and Rivière des Ha!Ha!.

During the aerial reconnoitering of the flood damage, areas of river erosion and deposition, and bank failures were mapped on 1:50 000 scale NTS maps and observations were recorded. Video and numerous oblique 35 mm pictures were taken along the rivers to photographically document the geomorphic effects and flood damage. Pre- and post-flood aerial photographs taken on May-June, 1994, and July 30, 1996, respectively, were obtained from the Québec government (for listing of the July 30, 1996, aerial photography see Table 3.1). We also had access to high resolution (1 m pixel size), low level, multi-spectral video (MSV) imagery of the study reaches provided by Canada Centre for Remote Sensing. Collectively, these photographs and MSV images represent important data sources which supplemented our field observations and mapping. However, it must be recognized that there has been major, and in some cases, dramatic, post-flood reconstruction which is not described in any detail in this report (March, 1997). The descriptive terminology of the river characteristics used in this report generally follows Kellerhals et al. (1976).

This study addresses the geomorphic effects of the flooding, but erosion generally was the dominant fluvial process. The locations of erosion and bank failures along Rivière aux Sables, Rivière Chicoutimi and Rivière du Moulin are depicted on pre-flood 1:50 000 scale digital base maps. The erosion and failure information depicted on these maps is approximate and subject to the limitations of the base map scale and the data sources. Users requiring larger scale maps should consult the post-flood aerial photographs listed in Table 3.1 rather than enlarging the relatively smallscale maps in this report.

The geomorphic effects along Rivière à Mars and Rivière des Ha!Ha! were much too complex to depict on the pre-flood 1:50 000 scale base maps. Therefore, separate pre- and post-flood channel morphologic diagrams were constructed for Rivière à Mars and the lower 4.5 km of Rivière des Ha!Ha! using the pre-flood base maps and post-flood mosaics of the MSV imagery. Also for the Rivière des Ha!Ha! study reaches (Fig. 1.2), the geomorphic effects were characterized by presenting selected MSV images adjacent to the base map.

On the 1:50 000 scale base map constructed for each river, a kilometer distance has been superimposed which approximately follows the river valley axis beginning from an arbitrary point just beyond the river mouth. This scale allows locations along the river that are mentioned in the text to be easily keyed to the base map. Therefore, reference to a feature at km 5.4 or km 3.1-3.4 along a given river refers to features located at these distances above the river mouth as defined by the distance scale on the base map.

Reference to the right and left sides of a given river channel is made with respect to the direction of flow of the river i.e., the downstream direction.

Table 3.1 List of immediate post-flood aerial photographs

River[1]	Date of photography	Approximate scale	Flight line	Aerial photograph numbers
Rivière aux Sables	July 30, 1996	1: 15 000	Q96304	10-19
Rivière Chicoutimi	July 30, 1996	1: 15 000	Q96304	20-44
Rivière à Mars	July 30, 1996	1: 15 000	Q96304	45-52
Rivière des Ha!Ha!	July 30, 1996	1: 15 000	Q96304	53-91

[1] No immediate post-flood aerial photographs of Rivière du Moulin were used in this report.

4. METEOROLOGY

Flooding in the Saguenay area was caused by a major storm system that stalled over the mouth of the St. Lawrence River between July 18-21, 1996 and dropped record amounts of rainfall (Environment Canada, 1996). As depicted in Fig. 4.1, in excess of 50 mm of rainfall fell upon a large area of southern Quebec during this storm. The largest zone of accumulation occurred just south of the Jonquière-Chicoutimi-La Baie area of the Saguenay Valley, where in excess of 200 mm of rain fell, reflecting orographic processes and the counter-clockwise rotation of the storm system. Individual locations within this zone reported receiving 210.9 mm (Portages-des-Roches station), 271.9 mm (Pikauba station) and 279.4 mm (Rivière-aux-Ecorces station) (Environnement et Faune Québec, 1996a). Although these are totals for a four day period, most of the rain in this area actually fell within a 36 hour period beginning at about 08:00 on July 19 and continuing until approximately 20:00 July 20 (Environnement et Faune Québec, 1996a), as exemplified by the rainfall record at the Bagotville airport station (Fig. 4.2).

Precipitation in the summer of 1996 to the end of July was above average in the Saguenay area. At the Bagotville airport station, 313.1 mm of precipitation fell in July producing the wettest month on the 1942-1996 record (Environment Canada, written communication, August 1, 1996). Of this total, 118 mm fell prior to the July 18-21 storm, exceeding the 1948-1995 July average of total precipitation (115 mm).

The intense rainfall from the July 18-21 1996 storm, in combination with the near-saturated ground conditions produced by the antecedent rainfall (Environment Canada, 1996) and the generally thin, discontinuous overburden cover blanketing the bedrock of the Laurentian Highlands produced widespread flooding throughout the northshore of southern Quebec. The most severe flooding occurred along rivers flowing northwards into the Saguenay Valley whose headwater areas were located within the greater than 200 mm rainfall accumulation zone. In particular, these are Rivière aux Ecorces, Rivière Pikauba, and Rivière Cyriac which flow into Lac Kénogami (and therefore are tributaries of Rivière aux Sables and Rivière Chicoutimi), and Rivière du Moulin, Rivière à Mars and Rivière des Ha!Ha! (Fig. 4.3).

Fig. 4.1 Isohyet map showing rainfall accumulation (mm) in southern Quebec between 08:00 July 18 to 08:00 July 21, 1996. Based upon a preliminary map released by Environnement et faune Québec (1996a).

Fig. 4.2 Daily precipitation (mm) in July 1996 received at C.F.B. Bagotville (data from Environment Canada).

Fig. 4.3 Map of the watersheds in the Jonquière, Chicoutimi and La Baie areas, southern Québec, that are discussed in this report.

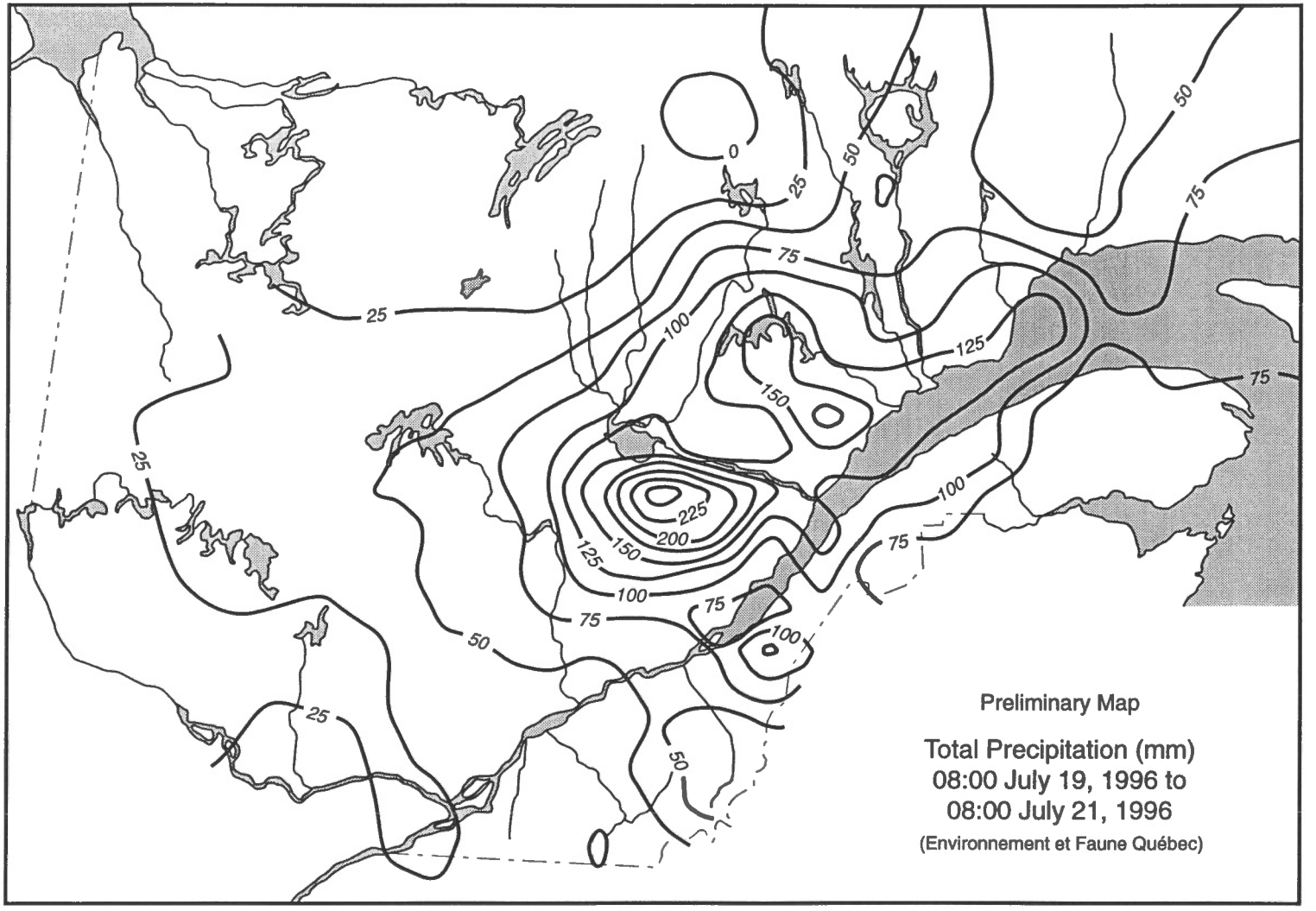
Preliminary Map
Total Precipitation (mm)
08:00 July 19, 1996 to
08:00 July 21, 1996
(Environnement et Faune Québec)
0
25
50
75
100
125
150
200
225

Fig. 4.1

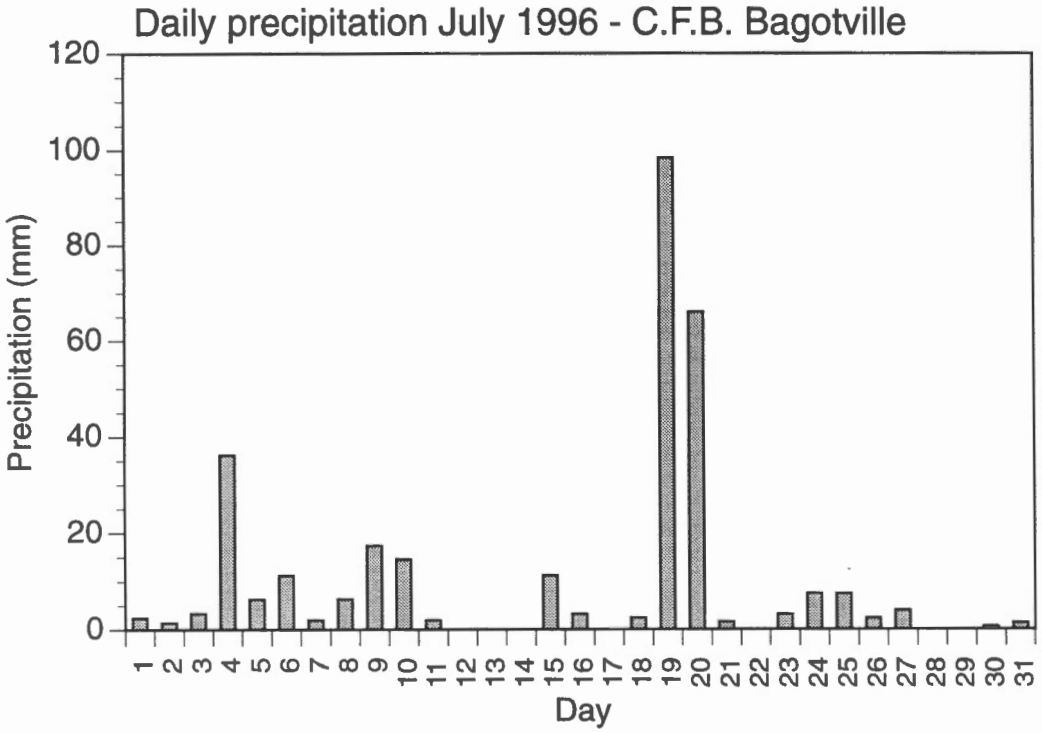
Daily precipitation July 1996 - C.F.B. Bagotville
Precipitation (mm)
120
100
80
60
40
20
0
1 2 3 4 5 6 7 8 9 10 11 12 13 14 15 16 17 18 19 20 21 22 23 24 25 26 27 28 29 30 31
Day

Fig. 4.2

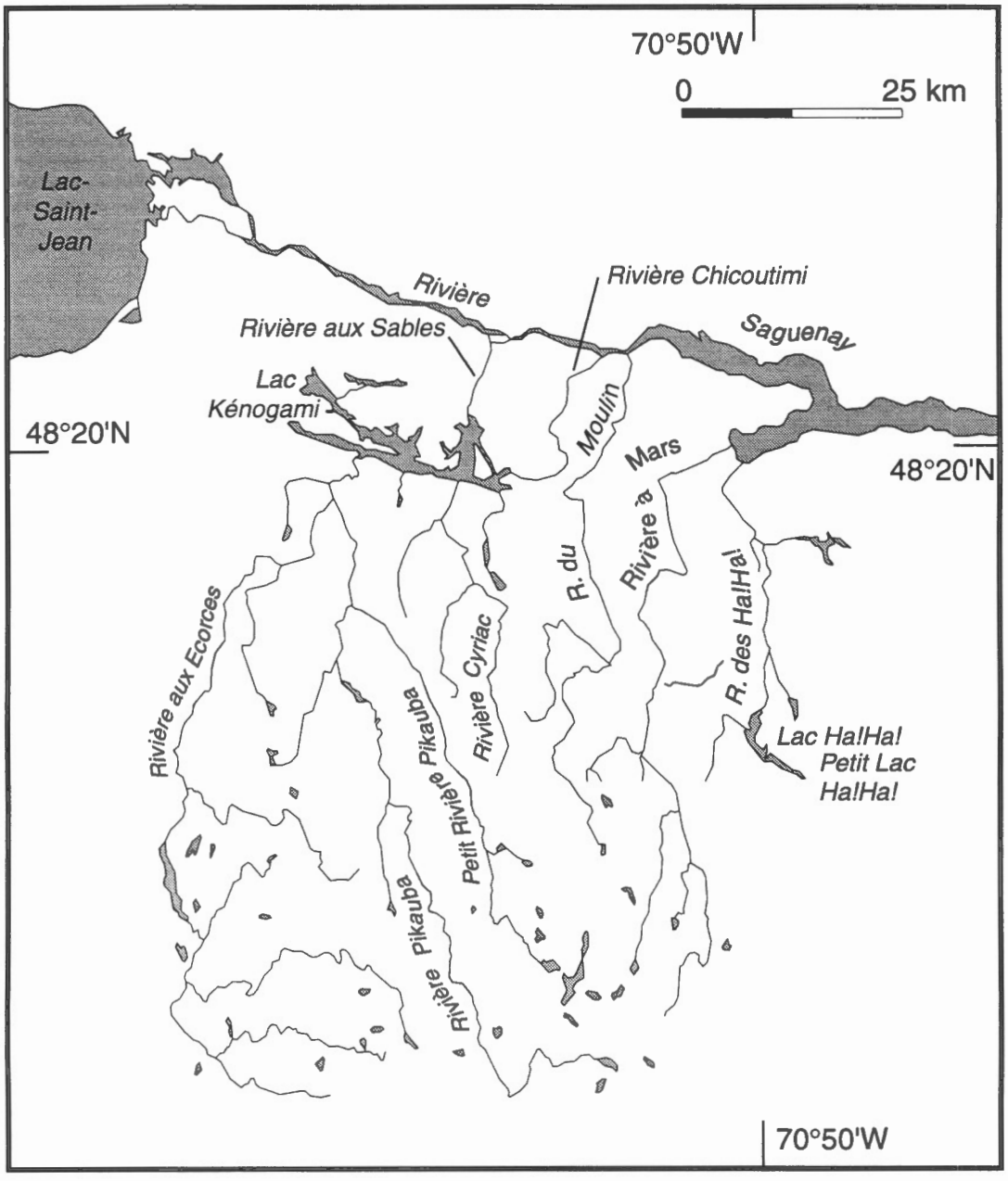
70°50'W
0
25 km
Lac-
Saint-
Jean
Rivière
Rivière Chicoutimi
Rivière aux Sables
Saguenay
Lac
Kénogami
48°20'N
Moulin
Mars
48°20'N
Rivière à
R. du
R. des Ha!Ha!
Rivière aux Ecorces
Rivière Cyriac
Pikauba
Petit Rivière Pikauba
Lac Ha!Ha!
Petit Lac
Ha!Ha!
Rivière Pikauba
70°50'W

Fig. 4.3

5. HYDROLOGY

Discharge regimes

The streamflow of Rivière aux Sables and Rivière Chicoutimi is regulated by dams controlling the level of Lac Kénogami (Fig. 4.3); Portage-des-Roches dam at the head of Rivière Chicoutimi and the east and west dams of the Pibrac dam complex at the head of Rivière aux Sables. Both rivers share the same contributing drainage basin (Fig. 4.3), the area of which is 3390 km^2 (Environnement et Faune Québec, 1996a). Smaller dams are present along both rivers; four along Rivière Chicoutimi and three along Rivière aux Sables. All seven small dams have relatively small reservoirs and have a negligible role regulating the discharges of the rivers.

The hydrology of Rivière aux Sables and Rivière Chicoutimi is particularly notable because of the regulated regimes that originate from the same reservoir. The outflow of the two rivers can be manipulated artificially at the dams, causing, for example, the discharge of one river to be increased with the other decreased proportionately so that the overall total volume of water released remains constant. More importantly, runoff into Lac Kénogami may be stored within the reservoir when the total outflow at the dams is maintained at a rate below the inflow into the reservoir. Such storage will cause the reservoir to rise and can be carried out only so long as 'safe' water levels are not exceeded beyond which point dams and dykes will eventually be overtopped.

During a given rainfall event, the manipulation of the level and outflow of Lac Kénogami has the potential to dampen (and delay) the peak discharge along Rivière aux Sables and Rivière Chicoutimi resulting from a given rainstorm. However, this storage process is dependent upon the antecedent level of the reservoir i.e., the higher the reservoir level, the lower the storage capacity and thus limiting dampening of the runoff from a given rainstorm. The summer levels of Lac Kénogami are normally maintained at high levels to satisfy the water demands of recreational users of the lake and energy producers (Environnement et Faune Québec, 1996a), which severely limits the potential for dampening runoff from a major summer rainstorm.

The discharge regime of the Rivière des Ha!Ha! is described as natural by the Water Survey of Canada (1992), despite the presence of the artificial reservoir at Lac Ha!Ha! (Fig. 4.3) and two smaller dams located downstream. Above the gauging station located 7.1 km above the river mouth, the drainage area of Rivière des Ha!Ha! is 572 km^2. Small dams are present along the Rivière du Moulin (two old dams) and Rivière à Mars (one abandoned dam), but these have very small reservoirs and thus have a negligible effect upon the natural discharge regimes.

Streamflow records exist for only the Rivière aux Sables, Rivière Chicoutimi and Rivière des Ha!Ha! watersheds. The mean monthly flows and the historic maximum daily flow

for each river are depicted in Figs. 5.1, 5.2 and 5.3. With all three rivers, the highest mean monthly flow occurs in May reflecting the combination of snowmelt and rainfall runoff. Not apparent from the mean monthly data are the maximum annual daily peak discharges which also usually occur in May, but relatively commonly occur in April and to a lesser extent in June. Occasionally, the maximum annual daily peak discharge will occur in a summer (July or August) or fall (September to November) month because of either a major rainfall event or an abnormally low spring discharge.

Flood levels along Rivière aux Sables and Rivière Chicoutimi

During the July 18-21, 1996 storm, the estimated maximum inflow into Lac Kénogami was 2780 m^3s^{-1} which exceeds the previously determined 1 in 10 000 year inflow (1550 m^3s^{-1}), but is less than the calculated maximum probable inflow (3610 m^3s^{-1}) (Carpentier, 1996). This inflow exceeded the outflow from Lac Kénogami causing the reservoir to rise to unprecedented levels. By 10:00 on July 21, the water level reached a maximum level of 166.08 m (above datum) from a level of 164.06 m recorded at 08:00 on July 17 (Environnement et Faune Québec, 1996a). This peak level was well above the historic maximum value of 164.5 m and exceeded the critical level of 165.7 m which represents the crest of the concrete dams (Environnement et Faune Québec, 1996a). As a result, all three dams (two at Pibrac and one at Portage-des-Roches) controlling the reservoir level were overtopped by Lac Kénogami waters, as were a number of the dykes (Environnement et Faune Québec, 1996a) with the resulting outflow spilling primarily into Rivière aux Sables and Rivière Chicoutimi. This produced flows that exceeded previously recorded discharges.

At the time of writing, streamflow records during the July 18-21, 1996 storm existed only for Rivière aux Sables and Rivière Chicoutimi and these were unofficial and fragmentary (Environnement et Faune Québec, 1996b). The accuracy of these records is not known. Summarized in Fig. 5.4, the records reveal that discharge increased dramatically along both rivers on July 20, beginning mid-day along Rivière aux Sables and late-afternoon along Rivière Chicoutimi. The obvious lag between the increase in streamflow and the timing of the rainfall which was most intense between 08:00 July 19 and 20:00 July 20, reflects the routing of water through the watershed into Lac Kénogami, but also the storage of water within the reservoir basin which caused the lake level to rise. Some of this stored water eventually had to be released to ease the rise in Lac Kénogami levels following the issuing of evacuation orders for lowlying areas along the two rivers (Environnement et Faune Québec, 1996a).

Despite the storage of some runoff within the reservoir, discharge levels eventually reached 660 m^3s^{-1} along Rivière aux Sables and 1200 m^3s^{-1} along Rivière Chicoutimi at 10:14, July 21 and 23:00, July 21, respectively (Environnement et Faune Québec, 1996b). These flows are the highest on record and are considerably larger than the historic maximum daily flows in the streamflow records, being 2.5 times larger than the 265 m^3s^{-1} level reported along Rivière aux Sables and 2.1 times larger than the 561 m^3s^{-1} reported along Rivière

Chicoutimi (data from Milieu Hydrique, Environnement et Faune Québec). For comparative purposes, the critical discharge beyond which the inundation of property occurs is 150 m^3s^{-1} and 255 m^3s^{-1} along Rivière aux Sables and Rivière Chicoutimi, respectively (Environnement et Faune Québec, 1996a). When 170 m^3s^{-1} along Rivière aux Sables and 310 m^3s^{-1} along Rivière Chicoutimi are exceeded, homes start being flooded (Environnement et Faune Québec, 1996a). The peak flows along the two rivers during the July 1996 flooding, obviously, are well above these critical levels.

Flood level along Rivière des Ha!Ha!

Drainage of Lac Ha!Ha! reservoir

The most severe flooding relative to the size of the drainage basin occurred along Rivière des Ha!Ha! because of events at Lac Ha!Ha! reservoir. The 12 km long reservoir is located about 34 km above the river mouth, and consists of Lac Ha!Ha! and Petit Lac Ha!Ha! which occupy separate, but connected basins (Fig. 4.3). Prior to the July flood, the level of Lac Ha!Ha! reservoir was controlled by a concrete dam located at the north end of Lac Ha!Ha! (Figs. 5.5 and 5.6). The water in the reservoir helped maintain discharge levels of Rivière des Ha!Ha! for use by two small power dams along the lower part of the river and a paper mill in the community of Grande-Baie (part of the City of La Baie) at the river mouth. The dam was built in 1950 at the site of a dam originally constructed in the early 1920's (Le Quotidien, 1996). The dam is owned by Consolidated-Stone Corporation, the dam consists of four 15' high gates, the levels of which are controlled by inserting and removing one foot square timbers. The reservoir level was normally maintained between 9 and 12' high relative to the heights of the gates (Le Quotidien, 1996).

During the July 18-21, 1996 rainstorm, the influx of runoff into the reservoir exceeded the outlet capacity of the gates at the time, causing the lake level to rise gradually. (As observed on July 28, 1996, three of the about 12 ft wide gates were open 3 ft, the fourth 7 ft.) The water level eventually rose to a height about 6 inches below the top of dam walls (14.5 ft relative to the height of the dam gates), as indicated by an organic matter line on the side of the dam and debris lines on the ground at both outer margins of the structure. Instead of rising further and overtopping the dam, the reservoir waters began to overtop a narrow dyke (known as 'Cut-away' dyke), 162 m long and 2-3 m high, which had been built across a saddle about 1 km to the south of the dam to help contain the reservoir (Figs. 5.5 and 5.7). Water spilling from the lake eroded into the dyke and then subsequently incised into the underlying surficial material of the saddle, eventually forming a new outlet channel, about 110 m wide at the site of the dyke. This new channel extends about 2 km downvalley and connects to the pre-flood Rivière des Ha!Ha! channel (Figs. 5.8 and 5.9). The erosion of the new outlet reduced the reservoir level by about 13±3 m (based upon GPS measurements; G. Fedosejevs, written communication, January 9, 1997), although the level of Petit Lac Ha!Ha! was reduced by only about 2 m being controlled by a narrows between the two basins (Fig. 4.3). The dam, which formerly

controlled the reservoir level, remained completely intact, but no longer impounding any water (Fig. 5.10).

The details of the erosion of the new outlet and consequent drainage of Lac Ha!Ha! reservoir are known only generally. As summarized from Le Quotidien (1996), drainage of Lac Ha!Ha! began on Saturday, July 20, 1996. Rivière des Ha!Ha! was in flood by 06:00 Saturday, by which time, a bridge (location uncertain) had been washed out downstream. By mid-morning, the residents of the hamlet of Boilleau, located along the valley bottom just downstream of the lake, were told to evacuate their homes because of flooding problems and roads being washed-out downstream. At about 14:30, the reservoir level was reported to be 12.4 ft with the dyke area having been overtopped and starting to erode. Massive erosion of the dyke is alleged to have occurred between 16:00 and 17:00. By 18:00, the water level had dropped to 10 ft and by 18:45 to 8.5 ft.

By deduction, the overtopping and erosion of the dyke must have began prior to 14:30 because the water mark at the dam had already dropped to the reported level of 12.4 ft from a maximum of 14.5 ft. Between 18:00 and 18:45, major erosion of the dyke/saddle area and drainage of the lake was well underway, producing the reported drop in the reservoir level of 1.5 ft from 10 to 8.5 ft. Based upon this drainage rate, the reservoir level dropped below the level of the gates probably late Saturday with the rapid erosion of the new outlet terminating perhaps sometime Sunday morning. The Nicolet Commission Report is reported to mention that the lake emptied in 18 hours (Ottawa Citizen, 1997), a time interval that is consistent with the previous interpretation. Overall, it appears that the drainage of Lac Ha!Ha! occurred rapidly over a period of many hours, but not catastrophically in a period of tens of minutes or up to several hours.

It should be noted that the uncontrolled drainage of water caused by the breaching of natural and artificial dams produces a peaked hydrograph consisting of rising and falling stages. During the rising stage, discharge increases over time because erosion progressively increases the size of the outlet. The rate of erosion of the outlet depends upon a number of factors, including the shape, height, width and composition of the 'dam' and the volume of impounded water available for drainage. The discharge will begin to decrease when the supply of water wanes because the reservoir has either fully drained or the erosion of the outlet has become arrested.

The drainage of Lac Ha!Ha! caused by the erosion of the dyke and saddle area, severely compounded the flooding problem downstream to the river mouth. The streamflow, already swollen by the runoff from the high rainfall, was augmented by the uncontrolled release of water from the reservoir which accentuated the height of flood wave. The flooding along the section of Rivière des Ha!Ha! below Lac Ha!Ha!, therefore, represents a combination of an 'outburst' flood resulting from the uncontrolled drainage of the reservoir superimposed upon a 'natural' hydrological event caused by the major rainstorm. Runoff from both 'sources' would have produced separate peak flows during the flood event, unfortunately, it is not known if the peaks coincided.

While the relationship between the magnitude and timing of the rainfall runoff and lake drainage components of the flood event are not known, there is no doubt that the drainage of Lac Ha!Ha! reservoir was the major cause of flooding downstream. Evidence for this is the width of the flood-eroded channel immediately below the new outlet which is 3 to 8 times wider than the pre-flood channel preserved just below the dam. The very high water marks within the hamlet of Boilleau located along the river just downstream of the reservoir, also indicate that a major influx of water entered the river system from the reservoir.

Discharge estimates

Streamflow records for Rivière des Ha!Ha! during and immediately after the July 18-21 rainstorm are not available because the discharge station was destroyed in the flood, but quantitative estimates of the flood along Rivière des Ha!Ha! can be calculated by three independent methods. Each is described separately.

Empirical relationship between peak discharge and drained lake volume

A number of empirical equations exist in the literature for estimating peak discharge resulting from failed glacier, landslide and constructed dams, using the volume of drained water. The most recent versions of these equations are contained in Costa (1988). The equation based upon constructed dam failures is the most suitable for use in the Lac Ha!Ha! scenario. From Costa (1988), the constructed dam failure equation is:

(1) $Q_{max} = 961\ V^{0.48}$ ($r^2 = 0.65$, SE=0.47 log-log units)

V - volume of drained water ($\times 10^6\ m^3$)

Q_{max} - peak discharge ($m^3 s^{-1}$)

However, log-log relations derived from least-squares regression analysis become biased during back-transformation of the logarithmic coefficients (see Miller, 1984; Ferguson, 1986) and result in the underestimation of the dependent variables (in this case peak discharge). To correct for this, following Desloges et al. (1989), an unbiased estimate (a') for the coefficient (a) in the power function:

(2) $\log_{Qmax} = a' + b \log V$

takes the form:

(3) $a' = a \exp (5.302 \times s^2 / 2)$

where s is the standard error of the estimate. In equation (1), s equals 0.47, thus the conversion factor is 1.8 and the unbiased equation becomes:

(4) $Q_{max} = 1730\ V^{0.48}$

Rather than using the total volume of water drained from Lac Ha!Ha! reservoir, it is more appropriate to use equation (4) with the volume drained from only the erosion of the 2-3 m high dyke. Using the estimate of this volume shown in Table 5.1, the peak discharge based upon equation (4) is 7650 m^3s^{-1}.

Drawdown of reservoir

As discussed in the *Drainage of Lac Ha!Ha! reservoir* section, Le Quotidien (1996) reports that the reservoir level dropped from 10 to 8.5 ft between 18:00 and 18:45 on July 20, 1996. This 1.5 ft drop in water level over a 45 minute period for the combined surface areas of Lac Ha!Ha! and Petit Lac Ha!Ha! produces a discharge estimate of 1380 m^3s^{-1} (Table 5.2). Because this discharge is based upon drawdown during a relatively early stage of lake drainage, it does not necessarily represent an estimate of the peak discharge. Discharge during a later stage of drainage may well have been larger because of subsequent enlargement of the outlet by erosion from the outflow.

Slope-area method

Estimation of discharge using the slope-area method is based upon the Manning and continuity equations:

(5) $$v = R^{0.667}\ s^{0.5}\ n^{-1}$$

(6) $$Q = v\ w\ d_{mean}$$

where,
- v - mean velocity
- R - hydraulic radius (assumed to be equivalent to d_{mean})
- s - slope
- n - Manning's 'n'
- w - width
- d_{mean} - mean depth

For this method, a cross-section of the river located 8.4 km above the river mouth and about 26.5 km below the outlet of Lac Ha!Ha!, was surveyed on July 29, 1996 (Figs. 5.11 and 5.12). Although located considerably downstream of Lac Ha!Ha!, this particular cross-section was chosen for several reasons: the valley bottom cross-section had not been severely altered by the flood; the river reach is relatively straight and of uniform width with the cross-section reasonably uncomplicated; no major tributaries join the river nearby; and there were good helicopter landing sites in close proximity along both sides of the river. The most significant modification that occurred at the cross-section during the flood was the deposition of sand, locally up to 2 m thick, within the thickly vegetated, flood channel margins (Fig. 5.12). This deposition results in the minor underestimation of the channel cross-sectional area, assuming the deposition occurred after the peak flow. The post-flood channel profile was not measured, but is assumed to be trapezoidal in shape and one metre deep. This almost certainly results in a slightly over-estimation of

the post-flood channel cross-sectional area, based upon the near bank water depth and the condition of the water surface. This error, however, is small relative to the cross-section of the flood channel and is to some extent self-canceling with the under-estimation of cross-sectional area caused by the sand deposition along the flood channel margins, mentioned above.

A high water surface slope of 0.0007 was surveyed on November 14, 1996, over a distance of 268 m. This slope, however, is considerably smaller than the slope of the post-flood water surface (0.0018) surveyed over a distance of 91 m on July 29, 1996. Conceivably, the lower high water slope could reflect a backwater effect formed behind a bridge located 1.5 km downstream that was later washed out by the flood or, alternatively, there was an error either in the identification or correlation of the high water marks or in the surveying of the high water slope. Discharge estimates, therefore, were calculated using both slopes to determine a range of viable peak flows at this site.

The channel roughness coefficient (Manning's 'n') was estimated using Barnes (1967). A range of roughness coefficients were selected to reflect uncertainty with defining this variable.

The surveyed cross-section and relevant data are depicted in Fig. 5.12, and the volume calculations based upon equations (2) and (3) are summarized in Table 5.3. The estimated peak discharge at the cross-section is 1080-1260 m^3s^{-1} based upon the 0.0007 slope and 1620-1980 m^3s^{-1} using the 0.0018 slope. The discharge calculated using the slope of 0.0007, however, is the estimate based upon the observed high water data.

Discussion

Of the three methods of discharge estimation, the empirical relationship between lake volume and peak flow produced, by far, the largest discharge (7650 m^3s^{-1}). This discharge estimate is 3.9-7.1 times larger than that calculated by the slope-area method at a cross-section located 26.5 km downstream and thus seems unreasonably high. It, therefore, is regarded as an absolute upper limit of the peak discharge.

The discharge estimates based upon lake drawdown (1380 m^3s^{-1}) and the slope-area method (1080-1260 and 1620-1980 m^3s^{-1}) are reasonably close. However, the discharges are not directly comparable because the former does not necessarily represent the peak flow (as mention in the *Drawdown of reservoir* section, above) while the latter should, but is based upon a cross-section of the flood channel located 26.5 km downstream of the lake outlet. Since the peak discharge at this cross-section may consist of a significant portion of rainfall runoff contributed from elsewhere in the drainage basin, it would be expected to be larger than the reservoir drawdown discharge, regardless of whether the latter represents the peak discharge or not. Therefore, intuitively, 1620-1980 m^3s^{-1} seems a more reasonable estimate than the 1080-1260 m^3s^{-1} range. However, if the rainfall runoff forms a very small component of the peak flow at the cross-section, the peak

discharge could be lower than upstream because of attenuation of the flood wave from the lake drainage as it travels downstream (Richards, 1982; Costa, 1988).

Significantly, all of the discharge estimates are more than a full order-of-magnitude larger than the previously recorded maximum daily discharge (108 m^3s^{-1}; Table 5.4). Despite the relatively short duration of the discharge record along this river (Fig. 5.3), the large difference between any of the estimated discharges and the previously recorded maximum daily discharge clearly indicates that the July 1996 flood along Rivière des Ha!Ha! was an extremely high magnitude event. Because of the unusual combination of very high rainfall and the uncontrolled drainage of Lac Ha!Ha! reservoir, it seems unlikely that a flood of this magnitude will be repeated by a strictly natural occurrence (i.e., rainfall or snowmelt event). However, the discharge estimate based upon the drawdown of Lac Ha!Ha! (the lower of the two diamond points on the graph in Fig. 5.13) is approaching, but does not exceed the distribution of maximum rainfall-runoff floods for the U.S. and the world. This suggests that it is not totally inconceivable that a discharge of 1380 m^3s^{-1} could be exceeded by a rainfall event. (The higher diamond point in Fig. 5.13 is the empirical estimate of discharge based upon the volume of drained lake water which, as discussed above, seems too high.)

The drainage scenario of Lac Ha!Ha! reservoir is significantly different to many dam failures in that the majority of the erosion which resulted in the drainage of the lake, involved up to 10-12 m of incision into surficial material underlying the dyke. This surficial material seems to have been relatively resistant to fluvial erosion because, as described above (*Drainage of Lac Ha!Ha! reservoir* section), drainage of the lake occurred over a period of many hours, and thus was not catastrophic in the sense of occurring over a period of tens of minutes or up to several hours. The surficial material underlying the dyke consists of a compact, massive, matrix-supported glacigenic diamicton. Clasts, occasionally up to 50 cm, form about 10% of the diamicton, while the matrix is a silty sand. Following the erosion of the dyke, fluvial incision into the diamicton took place through the development and recession of a knickpoint as suggested by the presence of an active knickpoint at the head of the outlet channel, and several deeply scoured channels branching off from the 'main' channel each headed by a well-defined 'step', apparently representing a dry knickpoints. Once the knickpoint erosion developed, drawdown of the lake would have been controlled directly by the rate of knickpoint retreat into the reservoir basin.

Table 5.1 Volume of water drained from Lac Ha!Ha! reservoir because of erosion of saddle dyke

Water body	Pre-flood area (km^2)	Change in water level (m)	Volume of drained water (10^6 m^3)
Lac Ha!Ha!	5.9	3[a]	17.7[c]
Petit Lac Ha!Ha!	2.2	2[b]	4.4[c]
Lac Ha!Ha! reservoir			22.1[c]

[a] maximum height of 2-3 m high of the dyke.

[b] the drop in water level of Petit Lac Ha!Ha! was limited by the level of the narrows between the two lake basins.

[c] volume is slightly overestimated because no allowance has been made for the constriction of the lake surface which would have occurred as the level dropped.

Table 5.2 Discharge estimate based upon drainage rate of Lac Ha!Ha!

Surface area (km^2)	Drop in water surface (m)	Time interval (min)	Discharge (m^3s^{-1})
8.1[a]	0.46[b]	45[b]	1380

[a] combined pre-drainage water surface of Lac Ha!Ha! and Petit Lac Ha!Ha! which together form the Lac Ha!Ha! reservoir (see Table 5.1).

[b] this drop in the water surface is reported to have occurred between 18:00 and 18:45, July 20, 1996 (Le Quotidien, 1996).

Table 5.3 Discharge estimate for cross-section located at km 8.4 based upon slope-area method

Slope	Manning 'n'	Width (m)	Mean depth (m)	Mean velocity (m^3s^{-1})	Discharge (m^3s^{-1})
0.0007[a]	0.036-0.043[c]	131	4.6	1.8-2.1	1080-1260
0.0018[b]	0.036-0.043[c]	131	4.6	2.7-3.3	1980-1620

[a] high water slope
[b] post-flood water surface observed on July 29, 1996
[c] from Barnes (1967)

Table 5.4 Comparison of estimated flood discharges with previously recorded maximum daily discharge

Source of discharge	Discharge (m^3s^{-1})	Ratio of estimated flood discharge to maximum reported daily discharge (108 m^3s^{-1})
Maximum daily discharge[a]	108	na
Estimates of July 1996 flood		
Empirical relationship between lake volume and peak flow	7650[cd]	70.8
Drawdown of reservoir	1380[def]	12.8
Slope-area method[b]		
- high water slope	1080-1260	10-11.7
- observed slope	1620-1980	15-18.3

[a] from the 1976-1994 streamflow record (data from Milieu Hydrique, Environnement et Faune Québec)

[b] based upon a surveyed cross-section of the flood channel located 26.5 km downstream of Lac Ha!Ha! reservoir

[c] see *Chapter 5 Hydrology - Drawdown of reservoir* section

[d] represents outflow from drainage of lake only

[e] from Table 5.2

[f] this discharge estimate may be smaller than peak discharge

[g] from Table 5.3

[h] includes flow from the drainage of the lake and rainfall runoff from elsewhere in the watershed

Fig. 5.1 Mean monthly and historic maximum daily flows of Rivière Chicoutimi at station number 061004 (data from Milieu Hydrique, Environnement et Faune Québec).

Fig. 5.2 Mean monthly and historic maximum daily flows of Rivière aux Sables at station number 061023 (data from Milieu Hydrique, Environnement et Faune Québec).

Fig. 5.3 Mean monthly and historic maximum daily flows of Rivière des Ha!Ha! at station number 060601 (data from Milieu Hydrique, Environnement et Faune Québec).

Fig. 5.4 Hydrographs of Rivière aux Sables and Rivière Chicoutimi during the July 18-21, 1996, storm, based upon unofficial and fragmentary streamflow records (Environnement et Faune Québec, 1996b).

Fig. 5.5 Map of the northern portion of Lac Ha!Ha! reservoir prior to the flood event showing the location of the dam which controlled the water levels, and the dyke that was overtopped.

Fig. 5.6 The dam which formerly controlled the level of Lac Ha!Ha! reservoir, viewed from above the drained lake basin (GSC photograph 1997-42A).

Fig. 5.7 Photostereogram of the pre-flood morphology of the dyke and saddle across which a new channel was eroded causing the drainage of Lac Ha!Ha! reservoir (Photocartothèque quebécoise 22D3-92; -93, June 15, 1994).

Fig. 5.8 The new outlet at Lac Ha!Ha! reservoir a) looking downstream from above the lake basin (GSC photograph 1997-42B) and b) looking upstream into the drained lake basin (GSC photograph 1997-42C). Photographs taken on July 28, 1996.

Fig. 5.9 Vertical multi-spectral video image of the northern portion of Lac Ha!Ha! reservoir showing the drained lake and new outlet, taken August 6, 1996 (Courtesy of Canada Centre of Remote Sensing).

Fig. 5.10 The dam, intact but non-functional, (bottom of photograph, just to left of centre) that impounded Lac Ha!Ha! with the drainage lake bed behind it. Photograph taken on July 28, 1996 (GSC photograph 1997-42D).

Fig. 5.11 Site along Rivière des Ha!Ha! at km 8.4 where a cross-section of the flood channel was surveyed (marked by solid line) to estimate the flood discharge. Photograph taken on July 28, 1996 (GSC photograph 1997-42E).

Fig. 5.12 The surveyed cross-section and the channel parameters used to estimate the flood discharge (no vertical exaggeration).

Fig. 5.13 Plot of the range of comparable discharge estimates caused by the drainage of Lac Ha!Ha! (diamonds symbols) superimposed upon the distribution of the maximum

rainfall-runoff floods (cross symbols; data from Costa, 1987). The lower of the Rivière des Ha!Ha! discharges is based upon the drawdown of the reservoir while the other is based upon the empirical relationship between discharge and the volume of drained water, as described in the text. The drainage basin area of the two diamond points is represented by the portion of the Rivière des Ha!Ha! watershed contributing to Lac Ha!Ha!.

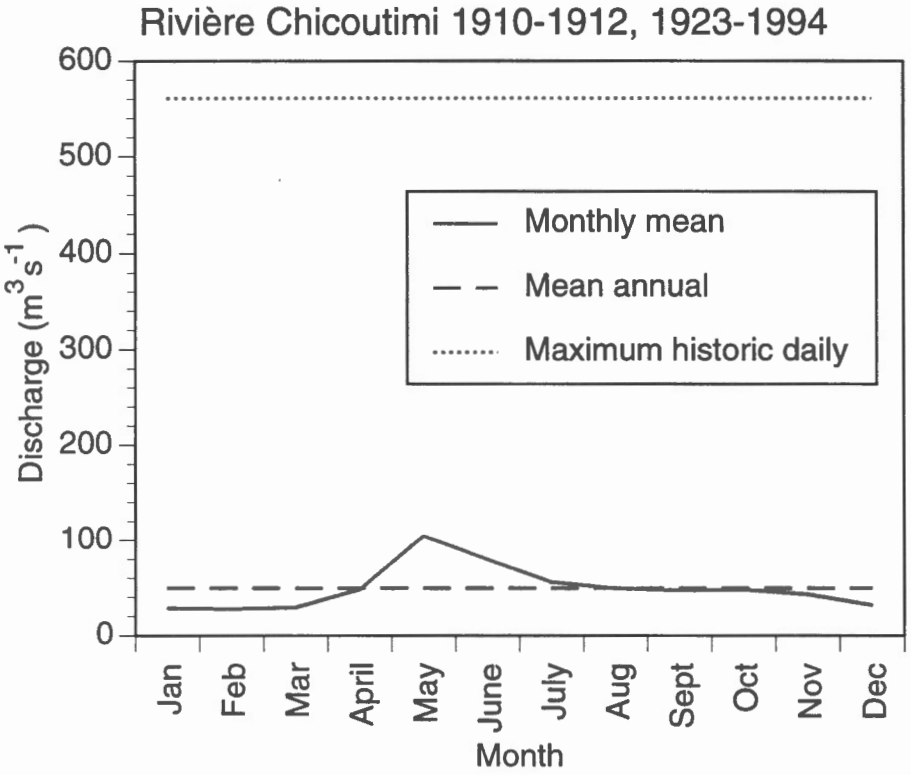
Rivière Chicoutimi 1910-1912, 1923-1994
600
500
400
300
200
100
0
Discharge (m3 s-1)
Monthly mean
Mean annual
Maximum historic daily
Jan
Feb
Mar
April
May
June
July
Aug
Sept
Oct
Nov
Dec
Month

Fig. 5.1

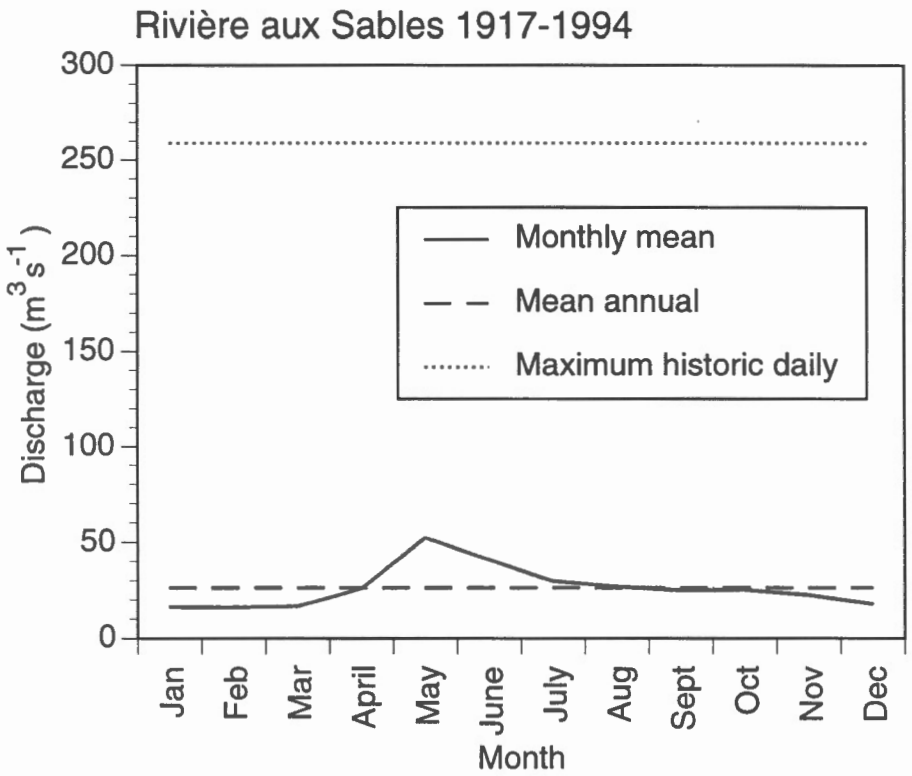
Rivière aux Sables 1917-1994
300
250
200
150
100
50
0
Discharge (m3 s-1)
Monthly mean
Mean annual
Maximum historic daily
Jan
Feb
Mar
April
May
June
July
Aug
Sept
Oct
Nov
Dec
Month

Fig. 5.2

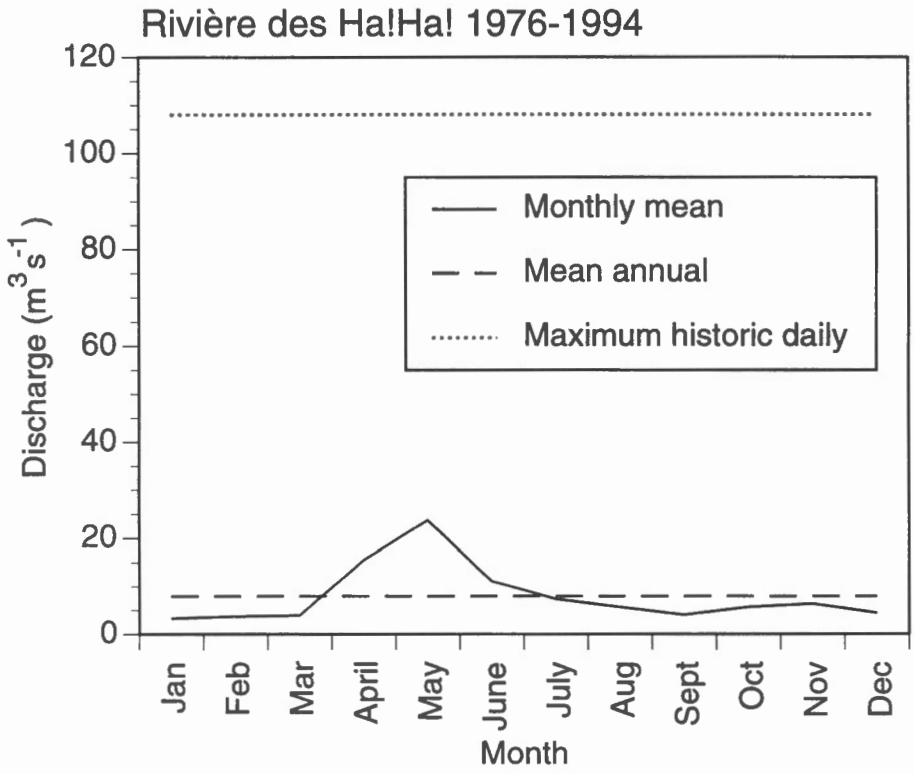
Rivière des Ha!Ha! 1976-1994
120
100
80
60
40
20
0
Discharge (m3 s-1)
Monthly mean
Mean annual
Maximum historic daily
Jan
Feb
Mar
April
May
June
July
Aug
Sept
Oct
Nov
Dec
Month

Fig. 5.3

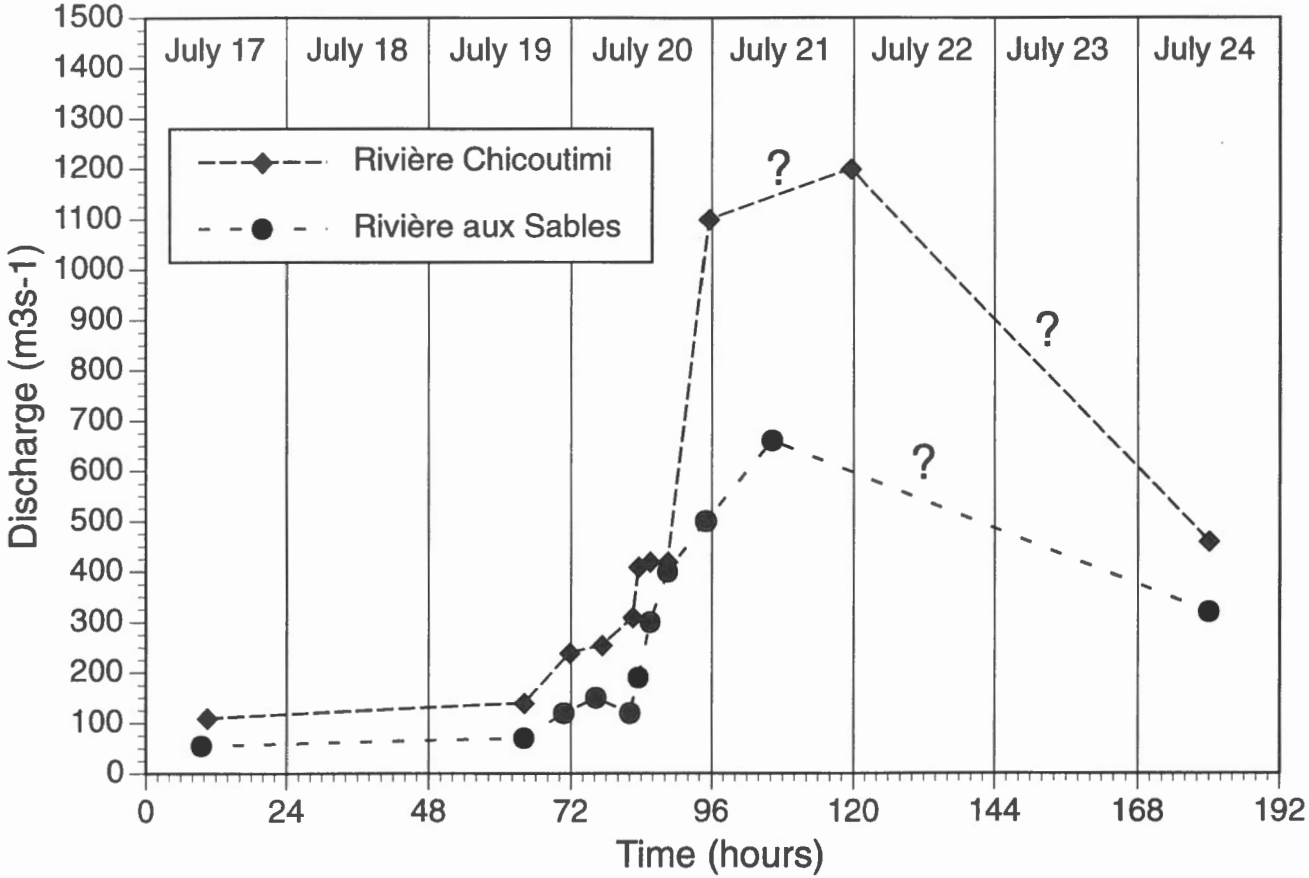
July 17
July 18
July 19
July 20
July 21
July 22
July 23
July 24
Rivière Chicoutimi
Rivière aux Sables
?
?
?
Discharge (m3s-1)
1500
1400
1300
1200
1100
1000
900
800
700
600
500
400
300
200
100
0
0
24
48
72
96
120
144
168
192
Time (hours)

Fig. 5.4

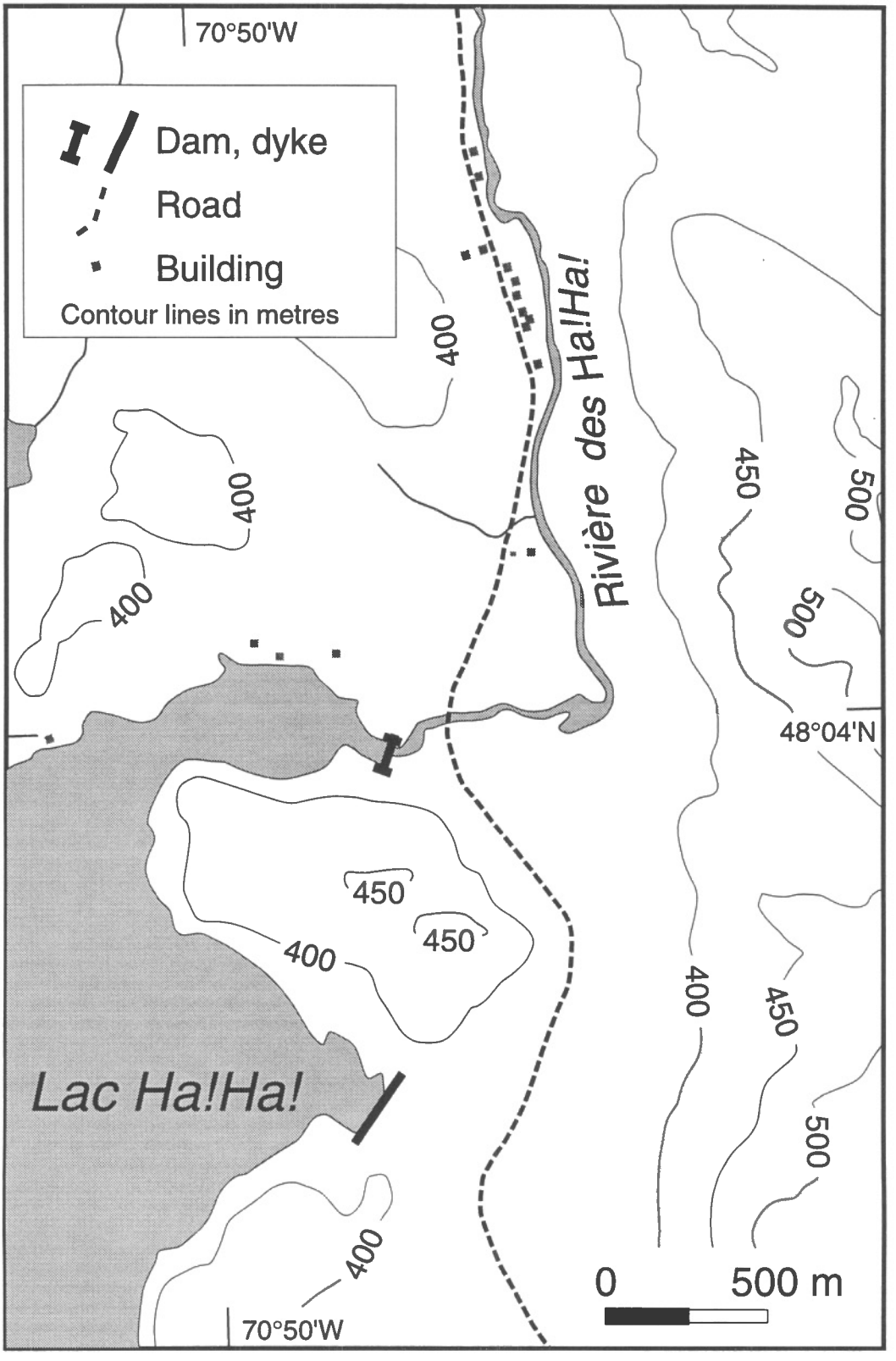
70°50'W
Dam, dyke
Road
Building
Contour lines in metres
400
400
400
Rivière des Ha!Ha!
450
500
500
48°04'N
450
450
400
400
450
500
Lac Ha!Ha!
400
0
500 m
70°50'W

Fig. 5.5

Fig. 5.6

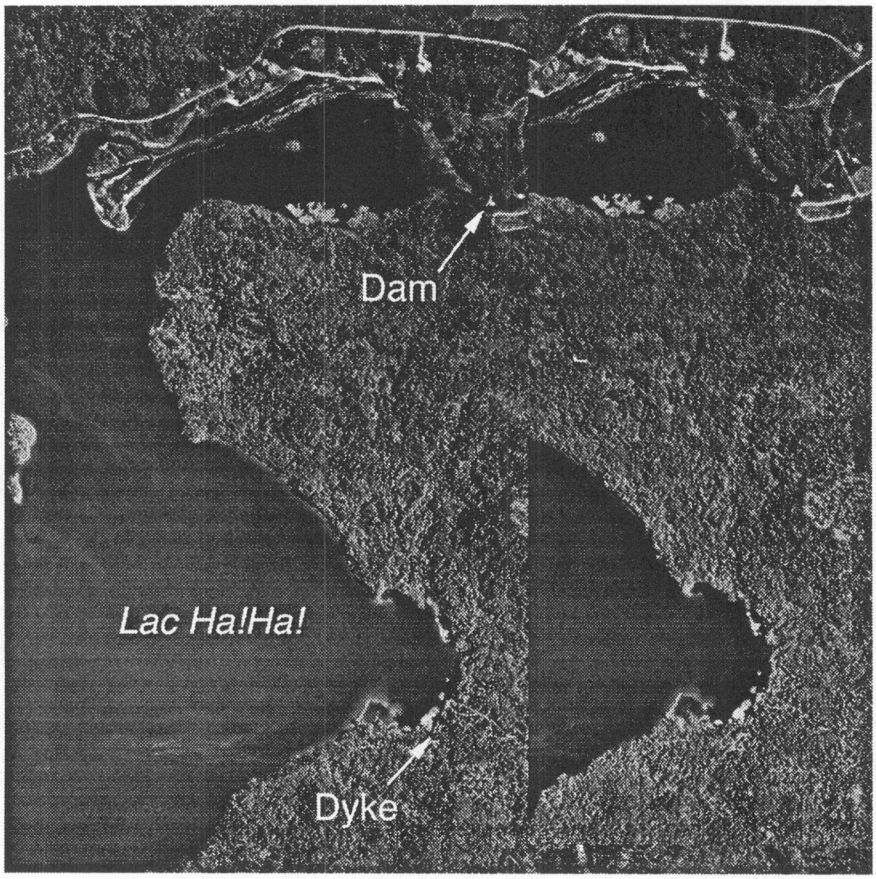

Fig. 5.7

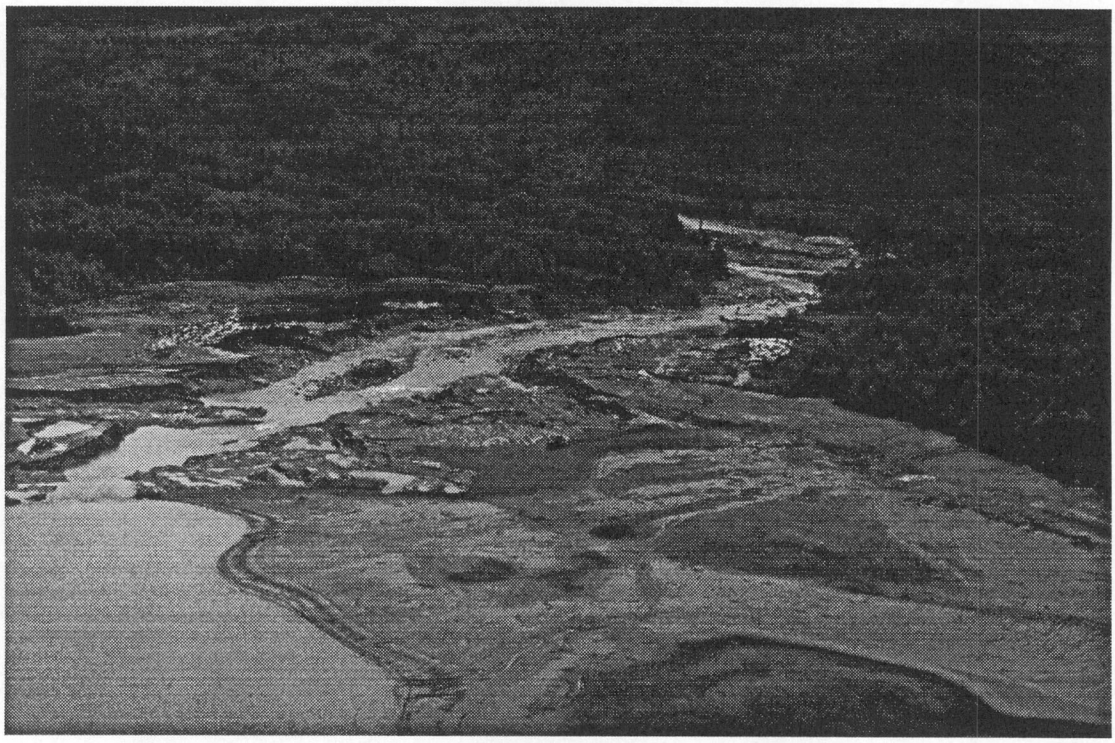

Fig. 5.8a

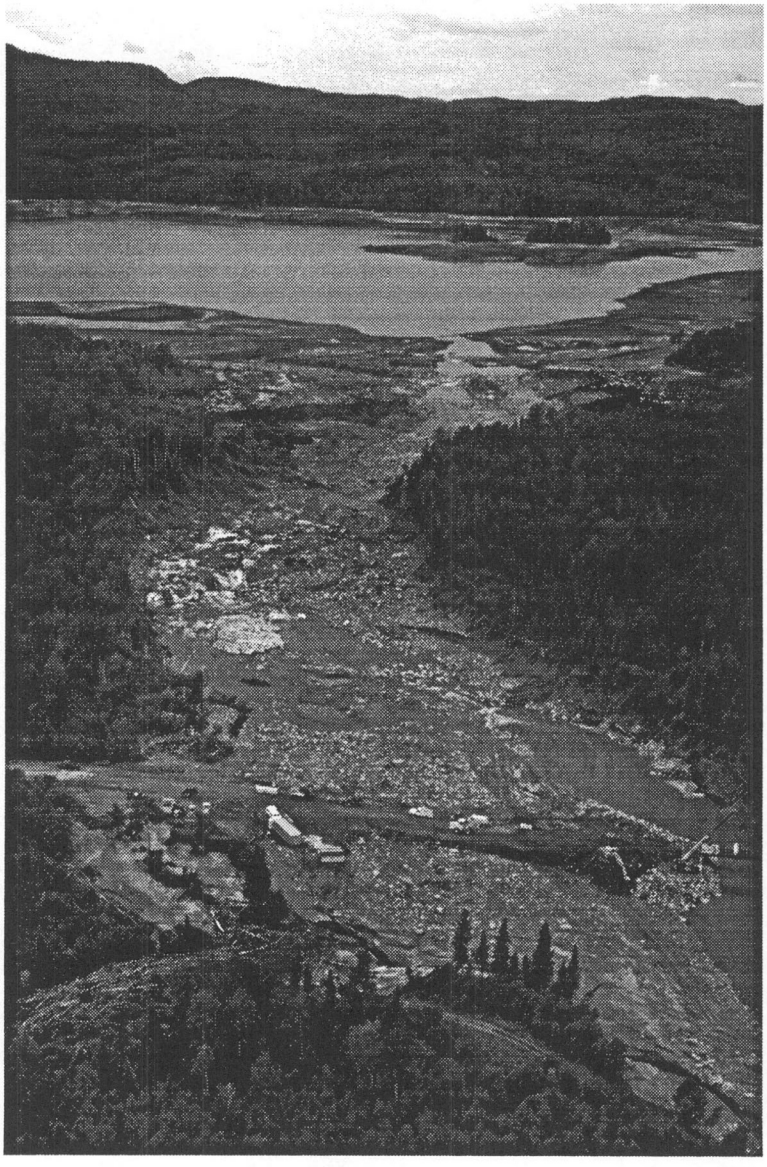

Fig. 5.8b

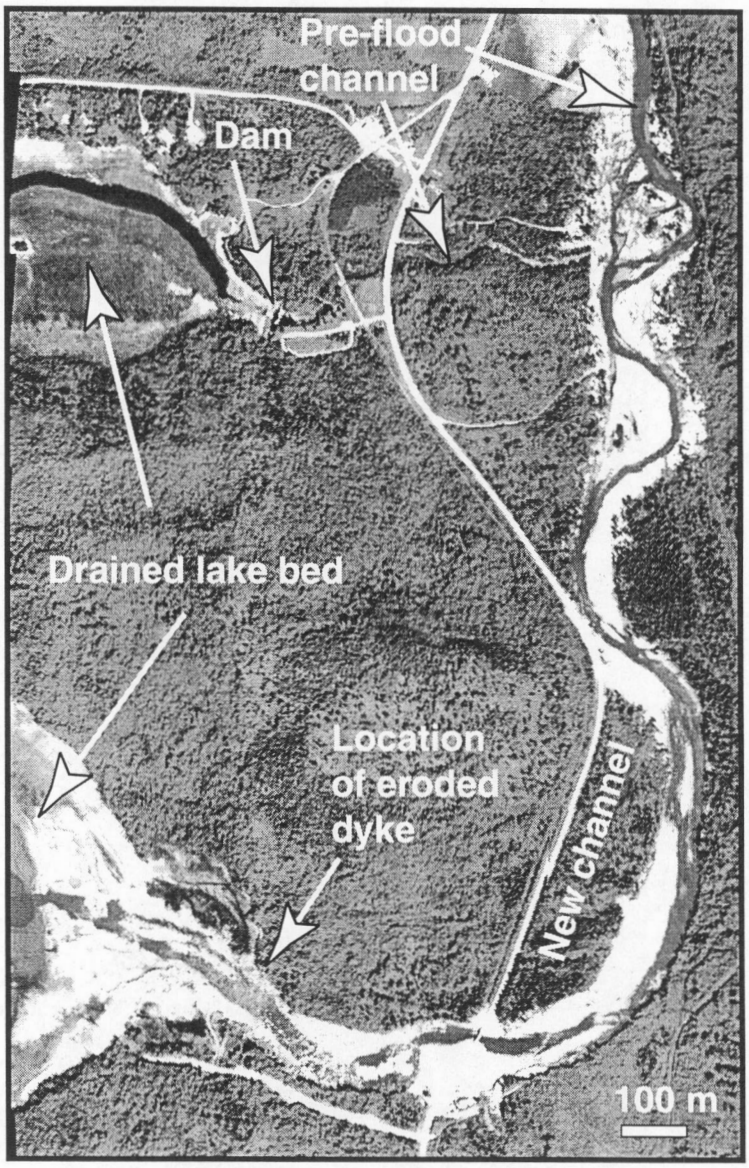
Pre-flood
channel
Dam
Drained lake bed
Location
of eroded
dyke
New channel
100 m

Fig. 5.9

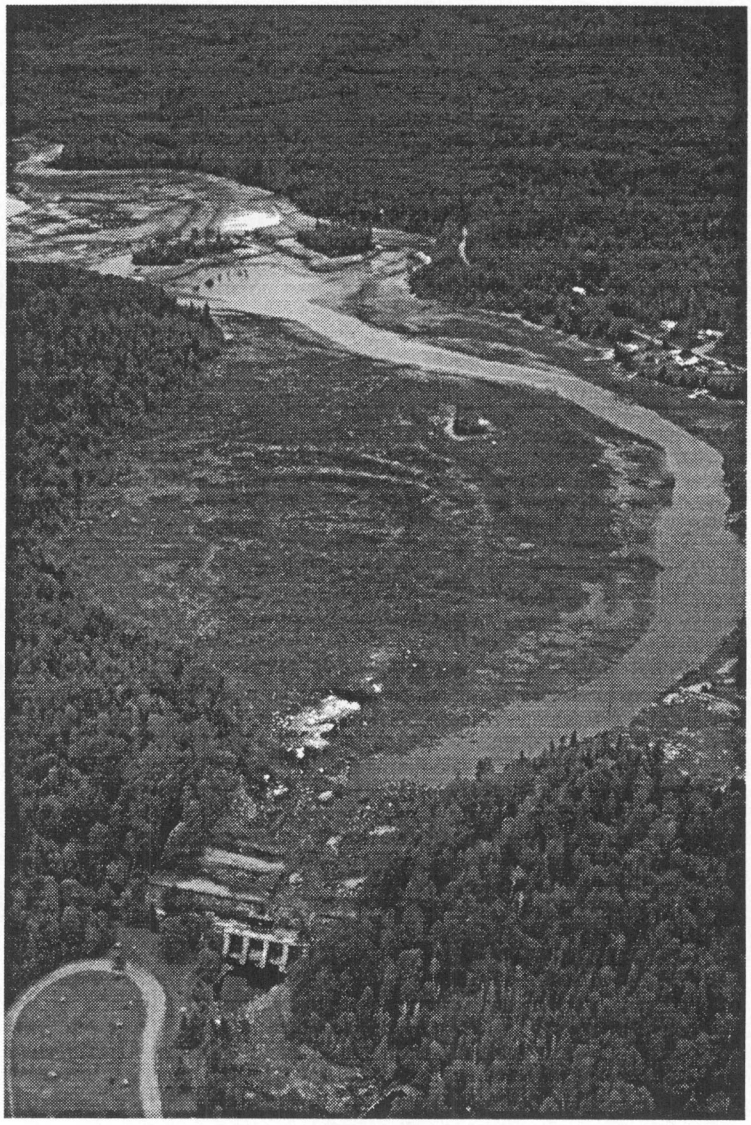

Fig. 5.10

Fig. 5.11

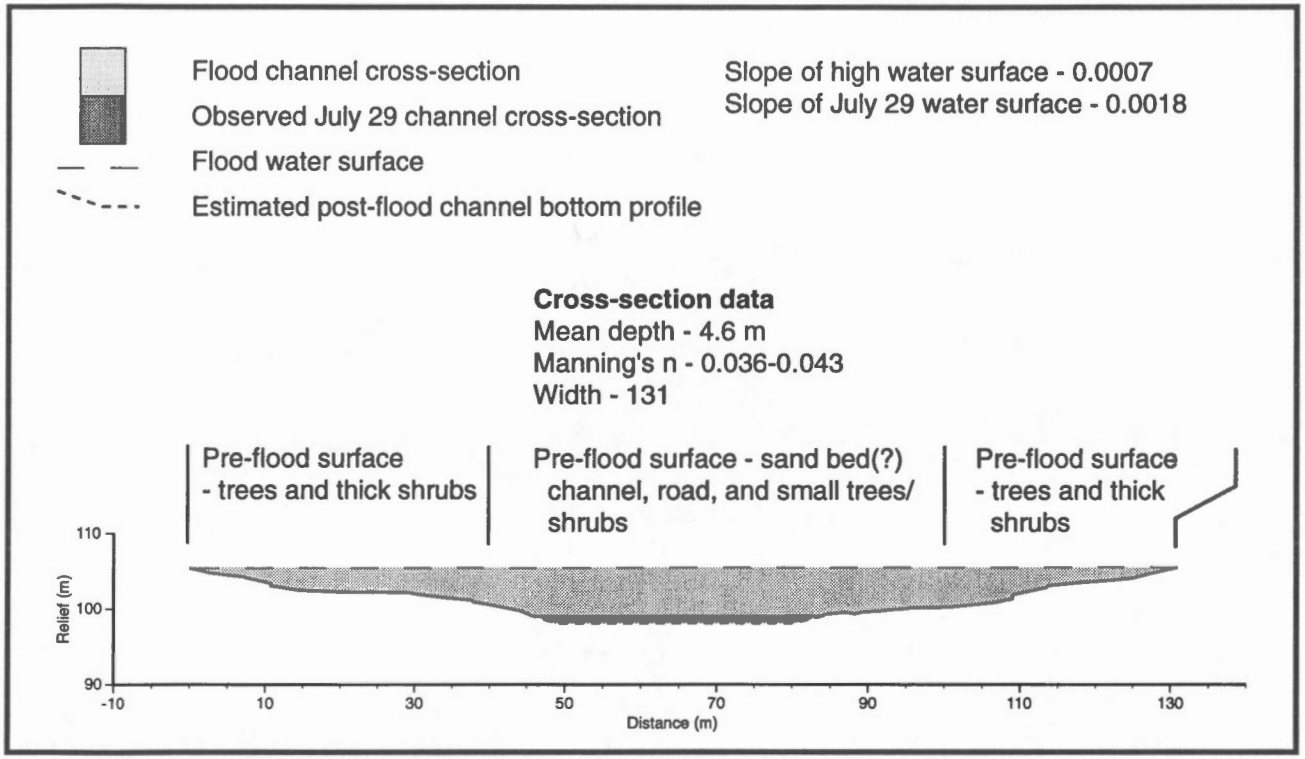
Flood channel cross-section
Observed July 29 channel cross-section
Flood water surface
Estimated post-flood channel bottom profile
Slope of high water surface - 0.0007
Slope of July 29 water surface - 0.0018
Cross-section data
Mean depth - 4.6 m
Manning's n - 0.036-0.043
Width - 131
Pre-flood surface - trees and thick shrubs
Pre-flood surface - sand bed(?) channel, road, and small trees/ shrubs
Pre-flood surface - trees and thick shrubs
Relief (m)
110
100
90
-10
10
30
50
70
90
110
130
Distance (m)

Fig. 5.12

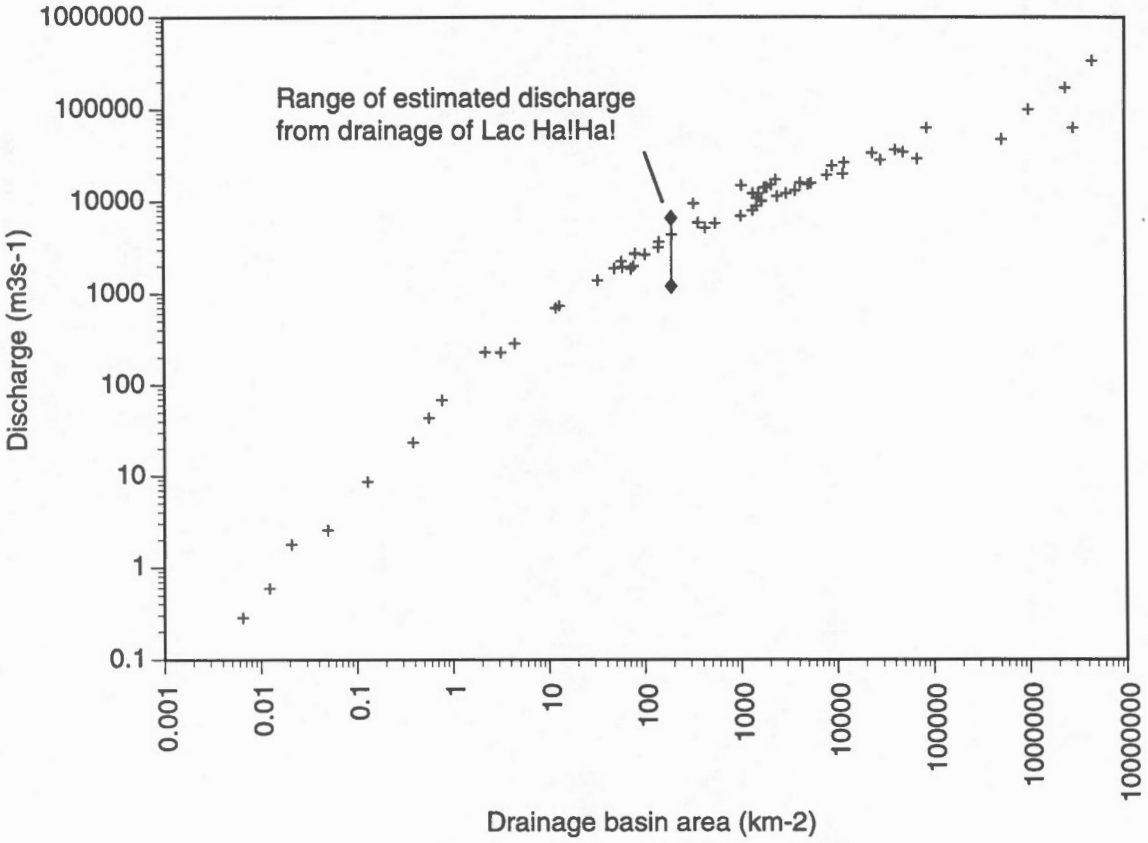
Range of estimated discharge
from drainage of Lac Ha!Ha!
Discharge (m3s-1)
1000000
100000
10000
1000
100
10
1
0.1
0.001
0.01
0.1
1
10
100
1000
10000
100000
1000000
10000000
Drainage basin area (km-2)

Fig. 5.13

6. RIVIÈRE AUX SABLES

General

Rivière aux Sables flows northward from Lac Kénogami reservoir to Rivière Saguenay, a distance of about 11 km (Figs. 1.2 and 6.1). The river is situated entirely on the Saguenay Valley lowland. It flows within a narrow, shallow stream-cut valley lacking a floodplain and alluvial terraces, that becomes deeper and better defined along the lower 3.5 km. The channel is primarily non-alluvial and laterally stable, and follows an irregular meandering course. The longitudinal profile is relatively gently sloped over the upper 7.5 km (average 0.0018) and steepens markedly over the lower 3 km where the river is incised to bedrock with two well-defined 'steps' present in the profile (Fig. 6.2).

The river flows through the hamlet of Pibrac and the downtown area of the City of Jonquière (Fig. 6.1). Between these two centres, numerous homes are situated on the lowland surface along two major roads located on either side of the river (Fig. 6.1). A large paper mill complex is located at km 1.5-1. Four sets of dams are situated along the river (Fig. 6.1): the Pibrac dam complex consisting of two dams and two dyke situated at the head of the river; the Abitibi power station dam owned by Abitibi-Price at km 3.2; Jonquière power station dam owned by the City of Jonquière at km 2.6; and the Abitibi paper mill dam at km 1 (Fig. 6.1). The river is crossed by four road bridges and two railway bridges.

Geomorphic effects of the flood

The effects of the flood along Rivière aux Sables vary markedly between km 11-3.5 and km 3.5-0, corresponding with the general downstream variation in river profile (Fig. 6.2). Along the relatively gently-sloped upper portion of the river (km 11-3.5), there was inundation of the valleysides and lowlying areas affecting numerous homes, particularly within the hamlet of Pibrac. Notable geomorphic effects were: scouring on the leeside of two concrete dykes at the Pibrac dam complex caused by overtopping of Lac Kénogami waters (Fig. 6.1 and 6.3a); bank scouring along the narrow reach immediately below the west control structure at the Pibrac dam complex (Fig. 6.1); bank scouring along narrow reaches at the base of the bridge crossing the river at about km 9.4 and adjacent to and just below a rapids at km 9-8.2 (where local gradient steepened); the formation of, or minor to major deposition on several point, mid-channel and side bars between km 9.1 and 6.2 (Fig. 6.3b); and the occurrence of a number of small (<100 m^2) bank and valleyside failures (Fig. 6.3c; see *Chapter 11 Landsliding and bank instability - Rivière aux Sables* section). Overall, however, the geomorphic effects of the flood were minor to moderate in extent with many sections of the river showing negligible effects from the flood i.e., no obvious erosion or deposition along the river banks or valleysides (Fig. 6.1). The relatively low gradient of the river would have been a factor in limiting the fluvial erosion.

In marked contrast, extensive erosion occurred along the lower 3.5 km of the river, most of this relating directly or indirectly to the presence of the three small dams. At the Abitibi power station dam (3.2 km), the overtopping of the structure and adjacent left bank by flood water resulted in up to about 45 m of lateral erosion of fine-grained marine sediment along the left valleyside (Fig. 6.4). Downstream at the Abitibi paper mill dam (km 1), overflow breached a low, narrow berm built on marine sediment forming the left valleyside, and laterally eroded up to about 85 m of the valleyside (Fig. 6.5). At both locations, deep incision occurred down to bedrock, resulting in the formation of large new channel courses adjacent to and significantly lower than the outlet gates of the dams (Figs. 6.4 and 6.5). At the Abitibi power station dam site, the river seems to have re-excavated an ancestral channel course that had been incised into the bedrock, most likely in the Pleistocene.

With the formation of these new channel courses, the reservoirs associated with both dams drained leaving the dams non-functional and the original spillways dry. Buildings located along the left valleyside adjacent to both dams collapsed or were damaged by undermining because of the extensive valleyside erosion associated with the formation of the new channels. At the Abitibi paper mill dam, during a stage of the flood prior to the erosion of the new channel, overflow across the right concrete wing of the dam resulted in channelized flow immediately downstream of the dam which eroded vegetation, overburden and fill exposing the underlying bedrock.

The Jonquière power station dam (km 2.6) was also overtopped during the flood causing minor erosion and failure of marine sediment along the left abutment. A breach about 20 m wide occurred in the right wing of the dam which lowered the reservoir several metres (Fig. 6.6). The outflow from this breach scoured the bedrock surface immediately downstream. Vertical incision at both the breach and at the left abutment was very limited because of the immediate presence of bedrock. However, the powerhouse below the dam was badly damaged by the overflow. After the flood, water remained impounded behind the dam structure although at a lower than normal level because of the breach.

The erosion adjacent to the three dams had consequences both upstream and downstream. The formation of the new channels during the flood which drained the Abitibi power station and Abitibi paper mill reservoirs resulted in strong currents being generated through previously tranquil reaches. At the former location, this flow caused minor to moderate scouring of the channel perimeter beginning at about km 4. A railway bridge located at km 3.5 partially collapsed because of erosion to the left abutment and scouring around the foundation of the left support located in the channel. A shallow retrogressive failure, about 50 m wide, occurred along the left bank just upstream of a railway bridge (km 3.5-3.6; Fig. 6.7), probably due to drawdown of the reservoir. Downstream, the powerhouse at the base of the dam was severely damaged by the flow along the new channel. Sediment derived from the erosion of the new channel beside the Abitibi power

station dam accumulated within the reservoir basin of the Jonquière power station dam located just downstream.

At the Jonquière power station dam, flow into and through the basin caused several zones of erosion and two small failures along the right side of the reservoir basin (Fig. 6.1). Up to 90 m of erosion occurred to a narrow point of land that extended upstream from the right wing of the dam (Fig. 6.1). Below the dam, the margins of a narrow bedrock reach were scoured with local erosion occurring to marine sediment along the valleysides. Sediments entrained from both here and upstream, were transported into and at least partially deposited within the reservoir of the Abitibi paper mill dam. A strong current through the Abitibi paper mill reservoir basin undoubtedly developed after the creation of the new channel adjacent to the dam (Fig. 6.1) and caused major lateral erosion along the right bank between km 1.5 and 1.2. This current caused up to about 15 m of lateral erosion to the right side of the reservoir beside a large paper mill building and incision into the bed of the basin. Just below the dam, flow along the lower part of the new channel scoured the vegetation and overburden cover from the underlying bedrock from a broad area (Fig. 6.5). Downstream to the river mouth, the pre-flood channel margins were extensively eroded widening the river channel (Fig. 6.1). About 130 m of erosion occurred along the left bank at the road bridge located just above the confluence with Rivière Saguenay (Fig. 6.8). Also at the river mouth, a large fan consisting of sand and gravel was deposited within Saguenay River channel (Fig. 6.8).

Fig. 6.1 (see POCKET) Map of Rivière aux Sables showing the locations of major communities, roads, bridges and dams. The locations of erosion and failures resulting from the flood are also shown. The scale (in blue) following the river marks kilometer distance allowing locations mentioned in the text to be keyed to the map. The yellow zones follow Dion (1986b) and designate areas having a medium to low potential for landsliding. Here, slopes are greater than 25% (14°), but there was no erosion at the toe of the slopes or evidence of major instability at the time of the original mapping. See Fig. 1.2 for the location of the map.

Fig. 6.2 Longitudinal profile of Rivière aux Sables from Lac Kénogami to Rivière Saguenay (data from 10 m contour lines on Québec Ministère de L'Energie et des Ressources maps 'Chicoutimi' (22D06-200-0202), 'Jonquière' (22D06-200-0201) and 'Lac Kénogami' (22D06-200-0101), 1:20 000 scale). The location of the dams are also shown although the change in water surface at some of these sites may fall between contour line intervals.

Fig. 6.3 Selected examples of geomorphic effects along Rivière aux Sables located between km 11 and 4: a) scouring to the lee of the west dyke at Pibrac dam complex (GSC photograph 1997-42F); b) fresh point bar deposit at 7.2 km (left side of picture; GSC photograph 1997-42G); and c) small bank failure along the left bank at 5.3 km (centre of picture; GSC photograph 1997-42H). Pictures taken on July 26, 1996.

Fig. 6.4 The Abitibi power station dam located at km 3.2: a) the intact dam and dry spillway along the right side of the river (upper centre of photograph; GSC photograph 1997-42I) and b) the extensive erosion along the left valleyside that undermined several apartment buildings, one of which has almost completely collapsed into the river gorge (GSC photograph 1997-42J). Pictures taken on July 26, 1996.

Fig. 6.5 The new channel flowing adjacent to the Abitibi paper mill dam at km 1. The original dam remains intact (marked by arrow). The new channel has formed because of overflow and erosion of a berm and underlying marine sediment. Picture taken on July 26, 1996 (GSC photograph 1997-42K).

Fig. 6.6 The Jonquière power station dam which was overtopped during the flood causing minor erosion of the left abutting valleyside and an about 20 m wide breach in the right wing of the dam. Picture taken on July 26, 1996 (GSC photograph 1997-42L).

Fig. 6.7 Wide, shallow retrogressive failure located at km 3.5-3.6. Picture taken on July 26, 1996 (GSC photograph 1997-41A).

Fig. 6.8 Large fan at the mouth of Rivière aux Sables formed from the accretion of sediment derived from erosion upstream. Note the bridge just left of centre where the left

abutment and a large section of the road approach has been washed away. Picture taken on July 26, 1996 (GSC photograph 1997-42M).

Fig. 6.1 see POCKET

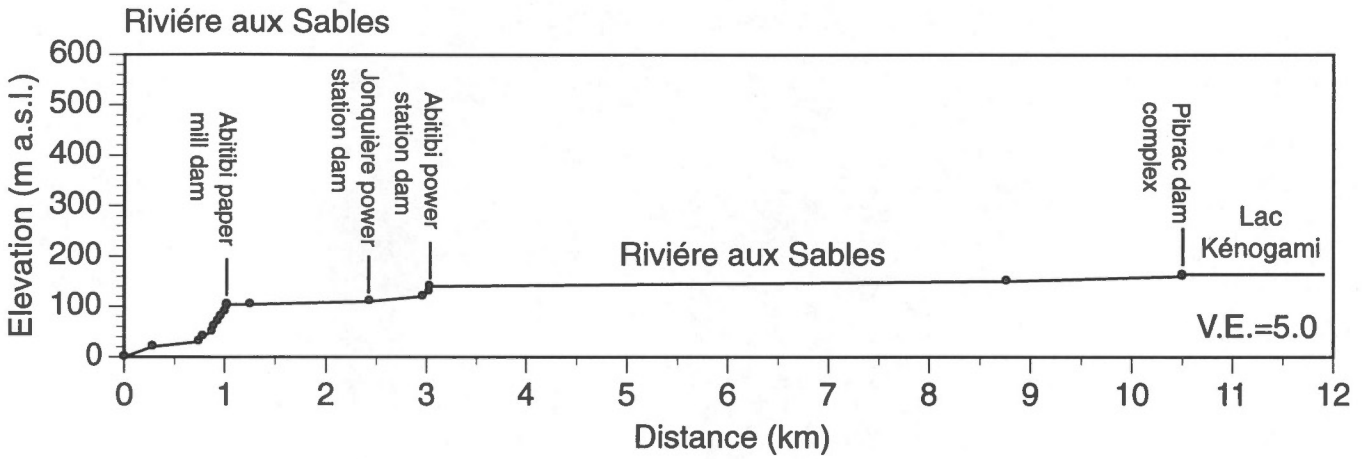
Riviére aux Sables
Elevation (m a.s.l.)
600
500
400
300
200
100
0
Abitibi paper mill dam
Jonquière power station dam
Abitibi power station dam
Riviére aux Sables
Pibrac dam complex
Lac Kénogami
V.E.=5.0
0
1
2
3
4
5
6
7
8
9
10
11
12
Distance (km)

Fig. 6.2

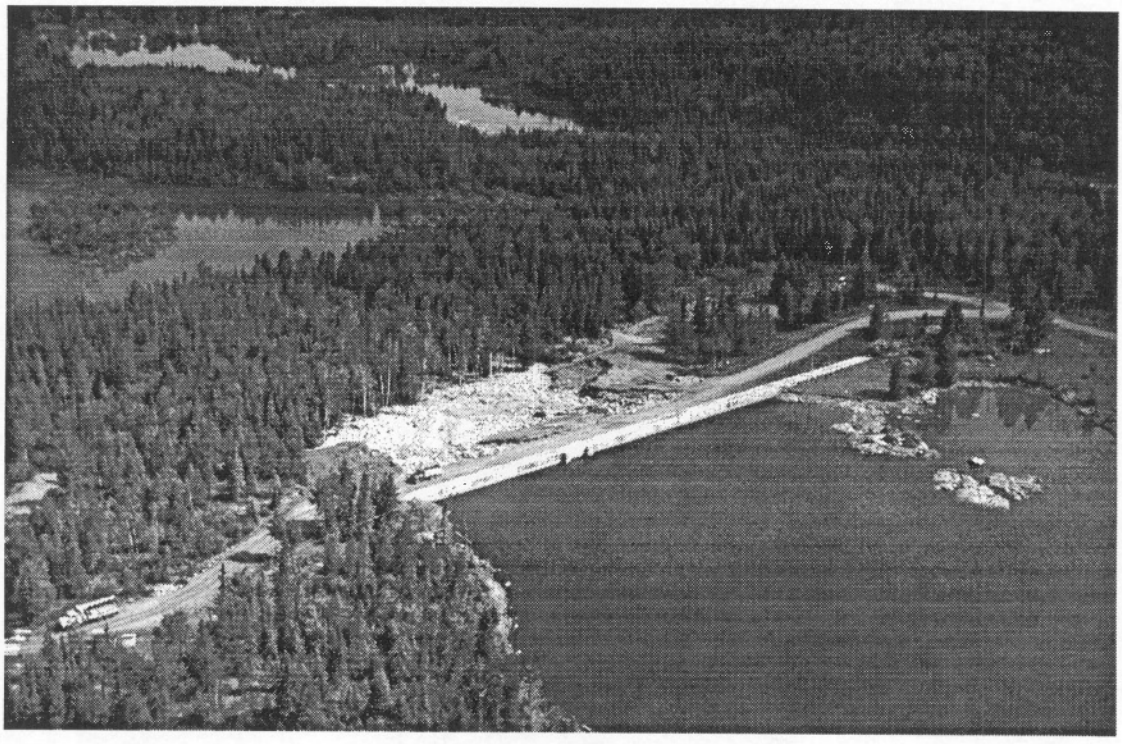

Fig. 6.3a

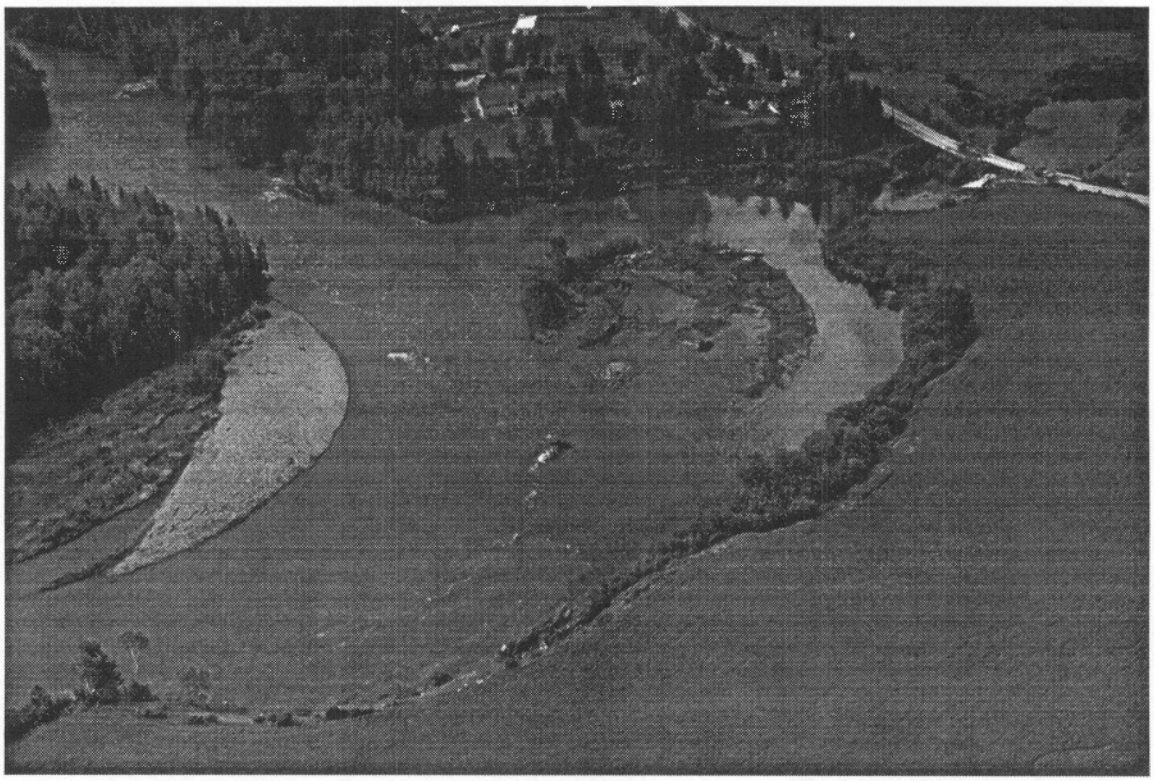

Fig. 6.3b

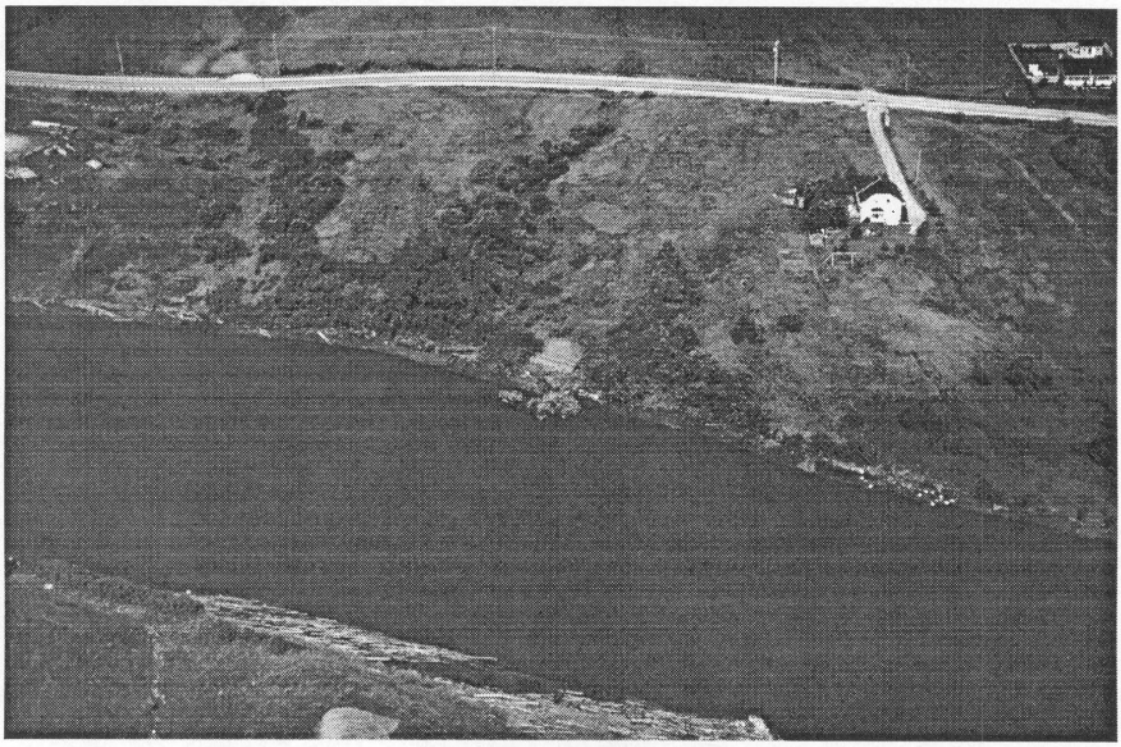

Fig.6.3c

Fig. 6.4a

Fig. 6:'b

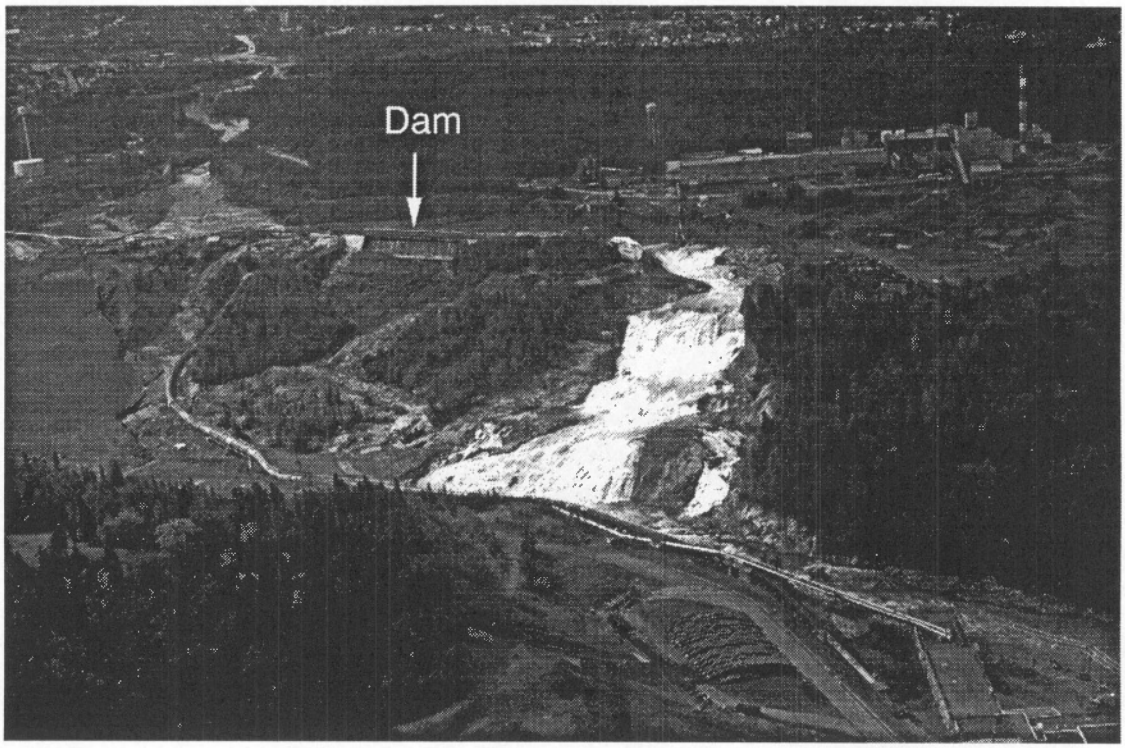

Fig. 6.5

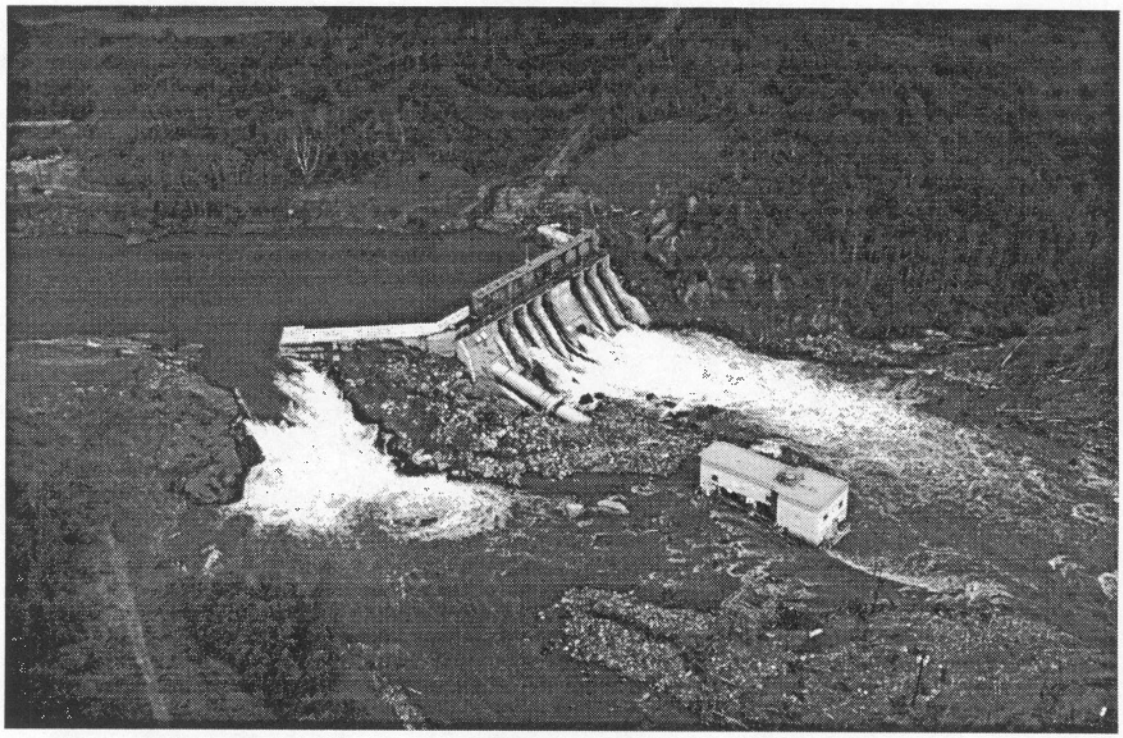

Fig. 6.6

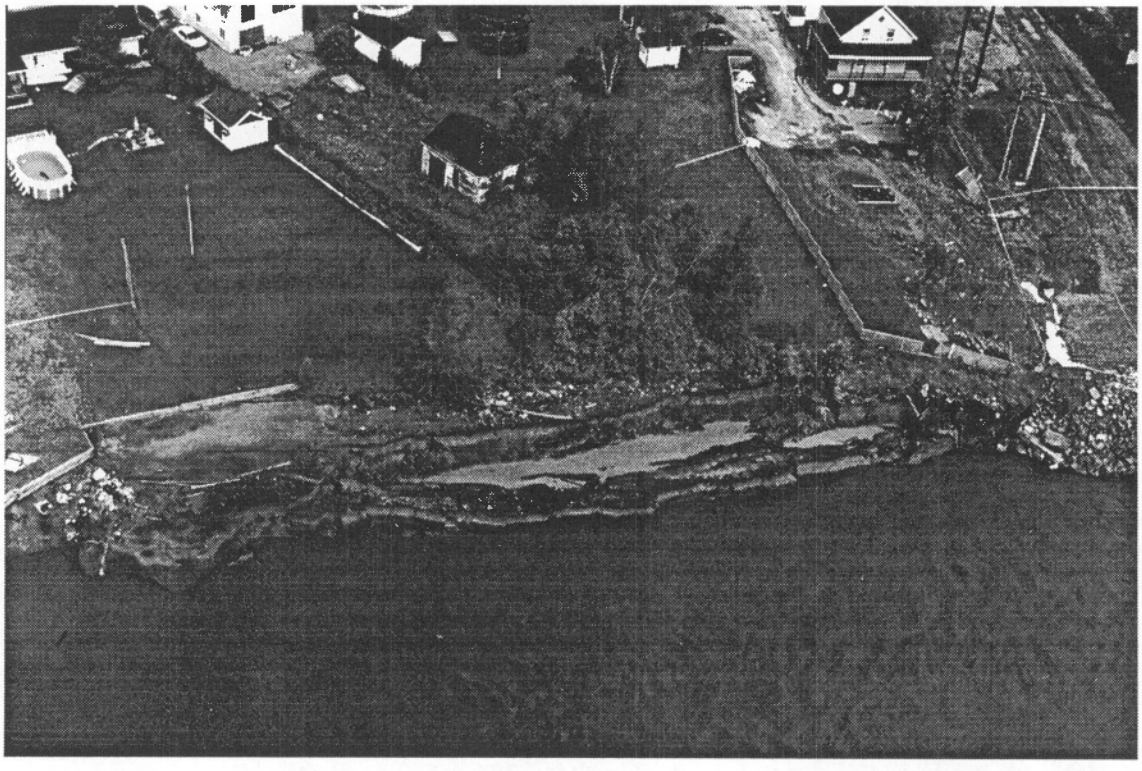

Fig.6.7

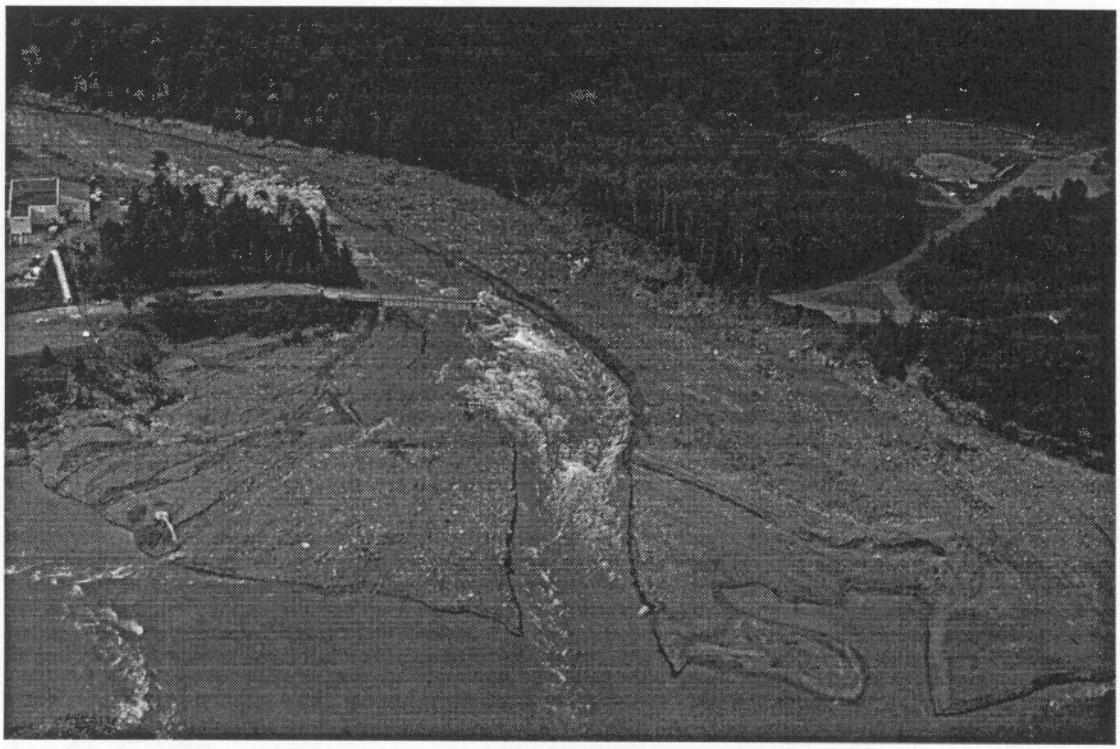

Fig. 6.8

7. RIVIÈRE CHICOUTIMI

General

Rivière Chicoutimi flows about 23.5 km from Lac Kénogami reservoir to the confluence with the Rivière Saguenay (Fig. 7.1). Over its course, the river is confined within a relatively narrow and shallow (up to 10-15 m deep) stream-cut valley. The valley becomes deeper along the lower 3 km where the river profile steepens and flows into the Saguenay River Valley (Fig. 7.2).

The river exhibits an irregular channel pattern and a narrow, fragmented, discontinuous floodplain is present between km 18 to 6. Several isolated alluvial terrace fragments are present at different levels above the floodplain. The river channel consists of bedrock, non-alluvial, and short alluvial sections. From km 23.5 to 18.5, the channel width is irregular, reflecting the presence of bedrock forming the river banks. The channel between km 18.5 to 3 varies from alluvial to non-alluvial depending on the presence of a floodplain surface. Here, channel width varies from about 30 to 370 m and tracts of well-defined floodplain are present at prominent bends at km 16-15.7, 14-13.6 and 12.0-11.7. Short bedrock reaches forming rapids are present at km 19.2-18.7, 7.5-7.2 and 5-4.7 along an otherwise relatively gentle river profile above km 3 (the rapids are not apparent in Fig. 7.2 because of the contour line spacing on the topographic base maps). Few bars are present although point bars occur along the convex side at the previously mentioned bends. Several islands occur, formed by bedrock protruding through the channel. There is no obvious contemporary lateral channel change in recent aerial photographs suggesting that the channel is stable. Below km 3 to the confluence with Rivière Saguenay, the channel alternates between bedrock and alluvial.

There is considerable residential, commercial, and industrial development along Rivière Chicoutimi. Numerous homes are located adjacent to the river on the lowland or terrace surfaces, and on the valleysides and floodplain. The river flows through the City of Chicoutimi along its lower 2 km. Five dams are present along the river, including Portage-des-Roches dam at Lac Kénogami (km 23.5), Chute-Garneau dam (km 7.3), Pont-Arnaud dam (km 5), Elkem dam (km 3) and Abitibi power station dam (km 0.6) (Fig. 7.1). The latter four dams impound small reservoirs. The river is crossed by six road (only five are shown in Fig. 7.1) and two railway bridges.

Geomorphic effects of the flood

During the flood severe erosion occurred along Rivière Chicoutimi adjacent to two dam sites while major damage to a commercial-residential area in Chicoutimi was caused by overtopping at a third dam. At Chute-Garneau dam (Fig. 7.3), the pre-flood channel was split by a small bedrock island located just upstream of the dam causing the river channel to widen markedly (Fig. 7.1). Overflow during the flood of the left valleyside resulted in

extensive lateral erosion and incision of the marine sediment adjacent to the dam. This overflow formed a new channel, 70 m wide and roughly 10 m deep, adjacent to and lower than the base of the dam (Figs. 7.1 and 7.3). The new channel represents a downstream extension of the existing left channel. The relatively deep incision along the new channel was able to occur because the lateral extension of bedrock surface upon which the dam is situated happens to be of lower relief at the location of the new channel. The formation of the new channel drained the reservoir previously impounded by the dam.

In conjunction with the formation of this new channel, major lateral bank erosion occurred along the concave bank of the channel to the left of the island just above the dam (Fig. 7.1). This erosion probably occurred following the drainage of the reservoir which allowed a relatively strong current to develop along the left bank. Bank erosion was probably accentuated by the curved morphology of the left channel around the island and the lateral dip into the bank of the bedrock surface forming the island, both of which would have directed flow against the left bank of the channel, as occurs around the outer bank of a meander (Fig. 7.3). Overall in the area of Chute-Garneau dam, bank erosion occurred along an about 440 m length of the left bank adjacent to the island and extending downstream through the new channel (Fig. 7.3). Sediment derived from the erosion of river bank and new channel was deposited in bars within the reach just downstream of the dam where the river channel broadens markedly (Fig. 7.1).

The extensive erosion along the left bank adjacent to the island and the dam resulted in the major loss of property and threatened to undermine several homes located near to the river (Fig. 7.3b). After the recession of the flood, the entire streamflow was carried along the channel to the left of the island and the new extension beside the dam (Fig. 7.3). The formerly submerged banks of the drained reservoir were exposed along a reach extending about 2 km above the dam. Although intact, the Chute-Garneau dam was left non-functional because of the draining of the reservoir.

At the Pont-Arnaud dam (km 5) prior to the flood, water passing through the dam gates spilled down a relatively steep bedrock and coarse bouldery lag channel into a broad pool just downstream (Fig. 7.1). Water flowed downstream from the reservoir to the powerhouse situated about 150 m downstream of the dam via buried penstocks located immediately to the right of the dam. The dam itself is founded on bedrock which must have formed the local control of baselevel for the upstream reach, prior to the construction of the dam (Fig. 7.4).

During the flood, water overtopped a section of valleyside just to the right of the penstocks and powerhouse eroding a new channel 150 m long, 95 m wide and roughly 12 m deep (Figs. 7.1 and 7.4). In a situation similar to the Chute-Garneau dam, the local bedrock topography in this area is irregular and happens to be lower at the location of the new channel than at the dam. Thus, the new channel incised to a level below that of the dam, draining the reservoir and leaving the dam intact, but non-functional. This erosion also severed a railway line which crossed the river just below the dam (Fig. 7.1).

Upstream of the dam, two well-defined erosion surfaces were incised into the floor of the reservoir basin (Fig. 7.5). The higher of these two surfaces represents approximately the level of the marine sediment that underlies the floor of the basin. This surface forms a well-defined erosional terrace along the valley bottom into which the lower surface has eroded. The higher erosion surface is interpreted to be the bed of a broad channel that was eroded into the basin floor. It probably formed following the drainage of the reservoir which would have allowed a strong current to develop that scoured the bed of the reservoir. The outer margins of the channel are erosional and formed by either steeply-sloped, organic-rich sediments which probably were accreted on the basin floor, or marine sediment of the valleyside. The new channel probably follows the pre-dam channel course that was subsequently widened and scoured down to the marine sediment.

The second, lower erosion surface forms a vertically-sided channel, 30-115 m wide and 1200 m long, incised into the marine sediment that forms the level of the upper surface (Fig. 7.5). This channel is headed by a well-defined 'step', 2-4 m high, representing a knickpoint within the river profile (Fig. 7.5). On July 26, 1996, after the flood had receded, a major portion of the streamflow was routed over this step forming a short water falls (Fig. 7.5). Located about 350 m downstream of this falls, the left side of the channel widens abruptly and is headed by two separate 'dry' knickpoint forms that represent analogous, but inactive features, to the present knickpoint (Fig. 7.5). At higher river stages water would have also cascaded over these features.

The presence of the active and inactive knickpoints suggests that the channel forming the lower erosion surface was carved into the marine sediment of the upper erosion surface by the upstream migration of the knickpoints. The presence of the knickpoint erosion likely relates to the strength and horizontal bedding of the marine sediments. Such deposits commonly are relatively resistant to a flow shearing over the surface of the beds, but are vulnerable to undercutting and scouring by back eddies and cavitation at the lee of a knickpoint. The knickpoint erosion probably originated at the downstream end of the new channel and has migrated upstream. The marked narrowing of the lower erosion surface channel that occurs at the location of the two dry knickpoints (Fig. 7.5) could reflect a drop in river stage after which concentrated flow occurred only over the observed active knickpoint which continued to migrate upstream after the flood.

A number of small, shallow failures occurred along the steeply sloped, eroded sides of the former reservoir (Fig. 7.1). Most of these happened within organic-rich sediment along the right bank (Fig. 7.1). The largest, however, was along the left bank at km 5.2 within marine sediment and had an area of about 2100 m^2 (Fig. 7.6). The occurrence of the failures probably relates to the rapid drawdown of the reservoir and the erosion of the river into the floor of the basin (see *Chapter 11 Landsliding and bank instability - Rivière Chicoutimi* section).

The Abitibi power station dam located in downtown Chicoutimi, consists of a 'main' structure housing the powerhouse and control gates, and a long narrow concrete wing that

extends upstream to enclose the right side of the reservoir (Figs. 7.1 and 7.7). During the flood, the entire dam was overtopped by water, the greatest volume of which spilled over the right wing and followed the natural grade which slopes steeply downvalley into a residential-commercial area known as 'old' Chicoutimi located adjacent to the dam (Fig. 7.7). This rapid torrent stripped the vegetation and thin overburden from the bedrock, eroded roads and, damaged and destroyed buildings, some of which were literally washed off their foundations (Fig. 7.7). A broad erosional 'channel' thus was created within the urban area (Fig. 7.7). Coarse sediment eroded by the overflow was deposited as a bar in a broad pool where the flood water re-entered Rivière Chicoutimi just above the river mouth (Fig. 7.7). The dam structure itself appeared to have received only minimal damage, and continued to impound water after the flood. The spillage of water through the downtown area ceased when the flood receded.

Elsewhere along Rivière Chicoutimi, the geomorphic effects of the flood ranged from negligible to moderate, with there being very little geomorphic evidence of the flood along some sections of the river (Fig. 7.8). This reflects the generally low valley gradient between km 23.5 and 3 and the presence of bedrock along the steeper portion of the river between km 3 and the river mouth (Fig. 7.2). However, there were many areas severely effected by inundation, including, the lowlying sections of the valley bottom, floodplain areas, and relatively flat bedrock surfaces that protrude slightly above the river surface. Examples of severely flooded areas were the community of Laterrière-Bassin, floodplain surfaces at km 16-15.7, 14-13.6, and 12.0-11.7, and a lowlying area at km 7.1-6.2 (Fig. 7.9). Flooding of some of these areas was accentuated by the pooling of water behind the bridge at km 6.7 or the rise in stage of the reservoirs impounded behind the Chute-Garneau and Pont-Arnaud dams prior to the breaching of the impoundments. Residences located on such surfaces were flooded, damaged to varying degrees and in some cases destroyed. Some of these inundated areas experienced trace to moderate (<1 m) sand deposition and scouring that locally formed elongated scour holes (Fig. 7.9b).

Areas of bank erosion and scouring occurred sporadically along the river, most often where the channel was constricted by bedrock projecting into the channel. The most notable, erosion and scouring occurred along the left bank both upstream and downstream of the bridge located at km 6.7 (Fig. 7.10). Below the bridge, the erosion seems to have happened because of the marked constriction and therefore acceleration of flow through the narrow underpass creating a high speed current which extended a short distance downstream. Significant erosion also occurred: along the right bank of the large pool at the river mouth where there was up to about 80 m of bank erosion; along the alluvial left and right banks at km 1.1-0.8 within the reservoir above the Abitibi power station dam; and to the vegetative cover along the lower valleysides of bedrock reaches located between km 3 and 1. A number of minor, shallow bank failures of the valleyside occurred sporadically along the river, commonly located along the concave banks opposite the tight meander bends (Fig. 7.1; see *Chapter 11 Landsliding and bank instability - Rivière Chicoutimi* section).

Fig. 7.1 (see POCKET) Map of Rivière Chicoutimi showing the locations of major communities, roads, bridges and dams. The locations of erosion and failures resulting from the flood are also shown. The scale (in blue) following the river marks kilometer distance allowing locations mentioned in the text to be keyed to the map. The yellow zones follow Dion (1986b) and designate areas having a medium to low potential for landsliding. Here, slopes are greater than 25% (14°), but there was no erosion at the toe of the slopes or evidence of major instability at the time of the original mapping. See Fig. 1.2 for the location of the map.

Fig. 7.2 Longitudinal profile of Rivière Chicoutimi (data from 10 m contour lines on Québec Ministère de L'Energie et des Ressources maps 'Chicoutimi' (22D06-200-0202), and 'Laterrière' (22D06-200-0102), 1:20 000 scale). The location of the dams are also shown although the change in water surface at some of these sites may fall between contour line intervals.

Fig. 7.3 Chute-Garneau dam and the new channel eroded during the flood that bypasses the dam; viewed from a) downstream (GSC photograph 1997-42N) and b) upstream of the dam (GSC photograph 1997-42O). Photographs taken on July 26, 1996.

Fig. 7.4 The Pont-Arnaud dam (centre-right) left intact, but non-functional following the flood. A newly eroded channel carries the river flow and bypasses the dam. Photograph taken on July 26, 1996 (GSC photograph 1997-42P).

Fig. 7.5 The incised channel of Rivière Chicoutimi upstream of the Pont-Arnaud dam. Two distinct levels of erosion surface are carved into the floor of the drained reservoir. The lower erosion surface is extending upstream through knickpoint retreat. Note the two dry knickpoint in the centre-right of the photograph. Picture taken on July 26, 1996 (GSC photograph 1997-42Q).

Fig. 7.6 Retrogressive failure located along the left bank at km 5.2 within the area formerly inundated by the Pont-Arnaud reservoir. The failure most likely occurred in response to the combination of the incision of the river into the basin floor and the drawdown of the reservoir. Photograph taken on July 26, 1996 (GSC photograph 1997-42R).

Fig. 7.7 The Abitibi power station dam (just right of centre) and the channel (left of centre) where a torrent of overflow waters swept through a residential-commercial area of Chicoutimi. Photograph taken on July 26, 1996 (GSC photograph 1997-42S).

Fig. 7.8 Reach of Rivière Chicoutimi which experienced no significant geomorphic change during the flood, looking upstream of km 8.5. The unvegetated banks in the foreground are the result of drawdown of the Chute-Garneau reservoir and are not the

product of bank erosion. Photograph taken on July 26, 1996 (GSC photograph 1997-42T).

Fig. 7.9 Examples of local effects of the flood along Rivière Chicoutimi which were not associated directly with a dam: a) inundation and deposition on the floodplain along the convex side of a meander located at km 16-15.7 (GSC photograph 1997-42U); and b) erosion of elongated scour holes and deposition on the floodplain along the convex side of a meander located at km 14-13.6 (GSC photograph 1997-42V). Photograph taken on July 26, 1996.

Fig. 7.10 Eroded river bank (centre of photograph) immediately downstream of the bridge located at km 6.7. Photograph taken on July 26, 1996 (GSC photograph 1997-42W).

Fig. 7.1 see POCKET

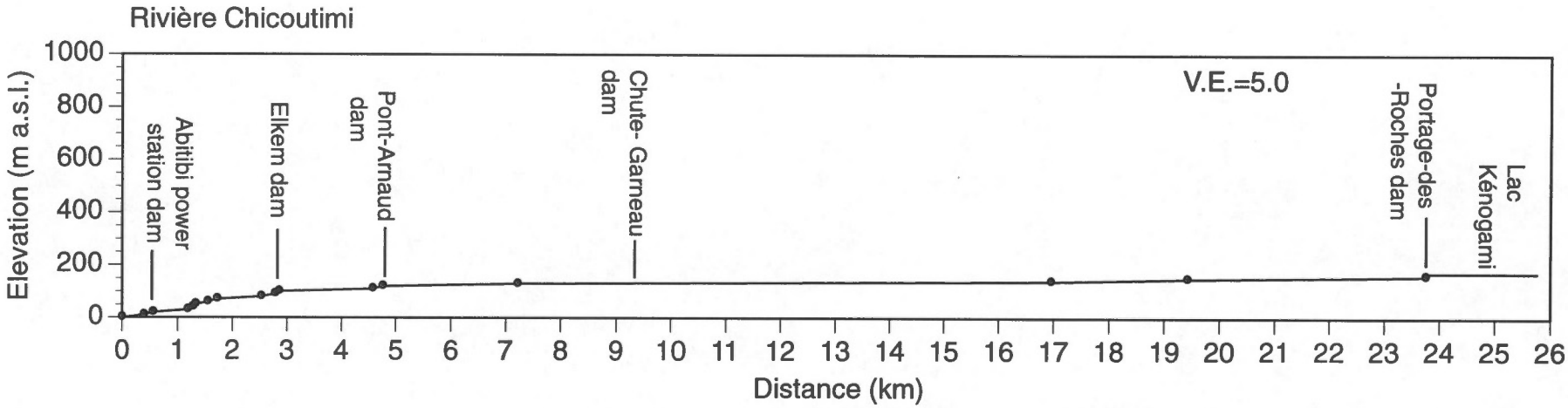
Rivière Chicoutimi
Elevation (m a.s.l.)
1000
800
600
400
200
0
Abitibi power station dam
Elkem dam
Pont-Arnaud dam
Chute- Garneau dam
V.E.=5.0
Portage-des -Roches dam
Lac Kénogami
0 1 2 3 4 5 6 7 8 9 10 11 12 13 14 15 16 17 18 19 20 21 22 23 24 25 26
Distance (km)

Fig. 7.2

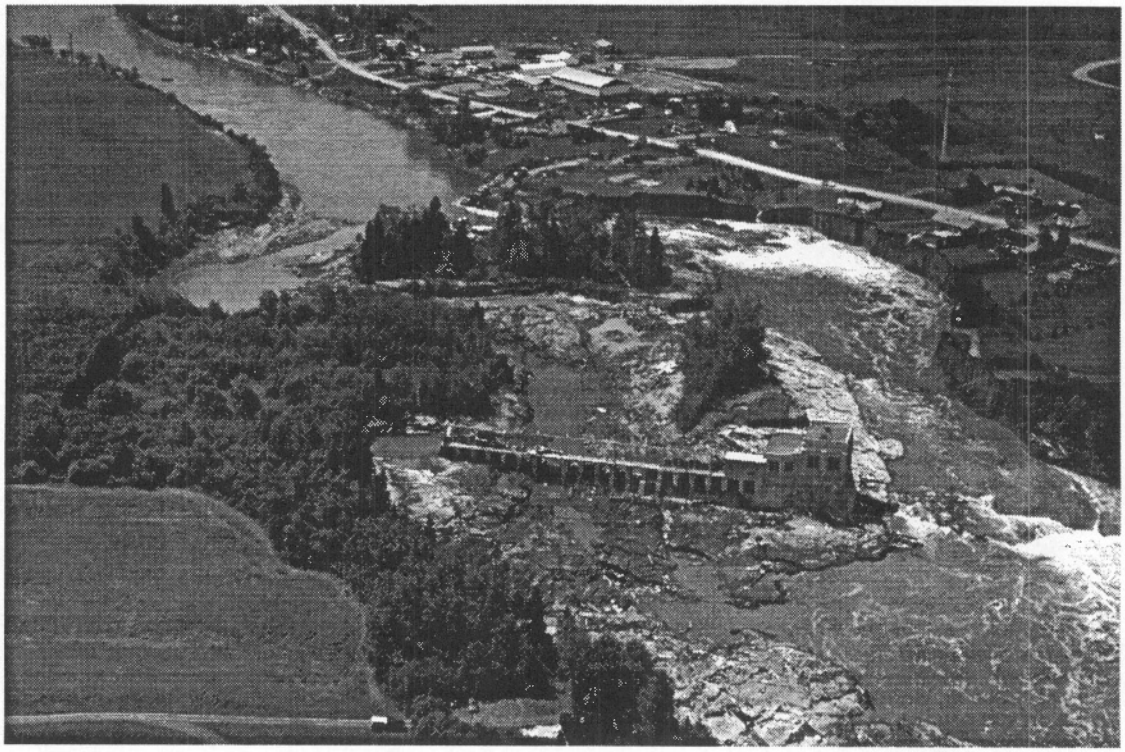

Fig. 7.3a

Fig. 7.3a

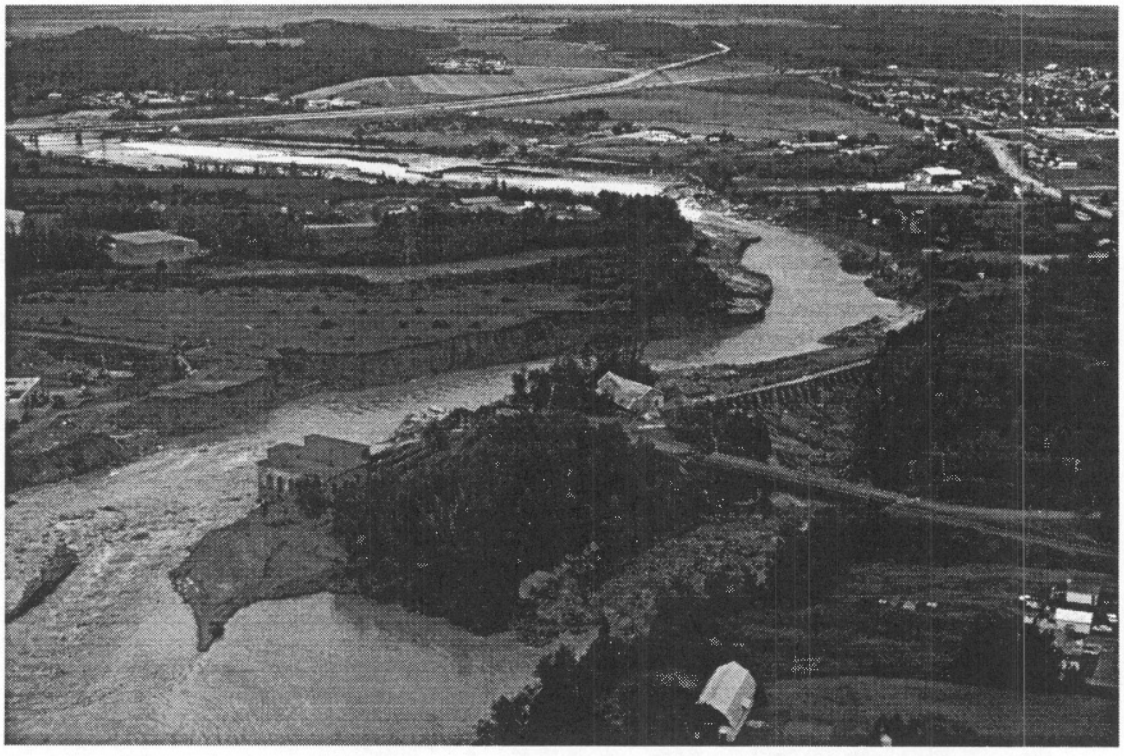

Fig. 7.4

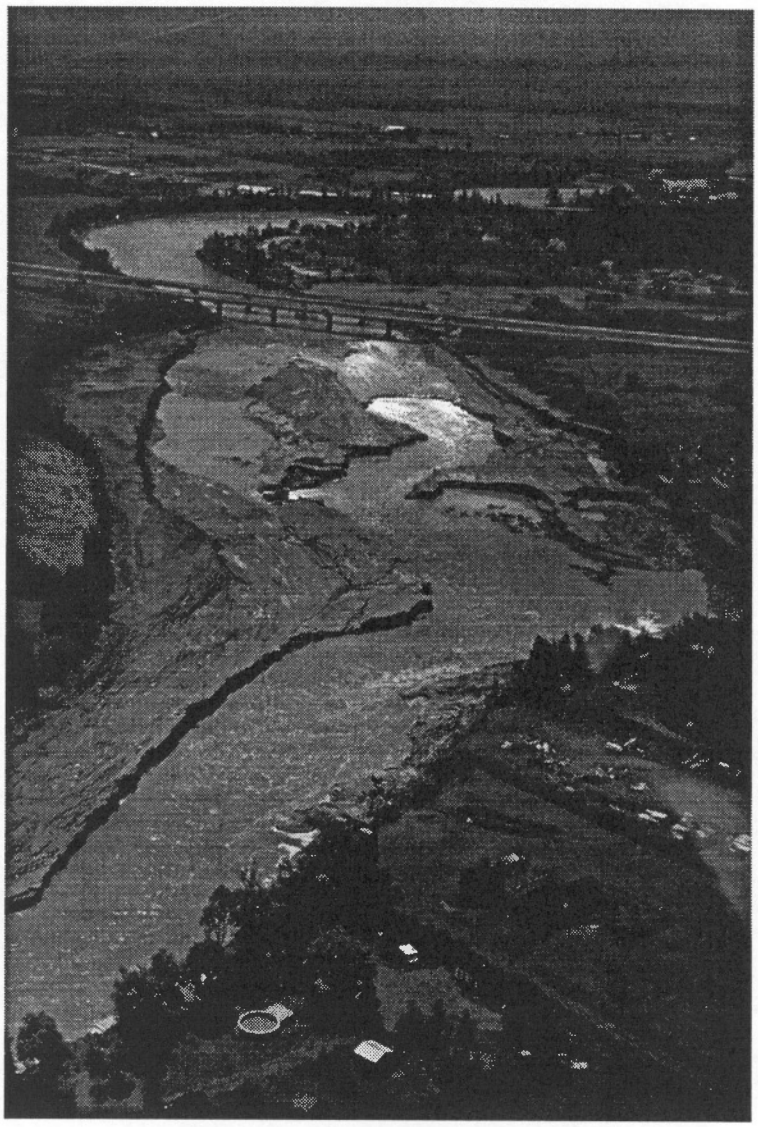

Fig. 7.5

Fig. 7.6

Fig. 7.7

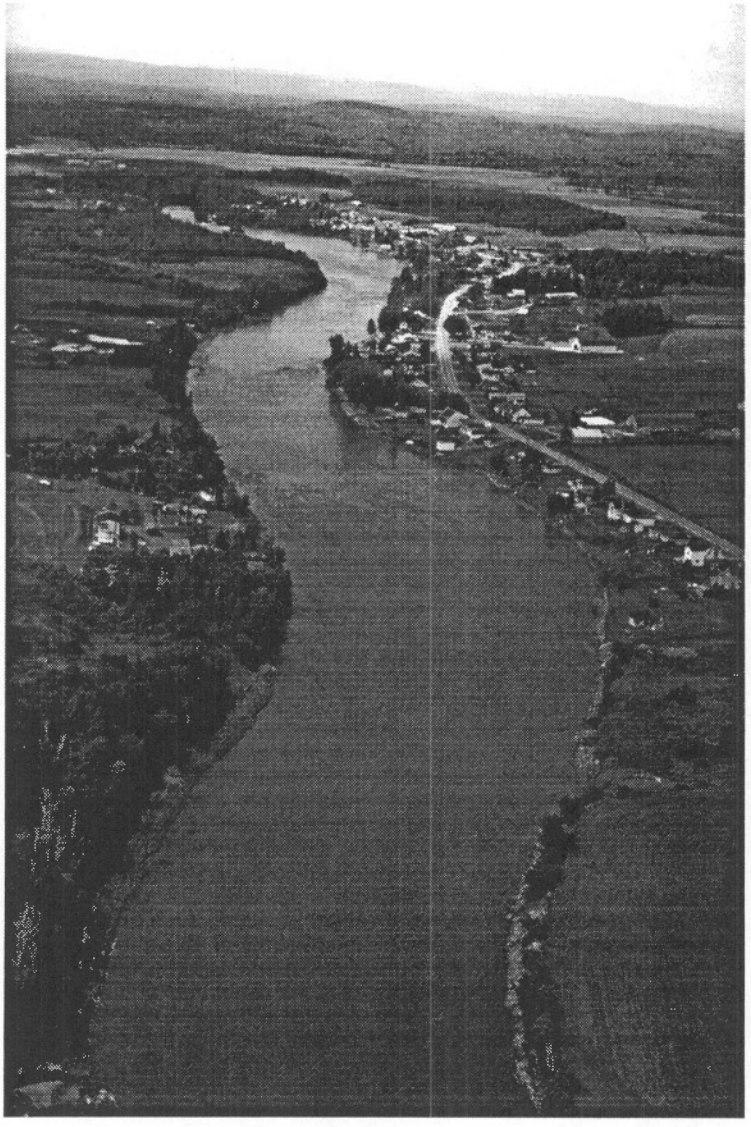

Fig. 7.8

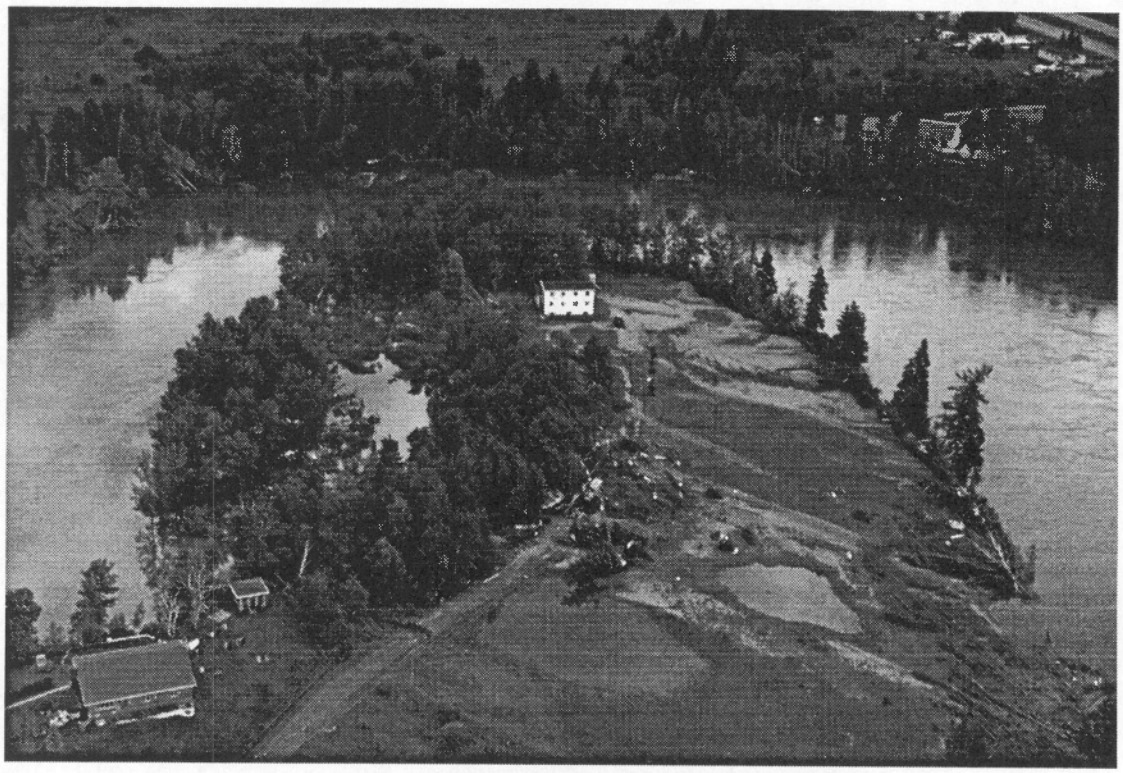

Fig. 7.9a

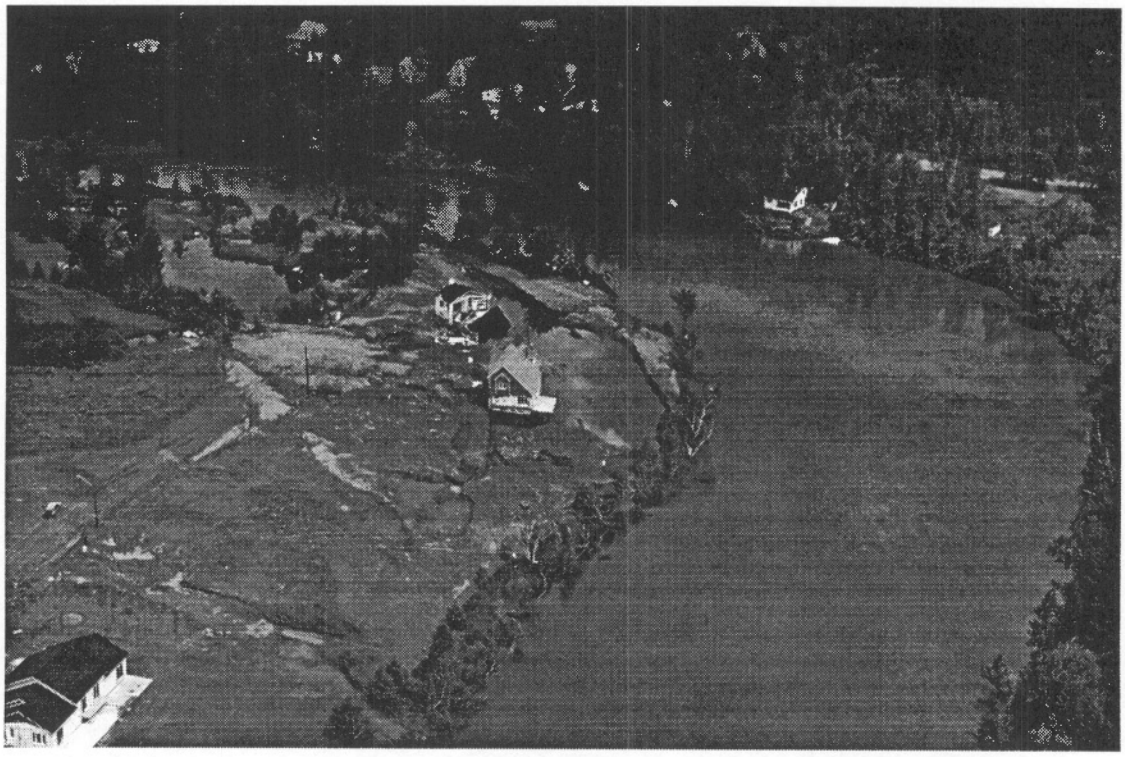

Fig. 7.9b

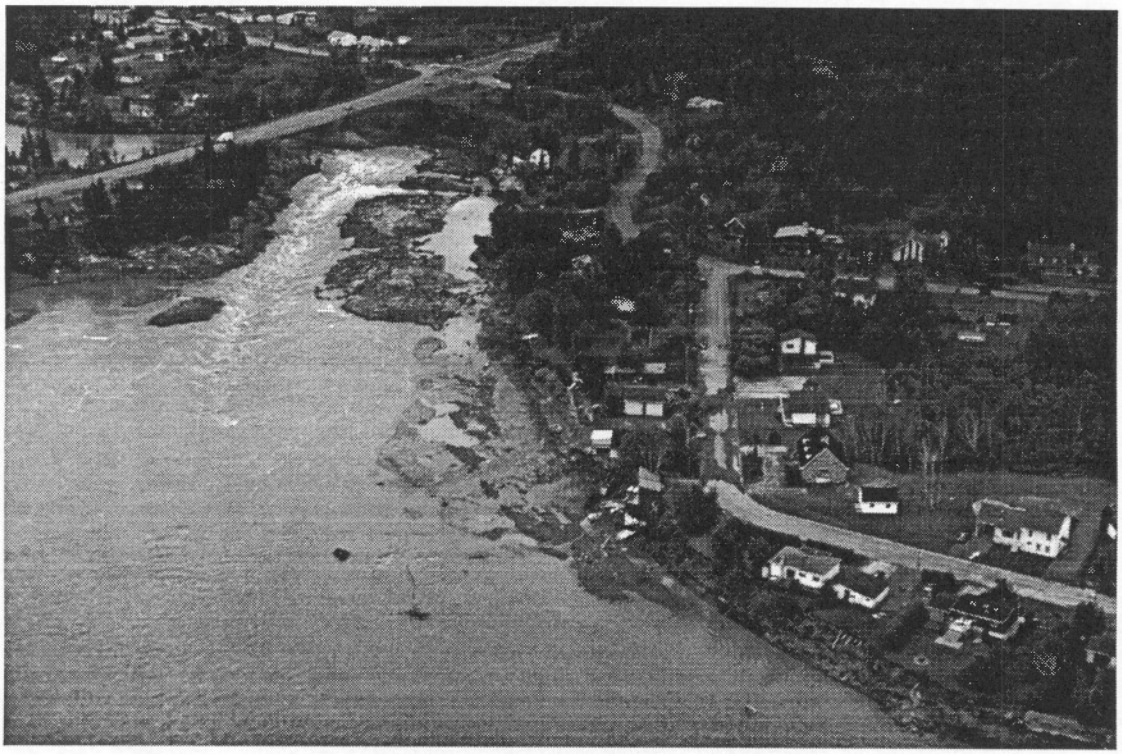

Fig. 7.10

8. RIVIÈRE À MARS

General

The study focuses on the lowest 10 km reach of Rivière à Mars where it flows across the lowland surface from the edge of the Laurentian Highlands to Baie des Ha!Ha! (Fig. 2.1). Along this reach, the river occupies a relatively straight stream-cut valley incised up to roughly 60 m into deltaic sands (upper 4.5 km) and marine sediment (lower 5.5 km) (Fig. 2.1). The valley bottom ranges from 200 m to 1200 m wide and consists of a 1-2 m high, wide floodplain, and various alluvial terraces, 3-10 m high.

Prior to the flood, the river meandered irregularly with a sinuosity of 1.2 (Fig. 8.1). The valley slope averages 0.012 between km 9.8 and the river mouth (Fig. 8.2). The gravel bed channel averages 20-40 m wide, but locally reaches 120 m wide (Fig. 8.1). Active point bars were present along the convex banks of many of the meanders; vegetated mid-channel bars and islands (observed on aerial photographs) occur within several clusters along the lower 6 km of the river that locally subdivide the channel. Numerous inactive (containing stagnant water) and abandoned (dry) channels, and channel scars (vegetated) are present on the floodplain along the study reach. The presence of the point bars, abandon and inactive channels and channel scars indicate collectively that the river is laterally unstable and experiences progressive lateral migration, channel abandonment, and avulsions. The channel morphology is generally characteristic of a meandering planform, but the presence of several separate multi-channeled reaches suggests that the planform is transitional between a meandering and braided morphology.

There is considerable settlement and infrastructure development along Rivière à Mars. The river is crossed by three major and one minor road bridges and two railway bridges. Numerous residences and a large trailer park are present on the floodplain between km 3.5 and 8.6. Major roads along the valley bottom, a railway line and many residences are situated above the floodplain on low terrace surfaces along the margins of the valley bottom (Fig. 8.1). A large residential-commercial-industrial development is present within the town of La Baie at the river mouth (Fig. 8.1). A fishway which forms a minor riffle in the river profile is present at km 2.9 while an abandoned dam with a small reservoir is present at the head of a canyon reach just above the upstream end of the study reach (Fig. 8.1).

Geomorphic effects of the flood

The combination of high discharge, relatively steep valley gradient and width of the flood flow along the lower 10 km of Rivière à Mars resulted in the flow energy (or unit stream power) exceeding the resistance of the valley bottom and largescale fluvial erosion ensued (see Baker and Costa, 1987; Kochel, 1988) This resulted in two major alterations of the morphologic character along the lower 10 km of Rivière à Mars. Most strikingly, the

channel width increased substantially, with the post-flood channel ranging from 50-380 m wide which locally is 1.3 to 19 times greater than the pre-flood morphology (Figs. 8.3 and 8.4). The largest amount of widening occurred between km 9.5 and 3.5 where the floodplain is widest and the pre-flood channel most sinuous, but significant widening also occurred along the more confined reaches both immediately upstream and downstream. Directly related to this widening, the immediate post-flood channel predominantly consisted of multi-channeled reaches flowing within the broad flood channel, a morphology that is consistent with a braided planform (Fig. 8.5). Thus, the flood has caused the river morphology to shift from a meandering (or transitional) to a braided planform.

The vast majority of the widening of Rivière à Mars resulted in the reworking of the floodplain and the erosion of terraces along the valley bottom margins. Only along the right bank at km 8.5-8.3 and 7.5 did lateral erosion impinge directly against and eroded the valleysides (Fig. 8.4). At both locations, this resulted in the cutbank erosion of a thick unit of deltaic sand and gravel that overlies marine sediment. The cutbank erosion at km 7.5 caused substantial retreat of the slope which undermined a railway bed located on the slope leaving the tracks suspended mid-air over a distance of about 125 m (Fig. 8.6)

The channel widening along Rivière à Mars occurred by several fluvial processes (as discussed below) that caused the erosion and dissection of the floodplain surface and erosion of terraces and, in isolates places, the valleysides. The processes are interrelated and apparent from the patterns of erosion, tracts of preserved floodplain, and close inspection of the pre- and post-flood aerial photographs. The overall widening of the river channel represents the coalescing of the erosion across valley bottom from these different processes.

The first process relates directly to concave erosion which is inherent to river meanders (Fig. 8.7). Although altered to considerably varying amounts, the basic morphology of a number of pre-flood meanders has been preserved at km 9.8, 7.8, 6.8, 2.9, and 2.5 (the distance referring to the meander apices). As depicted in Fig. 8.4, all have experienced considerable erosion along the concave banks resulting in the outward widening of the meander loop. In some cases, the post-flood apex of the outer bank has shifted slightly downvalley of the original position indicating that progressive downvalley translation of the meander form has accompanied the outward expansion (Figs. 8.3 and 8.4). Meander expansion and downvalley translation has also occurred where bends developed during the flood (e.g., right bank at 3.8 km; Fig. 8.4). Less obviously, major erosion to the outer banks of the channel occurred at several locations along the river that coincide approximately with the positions of many pre-flood meanders. These eroded areas are arcuate in shape and were probably formed during the earlier stages of the flood by the outward expansion and downvalley translation of original meanders which latter were obliterated by major local erosion of the floodplain. Examples of arcuate-shaped bank erosion which does not correspond to any post-flood meanders occur along the right bank

at km 4.8 km and the left bank at km 7.0, 6.6, and 5.9 (Fig. 8.4). Also, concave bank erosion probably occurred at the outer banks of sinuous channels along the multi-channeled sections that subsequently become obscured. Similarly, a concave style of bank erosion probably occurred elsewhere within the channel where flow became directed at a given bank because of deflection at channel junctions, or the presence of bars and other minor irregularities.

The second process of erosion pertains to the development of an avulsion whereby a cut-off channel forms across the floodplain surface behind the convex side of a meander. The best preserved example of this process is located on the left side of the flood channel at 6.8 km, where a cut-off channel now carries the entire flow of the river with the original channel left inactive (Figs. 8.3 and 8.4). A large tract of floodplain that was located immediately behind the convex bank of the original meander is preserved as a vegetated island within the flood channel.

Avulsions occur where floodwater overtops a bank and erodes a channel course into the floodplain surface. This can involve either the erosion of a new channel or the re-activation of an old channel scar. In either case, once formed, the gradient of the cut-off channel will be steeper than that around the meander loop because it is a shorter, more direct route down the valley, thus it will tend to increase in size and carry an increasingly larger portion of discharge at the expense of the initial channel. At some point the original channel may be abandoned with the entire flow being routed down the cut-off channel. Along Rivière à Mars, cut-off channels probably developed at meanders originally located at km 8.2 and 8.8 as indicated by preserved tracts of floodplain that occur as islands within the flood channel (Fig. 8.4). It is very likely that cut-off channels developed elsewhere along the study reach during the flood, but became subsequently obscured by the complete erosion of the local floodplain. Once a cut-off channel has formed, it functions like any other existing channel with erosion occurring along the concave banks as described above, or wherever flow is directed against the channel margin.

The final process is similar to the formation of cut-off channels, but does not result in the truncation a meander bend. It is caused by formation of a new channel or re-activation of an abandoned (vegetated) channel or channel scar, resulting in the erosion and dissection of the floodplain surface. The best preserved example of this process is located along the right side of the river between 3.5 and 4 km where a broad secondary flood channel is present on the floodplain (Fig. 8.8). This channel evidently is preserved at an early stage of formation since some parts of the channel surface have experienced erosion and other parts deposition.

As with the cut-off channel, once established, the margins of the new or re-activated channels would be subject to erosion along the concave banks or wherever flow was directed against the banks. The extent to which channel formation or re-activation is responsible for eroding the floodplain along Rivière à Mars is difficult to ascertain because of the widespread erosion of the floodplain.

The flooding and extensive erosion along the Rivière à Mars floodplain caused the inundation, damage and destruction of numerous residences (permanent, seasonal and trailers) located along both sides of the river, between km 8.6 and 3.5 (Fig. 8.9a). Within La Baie a residential-commercial area along the left side of the river was inundated. Localized bank erosion of terraces damaged and destroyed homes by undermining, but also severed both the main road and a railway line along the left side of the valley bottom in several places (Fig. 8.9b). This damage is especially notable because, in many instances, the terrace surfaces were not inundated and thus the damage relates exclusively to bank erosion. As mentioned above, cutbank erosion of the valleyside at km 7.5 undermined the bed of the railway tracks leaving the track and ties suspended in mid-air (Fig. 8.7b). Bank erosion along one of the abutments caused the collapse or damage to two railway and three road bridges crossing the river (Fig. 8.9c).

Fig. 8.1 (see POCKET) Map of the lower 10 km of Rivière à Mars showing the locations of major communities, roads, and bridges. The scale (in blue) following the river marks kilometer distance allowing locations mentioned in the text to be keyed to the map. See Fig. 1.2 for the location of the map.

Fig. 8.2 Longitudinal profile of the lower about 10 km of Rivière à Mars (data from 10 m contour lines on Québec Ministère de L'Energie et des Ressources map 'La Baie' (22D02-200-0101), 1:20 000 scale).

Fig. 8.3 Aerial photographs of the Rivière à Mars between km 9.5 and 6.4 a) pre-flood taken on May 24, 1994 (Photocartothèque québécoise HMQ94-119 -230) and b) post-flood taken on July 30, 1996 (Photocartothèque québécoise Q96304-47).

Fig. 8.4 Maps showing a) the pre-flood and b) post-flood channel width of Rivière à Mars. The pre-flood width is based on Québec Ministère de L'Energie et des Ressources map 'La Baie' (22D02-200-0101), 1:20 000 scale. The post-flood width was obtained from tracing a rectified mosaic of multi-spectral video images acquired on August 6, 1996 (courtesy of Canada Centre for Remote Sensing). The scale following the river in b) marks kilometer distance allowing post-flood characteristics of the channel that are discussed in the text to be keyed to the map.

Fig. 8.5 The post-flood Rivière à Mars looking downstream of km 4.2 (Fig. 8.4), showing the braided morphology of the river and the wide flood channel. Photograph taken on July 27, 1996 (GSC photograph 1997-42X).

Fig. 8.6 Railway tracks at km 7.5 (Fig. 8.4) suspended mid-air because of undermining by cutbank erosion of the valleyside. Photograph taken on July 27, 1996 (GSC photograph 1997-42Y).

Fig. 8.7 Concave bank erosion at a) the bend at km 9.8 (Fig. 8.4), where a road along the outer bank has been severed (GSC photograph 1997-42Z), and b) the bend at km 7.8 (Fig. 8.4), where a railway bridge has collapsed because of erosion of the left abutting bank (GSC photograph 1997-42AA). Photographs taken on July 27, 1996.

Fig. 8.8 A broad secondary channel on the right side of the flood channel which is the result of overflow on, but only partial erosion into the floodplain. The view of the river is downstream of km 4.1. Photograph taken on July 27, 1996 (GSC photograph 1997-42BB).

Fig. 8.9 Examples of flood damage along Rivière à Mars: a) undermined and displaced home resting on a bar in the flood channel at km 8.3 (Fig. 8.4; GSC photograph 1997-42CC), b) homes located on a terrace surface at km 4.6 undermined by lateral bank erosion (Fig. 8.4; GSC photograph 1997-42DD), and c) collapsed bridge caused by

erosion of left abutting bank at km 2.8 (Fig. 8.4; GSC photograph 1997-42EE). All photographs taken on July 27, 1996.

Fig. 8.1 see POCKET

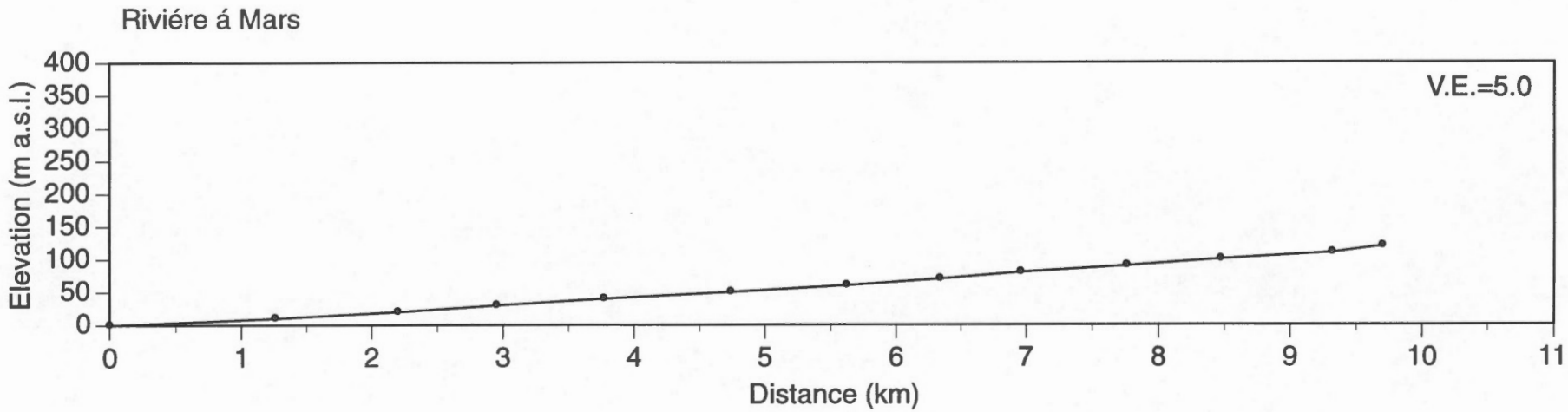
Riviére á Mars
V.E.=5.0
Elevation (m a.s.l.)
400
350
300
250
200
150
100
50
0
0
1
2
3
4
5
6
7
8
9
10
11
Distance (km)

Fig. 8.2

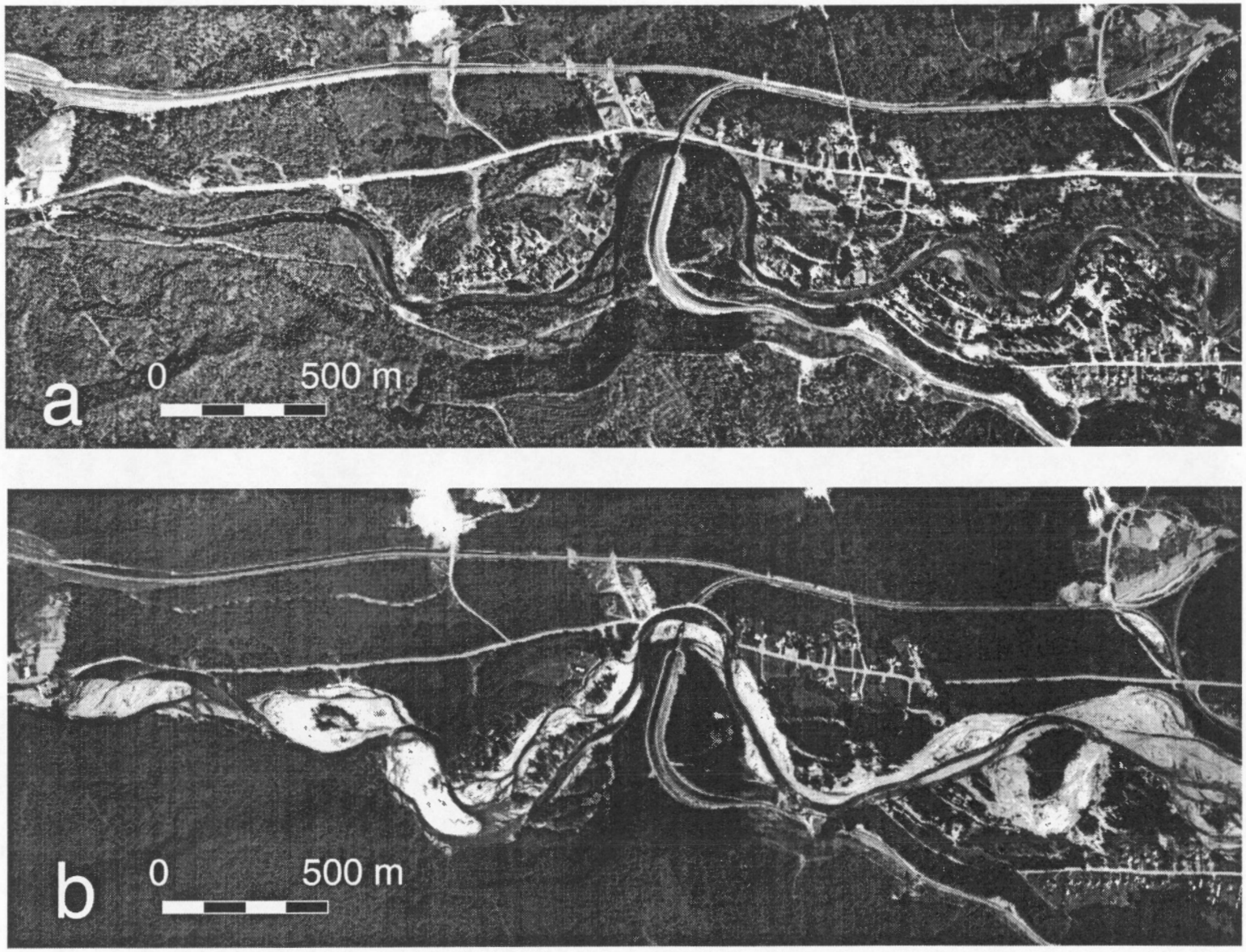

Fig. 8.3

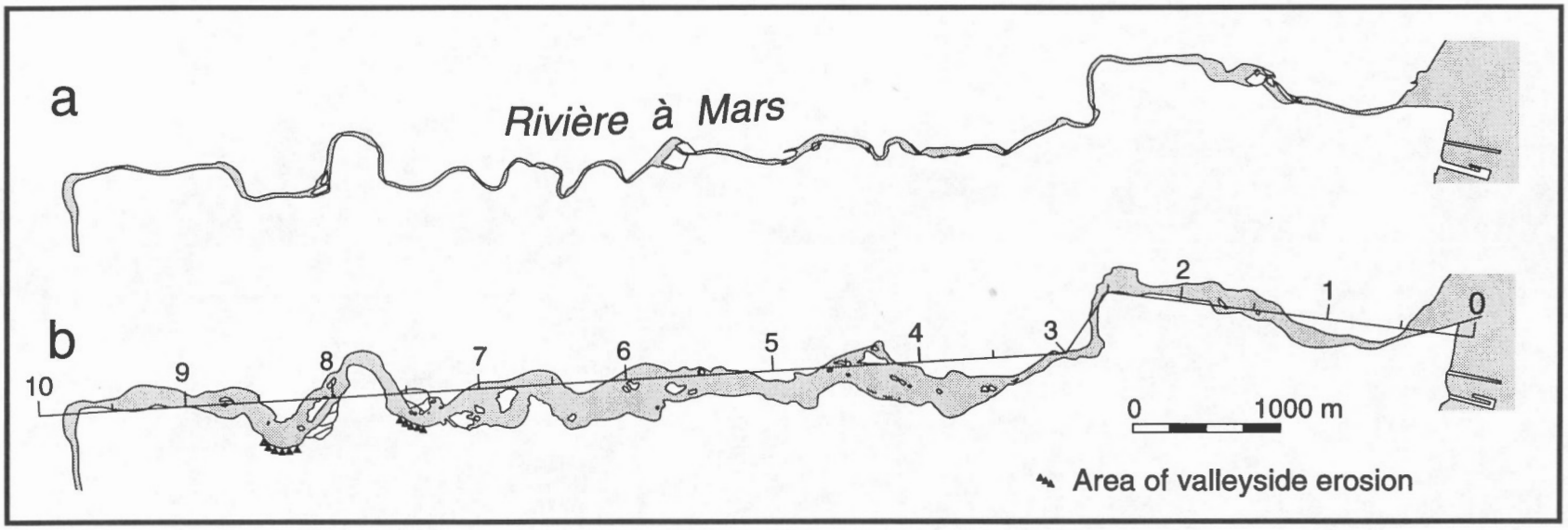
a
Rivière à Mars
b
10
9
8
7
6
5
4
3
2
1
0
0
1000 m
Area of valleyside erosion

Fig. 8.4

Fig. 8.5

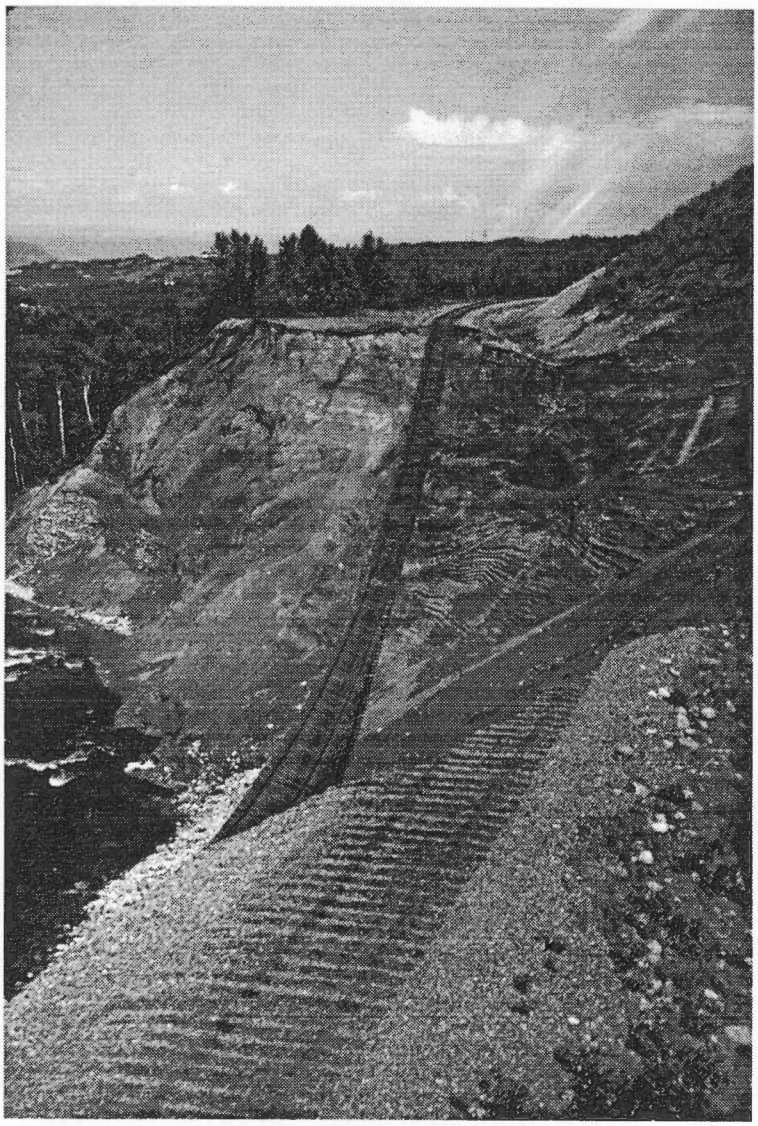

Fig. 8.6

Fig. 8.7a

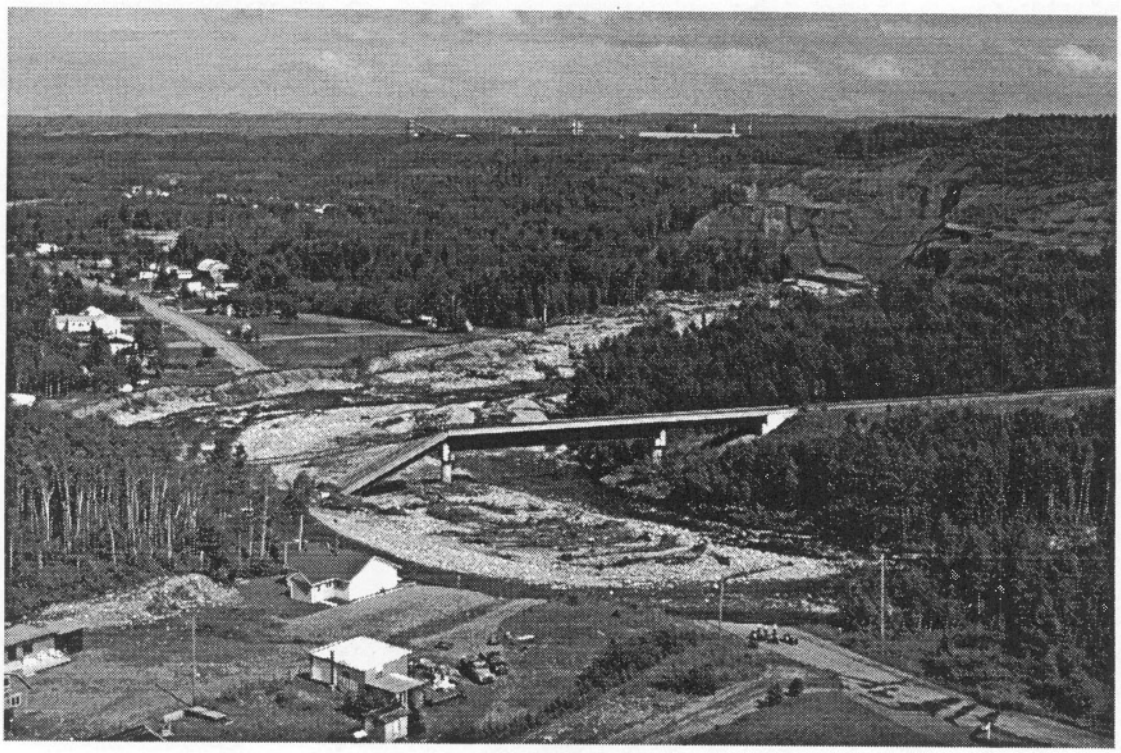

Fig. 8.7b

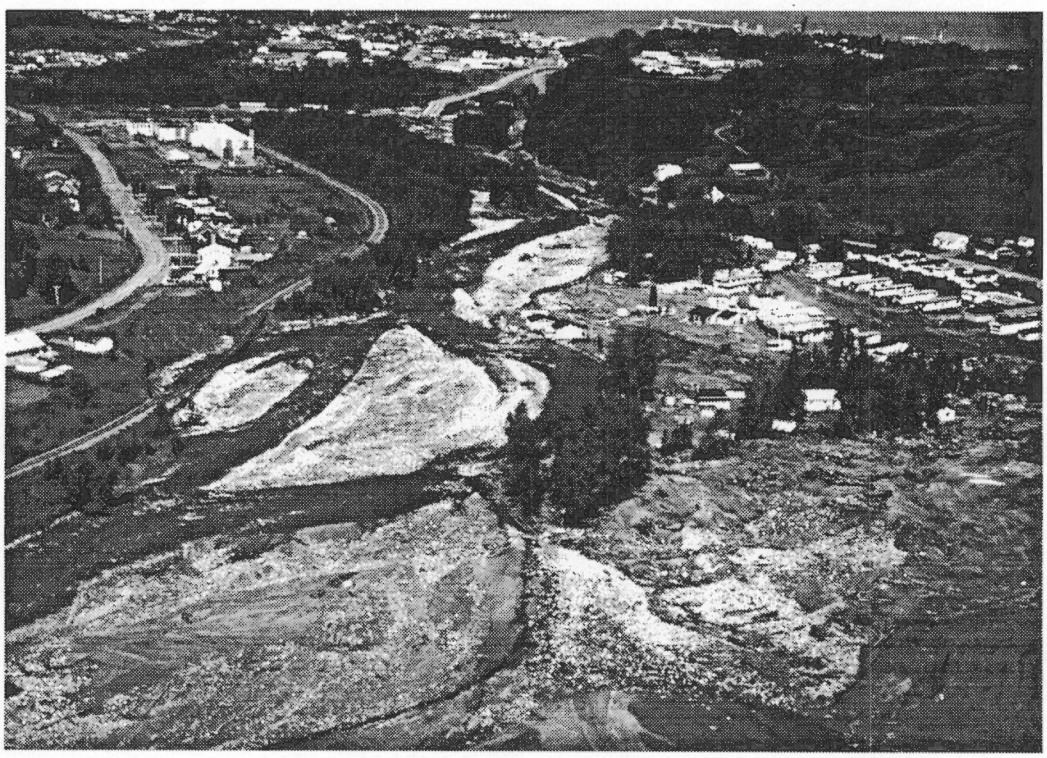

Fig. 8.8

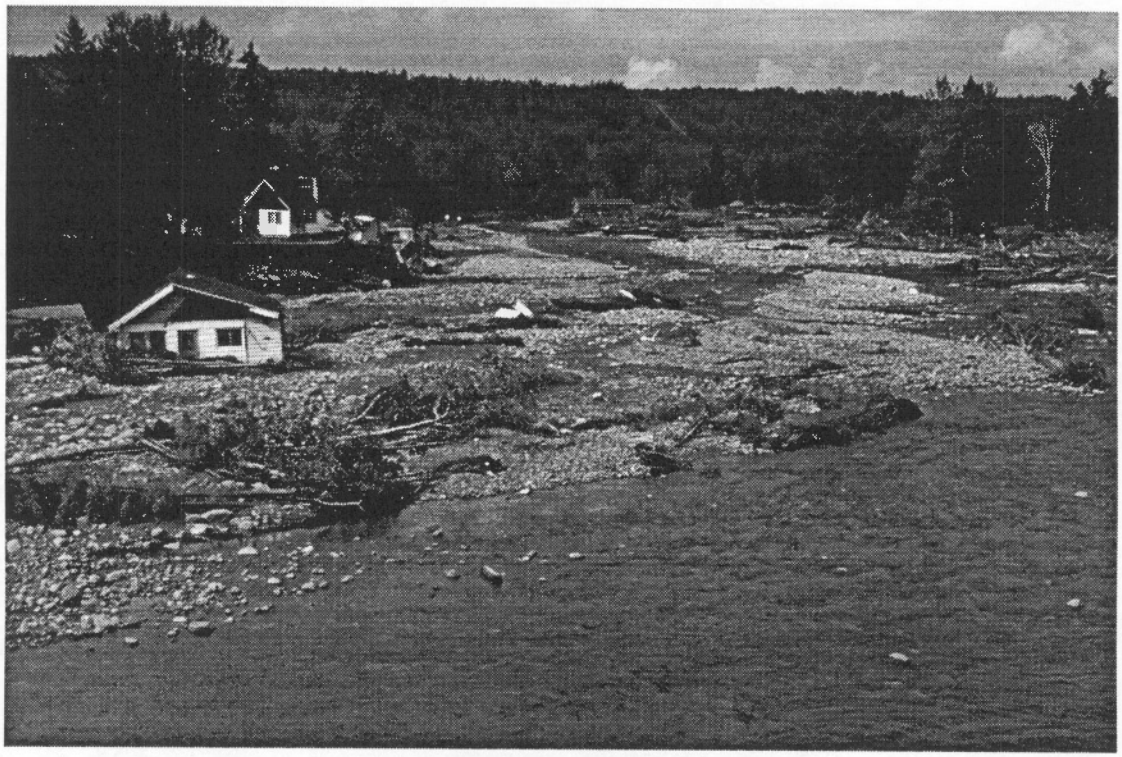

Fig. 8.9a

Fig. 8.9b

Fig. 8.9c

9. RIVIÈRE DES HA!HA!

General

Flooding along Rivière des Ha!Ha! severely affected a 35 km length of valley bottom extending from Lac Ha!Ha! to the river mouth (Fig. 9.1). As discussed above (see *Hydrology section*), flooding along Rivière des Ha!Ha! was accentuated by the breaching of a saddle dyke that caused the uncontrolled drainage of Lac Ha!Ha!.

The pre-flood Rivière des Ha!Ha! exhibited a varied morphologic character over its 34 km length, consisting of alluvial, non-alluvial and short bedrock reaches. Although the flood affected the entire length of river from Lac Ha!Ha! to the river mouth, this summary focuses on those sections where there were direct impacts on adjacent communities (see Fig. 1.2). Thus, there is a gap in the descriptions and maps between km 27 and 10.5 where the areas adjacent to the river are uninhabited. The remaining portions of the river are described in three segments that are referred to by kilometer distance measured upstream from an arbitrary point just beyond the river mouth. The segments are described in separate sections that summarize the pre- and post-flood river morphologies, beginning with the upstream segment.

Geomorphic effects of the flood

km 35-27 segment

Pre-flood

The segment from km 35-27 forms the upper part of Rivière des Ha!Ha! extending below Lac Ha!Ha! reservoir (Fig. 9.1). The described length of river pertains specifically to the reach situated immediately downstream of the confluence at km 33 where the post-flood river channel meets the pre-flood outlet channel that previously drained the lake (Fig. 9.1). Below this confluence, the river follows a lowland valley within the Laurentian Highland. The valley bottom consists of alluvial floodplain and undulatory non-alluvial surface. The valley gradient between km 33.3 and 27 averages 0.0017 (Fig. 9.2).

The pre-flood river exhibited an irregular meandering planform with a sinuosity of 1.3 and channel 20-40 m wide. There were no active bars nor vegetated islands present along the river suggesting that the channel was laterally stable. The floodplain ranges from roughly 80 to 400 m wide, the wider section occurring where several successive well-developed meanders are present (Fig. 9.1). A large lowlying area branches from the Rivière des Ha!Ha! floodplain between km 29.5-30, where a minor tributary flows across the valley bottom from the west. The floodplain is heavily vegetated with either grass or forest cover.

The hamlet of Boilleau is located along the river between km 32-28 adjacent to a major road that follows the left side of the valley (Fig. 9.1). A number of homes located beside the road are situated on the floodplain and lowlying areas of the valley bottom.

Post-flood

The km 35-27 section of the river was severely impacted by the flood. Most strikingly was the formation of a new outlet of Lac Ha!Ha! and 2 km long channel that joins the pre-flood channel at km 33 (Fig. 9.1a). The outlet and new channel formed because of overtopping and erosion of a dyke and the underlying surficial material, by rising Lac Ha!Ha! waters (see *Drainage of Lac Ha!Ha! reservoir* section).

The channel extending below the new lake outlet joins the pre-existing channel at km 33 (Fig. 9.1). It ranges from 60 to 170 m wide which is locally 3 to 8 times wider than the pre-flood channel immediately below km 33. The continued function of the new outlet and channel will be shortlived as Consolidated Stone Corporation, the owner of the eroded dyke, is undertaking the construction of a new dyke across the mouth of the outlet to restore Lac Ha!Ha! to its pre-flood level. The new dyke is expected to be completed by the end of December 1996 (Emile Soucie, pers. comm., November 13, 1996).

Downstream of km 33, the flood wave swept across the valley bottom, but generally caused negligible erosion of the pre-flood channel margins and the inundated areas of the forest and grassland surfaces. Along the low sinuosity reaches of the river (km 33-30 and 29-28), very localized bank erosion occurred causing minor channel widening, the best of example of which is present at km 31.4 (Fig. 9.1b and c). Large tracts of forest on the floodplain were knocked over between km 29.9-29 and at km 27 (Fig. 9.1b and c), where the flood wave crossed the surface of several well-defined meanders (Figs. 9.3 and 9.4). The most significant erosion occurred at km 33 where the floodplain was partially dissected, and at km 27 where an elongated scour hole 35 m wide and 150 m long, was eroded into the floodplain (Fig. 9.4). The scour hole development at km 27 represents an intermediate stage of the meander cutoff process which likely would have eventually caused the 'blowing out' of the meander had the flood wave been sustained for a longer period of time.

In contrast to the lack of erosion along this segment of the river, extensive deposition occurred on much of the inundated areas of the valley bottom, particularly between km 32.8-32 and 30.5-29 where up to about 2 m of sediment were deposited (Fig. 9.1b and c). These deposits form broad silt-very fine sand sheets that aggraded wide, lowlying areas where the flood waters spread across of the valley bottom (Figs. 9.1b, c, and 9.5). Deposition also occurred along the narrower parts of the valley bottom and within the forested areas of the floodplain where the vegetation contributed to the trapping of sediment. Overall, the considerable aggradation that occurred below km 33 reflects a combination of several factors: the gentle valley gradient and the high resistance to flow of the vegetative cover(s) both of which limited local flow velocities thus promoting

deposition of entrained sediment; and, perhaps most importantly, the large amount of sediment derived from the erosion of the new lake outlet and associated channel immediately upstream that was thus available for deposition.

Numerous residences within the hamlet of Boilleau located on low-lying areas adjacent to the river were damaged to varying degrees by flood water. Extensive damage also occurred to property by deposition of silt and sand on roads, lawns and fields (Fig. 9.1b and c). The formation of the channel below the new lake outlet washed-out the main road which provides access to the upper area of the watershed and a secondary road crossing the valley bottom at km 33.2.

km 10.5 to 4.5 segment

Pre-flood

Most of the km 10.5 to 4.5 segment of Rivière des Ha!Ha! is confined within a narrow, relatively straight valley bottom with a sharp bend occurring at km 5. The lower valleysides consist primarily of alluvium overlying Quaternary sediments (diamicton/marine sediment), except at km 6 where bedrock is exposed along the left bank. A narrow floodplain/terrace is present along the river between km 10.5 and 5. Below km 5.0, the river flows within a narrow bedrock canyon ending at km 4.5. In contrast to this confined morphology, two successive meanders occur within a broad floodplain in the upper part of the segment at km 10.5-10 (Fig. 9.1).

The pre-flood river channel ranged from 20-50 m wide. The valley gradient averages 0.002 between km 12.7 and 7.9, then steepens gradually downstream through to the bottom of the canyon (Fig. 9.2). No active bars were present along the 10-4.5 km reach, but a vegetated island was present at about km 5 (subsequently destroyed in flood). The pre-flood channel was laterally stable. At the two meanders situated at km 10.5-10, no lateral migration was detected on post-1962 aerial photograph, but scars on the floodplain are indicative of past progressive lateral migration.

A number of houses are present on the narrow floodplain/terrace surface or the lower part of the valley side between km 10.5-6, particularly along the right side of the river. Access to the homes is provided by roads also constructed on the floodplain/terrace surface, and bridges at about 6.9 km and 9.7 km (both washed-out during the flood). A small hydro-electric dam is located just above the canyon at 5 km with the powerhouse situated at the base of the canyon on the left bank at km 4.5.

Post-flood

The effects of flooding along the km 10.5 to 4.5 segment were considerably different upstream and downstream of km 7.8, reflecting the change in valley gradient (Fig. 9.2). Upstream at km 10.5-10, the flood wave inundated the broad, low-lying area adjacent to

the two meanders (see above) depositing a large sheet of sand up to several metres thick, particularly along the right valleyside (Figs. 9.1d, 9.6 and 9.7). The pre-flood meanders seem to have been cut-off during the flood causing a reduction in local sinuosity from 1.6 to 1.2 (Fig. 9.6). However, an inspection of oblique aerial photographs indicates that aggradation of the channel occurred in this area suggesting that the original meanders may, in fact, be preserved buried beneath flood alluvium.

Aggradation, representing the downstream extension to that present at km 10.5-10, is present downstream below km 10 where the river becomes confined within a narrow linear section of valley bottom and closely follows the pre-flood channel course. Up to several metres of sand aggraded the valley bottom adjacent to the river burying vegetation and road(s) (Fig. 9.8). The sand deposit thins gradually downvalley, disappearing by about km 8, although it persists downstream within areas of thick vegetation cover beside the river and the road. Channel incision begins abruptly at km 7.8, as discussed below (Figs. 9.1e and 9.9). Between km 10-7.8, very little erosion of the valley margins occurred and the pre-flood channel margins are generally well-preserved. However, in places, trees growing on the valley bottom were knocked over and damaged, and large asphalt slabs of the road (up to several metres long) were displaced by the flow.

Beginning at km 7.8 and extending downstream to the top of the canyon at km 5, the pre-flood channel was extensively eroded causing widening and deepening of the channel (Figs. 9.1e and 9.10). This erosion becomes more extensive downstream to about km 6 and has completely destroyed the pre-flood alluvial surface, forming a 'gorge' incised up to about 15 m into the late Pleistocene deposits along the valley bottom. Below 6 km, channel widening was more extensive than incision. A meander was washed-out at km 5.8. Between km 7.8 and 5, the post-flood channel ranged from 50 to 95 m wide along the straight reaches of valley representing local increases of 1.6 to 5 times the pre-flood channel width. The post-flood river flows on a surface consisting of either, or a combination of bouldery alluvial lag and exposed glacigenic diamicton with some minor areas of exposed bedrock (Fig. 9.10). Downstream along the canyon (km 5-4.5), the bedrock was extensively scoured by the flood water removing the vegetation cover (Fig. 9.11).

The transition from deposition to erosion along the valley bottom which occurred at approximately km 7.8 is notable because it corresponds with the steepening of valley slope (Fig. 9.2). Between km 10 and 6, if it can be assumed that the discharge, flow width and, valley bottom materials and roughness of this quite uniform reach of valley are sensibly constant, the increase in valley slope appears to be the critical variable which pushed the flow energy (or unit stream power; see Baker and Coast, 1987; Kochel, 1988) across an erosive threshold allowing largescale erosion of the valley bottom to take place. This erosion extended downstream to the river mouth and probably continued to be controlled by the valley slope which remains relatively steep (despite some variation). However, changes in the other variables complicate the picture downstream of km 6.

Between km 10.5-7.8, the road, numerous homes and property were damaged or destroyed by inundation and/or sedimentation (Fig. 9.7). Below 7.8 km, numerous homes were damaged or destroyed by undermined because of bank erosion (Fig. 9.10). Bridges were washed out at km 9.7 and 6.9. A small dam located at km 5 was breached and the reservoir partially aggraded with sediment. The powerhouse situated at km 4.5 was destroyed (Fig. 9.11).

km 4.5 to the river mouth segment

Pre-flood

Between km 4.5 and the river mouth, Rivière des Ha!Ha! flows within a stream-cut valley incised up to about 50 m into marine and deltaic sediments (Fig. 2.1). A floodplain is present below km 4.5 with an irregular width ranging from roughly 70 to 250 m wide. The adjacent valley bottom is heavily vegetated with either grass or forest cover. The margins of the floodplain abut directly against the lower valleysides between km 4.5-3.2 and against primarily relatively low terraces below km 3.2 to the river mouth. The valley slope averages 0.022 (Fig. 9.2). The valley bottom (and floodplain) is much narrow upstream of km 3.2 than downstream.

The entire lowest segment of the river is alluvial. The pre-flood channel followed an irregular meandering course with a sinuosity of 1.2. The gravel bed channel alternates between single channeled and divided reaches, the latter flowing around small islands representing stabilized mid-channel bars. The channel morphology, thus, seems to exhibit a transitional meandered-braided planform. River width along the single channeled reaches ranges from 20 to 60 m wide while along the divided channels it ranging from 50 to 110 m wide. A visual comparison of aerial photographs taken in 1962 and 1974 revealed that the channel had been laterally stable during this time period. No fresh point bars were present along the convex banks, but abandoned channels were occasionally present.

Considerable development is present along the lower 4.5 km of Rivière des Ha!Ha!. A large residential and commercial area is located on the floodplain and alluvial terraces along the lower 1 km of the river within the city of La Baie (specifically Grande-Baie). A major road extends along the left side (northside) of the valley located primarily on a discontinuous alluvial terrace. Along this road are a number of homes and several farms. In La Baie, the river is crossed by two bridges. A small hydroelectric dam complex is located at km 1.8.

Post-flood

The flood caused extensive geomorphic change along the lower 4.5 km of the river (Fig. 9.12). Between km 4.5-3.2, widening and deepening of the river destroyed the pre-flood channel, similar to what occurred upstream between km 7.8 and 5. In places, the alluvium was completely stripped and the river now flows on exposed marine sediments (Fig.

9.13). The post-flood channel ranges from 70-200 m wide which locally is 1.5-4 times the pre-flood width (Fig. 9.12), despite being restricted by the relatively narrow valleysides. The most extensive widening occurred at the bend located at 4 km where flow was concentrated along the concave bank (Fig. 9.12). Relatively deep channel incision occurred at km 3.5-3.2 due to the development and retreat of a knickpoint within the exposed marine sediment. The knickpoint was still present on July 29, forming an abrupt 3-5 m waterfalls in the river profile (Fig. 9.14).

Below km 3.2, the flood caused in major widening of the river channel due to extensive erosion of the floodplain and low terrace surfaces (Fig. 9.1f, 9.12 and 9.15). Here, the post-flood channel ranges from 80 to 320 m wide which locally is 4 to 10 times wider than the pre-flood channel (Fig. 9.12). The post-flood channel morphology, in places, is multi-channeled and forms a braided planform. Major widening also occurred adjacent to a small dam located at km 1.8 where overflow of the abutting left bank resulted in major incision of the floodplain forming a channel which now carries the river flow beside and lower than the dam (Fig. 9.16). This erosion drained the small reservoir, damaged the dam, severed penstocks, and destroyed the powerhouse.

Comparison of pre- and post-flood aerial photography indicates that several processes were responsible for the extensive channel widening below km 3.2. Several arcuate zones of erosion along the lower flood channel margins which correspond approximately to the pre-flood meanders positions indicate that the meanders have undergone considerable lateral expansion and downvalley translation (Fig. 9.1f). Since none of the original meanders are preserved, this suggests that they were later cut-off by flood waters spilling over the banks and, crossing and eroding into the floodplain. After the formation of the cut-off channels, the intervening floodplain probably was reworked by subsequent lateral channel migration, eventually resulting in the coalescing of channels to form a broad single 'flood' channel along the valley bottom. The floodwaters also likely induced the reactivation of abandoned and inactive channels which also underwent lateral migration.

At the river mouth, sediment derived from erosion upstream was deposited as a broad sheet on the tidal flat, the subaerial extent of which was considerably increased at low tide (Fig. 9.17). Debris from buildings destroyed by flooding and bank erosion upstream were also carried out and deposited on the tidal flat.

The extensive reworking of the floodplain and lateral erosion into terrace surfaces by flood waters resulted in severe damage and destruction to homes, businesses and infrastructure along the lower Rivière des Ha!Ha! between km 3.1 and the river mouth. Immediately upstream of the village of La Baie, most homes and roads were situated along the left side of the valley on a terrace surface above the maximum level of the flood. Despite this, extensive bank erosion resulted in the loss by undermining of numerous homes, a dairy farm (including barn and silo) and severed of the road in several places (Fig. 9.15). The dam located at km 1.8 was severely damaged, as mentioned above (Fig. 9.16). Within La Baie, extensive damage to residential and commercial areas located on

terrace and floodplain surfaces was caused by inundation and/or undermining (Fig. 9.17). The road approaches to two bridges were washed-out.

Fig. 9.1 (see POCKET) Map of Rivière des Ha!Ha! extending from Lac Ha!Ha! to Baie des Ha!Ha! showing the locations of major communities, roads, bridges, and dams. The scale (in blue) following the river marks kilometer distance allowing locations mentioned in the text to be keyed to the map. The geomorphic effects of the flood are depicted by representative multi-spectral video images (a to f) of the valley bottom acquired on August 6, 1996 (Courtesy of Canada Centre for Remote Sensing). See Fig. 1.2 for the location of the map.

Fig. 9.2 Longitudinal profile of Rivière des Ha!Ha! (data from 10 m contour lines on Québec Ministère de L'Energie et des Ressources maps 'La Baie' (22D02-200-0101), 'Ferland' (22D02-200-0201) and 'Boilleau' (22D07-200-0101), 1:20 000 scale). The location of the dams are shown although the change in water surface at these locations may fall between contour line intervals. The three segments of river discussed in the manuscript are also shown.

Fig. 9.3 Trees on floodplain knocked over by flood water a) at km 33 (GSC photograph 1997-42FF) and b) viewed upvalley from km 29.2 (GSC photograph 1997-42GG). Photographs taken on July 28, 1996.

Fig. 9.4 An elongated scour hole eroded by overbank flow across a meander at km 27.5 (GSC photograph 1997-42HH). Also note the trees on the floodplain knocked down by the flood water. Photograph taken on July 28, 1996.

Fig. 9.5 Overbank deposition on broad, low-lying areas of the valley bottom viewed upstream from a) km 32.2 (GSC photograph 1997-42II)and b) km 29.6 (GSC photograph 1997-42JJ). Photographs taken on July 28, 1996.

Fig. 9.6 Aerial photographs of the meanders located at km 10.5-10 a) pre- (June 5, 1994; Photocartothèque québécoise HMQ94-126-208) and b) post-flood (July 30, 1996; Photocartothèque québécoise Q96304-68). Note the change in channel position and increased channel width in the post-flood photograph relative to the pre-flood photograph.

Fig. 9.7 Extensive sand aggradation along the right side of the valley at km 10.5-10. Photograph taken on July 28, 1996 (GSC photograph 1997-42KK).

Fig. 9.8 Sand deposited along the margins of the valley bottom adjacent to river looking upstream of km 8. Photograph taken on July 28, 1996 (GSC photograph 1997-42LL).

Fig. 9.9 The incised and widened river channel extending downstream below 7.8 km. The transition from non-erosion to erosion is located just upstream of this view. Photograph taken on July 28, 1996 (GSC photograph 1997-42MM).

Fig. 9.10 The incised and widened channel looking upstream of km 6.1. Exposed diamicton and bedrock, and bouldery lag form the perimeter of the channel. Note the homes damaged by undermining along the right bank. Photograph taken on July 28, 1996 (GSC photograph 1997-42NN).

Fig. 9.11 Scoured bedrock along the canyon located at km 5-4.5. In the foreground along the left bank (lower centre-right side of picture) is a powerhouse severely damaged during the flood. Photograph taken on July 28, 1996 (GSC photograph 1997-42OO).

Fig. 9.12 Maps showing a) the pre-flood and b) post-flood channel width of Rivière des Ha!Ha!. The pre-flood map is from Québec Ministère de L'Energie et des Ressources map 'La Baie' (22D02-200-0101), 1:20 000 scale. The post-flood map was obtained from tracing of a rectified mosaic of multi-spectral video images acquired on August 6, 1996 (courtesy of Canada Centre for Remote Sensing).

Fig. 9.13 Post-flood channel at about km 4.2 where the pre-flood alluvium has been stripped exposing the underlying marine sediment. Photograph taken on July 28, 1996 (GSC photograph 1997-42PP).

Fig. 9.14 Incised channel below km 3.5 produced by knickpoint erosion into marine sediment. Photograph taken on July 28, 1996 (GSC photograph 1997-42QQ).

Fig. 9.15 The broad post-flood channel of Rivière des Ha!Ha! viewed downstream from km 3. Note the extensive reworking of the floodplain and lateral erosion into low terrace surfaces along the valley side. Photograph taken on July 28, 1996 (GSC photograph 1997-42RR).

Fig. 9.16 The new channel situated adjacent to the dam located at km 1.8 (centre-right of photograph). Photograph taken on July 28, 1996 (GSC photograph 1997-42SS).

Fig. 9.17 Tidal flats at the river mouth looking upstream into the Rivière des Ha!Ha! valley. Note the debris from destroyed buildings on the tidal flats. The flood resulted in considerable damage to residential and commercial areas within La Baie at the river mouth. Photograph taken on July 28, 1996 (GSC photograph 1997-42TT).

Fig. 9.1 see POCKET

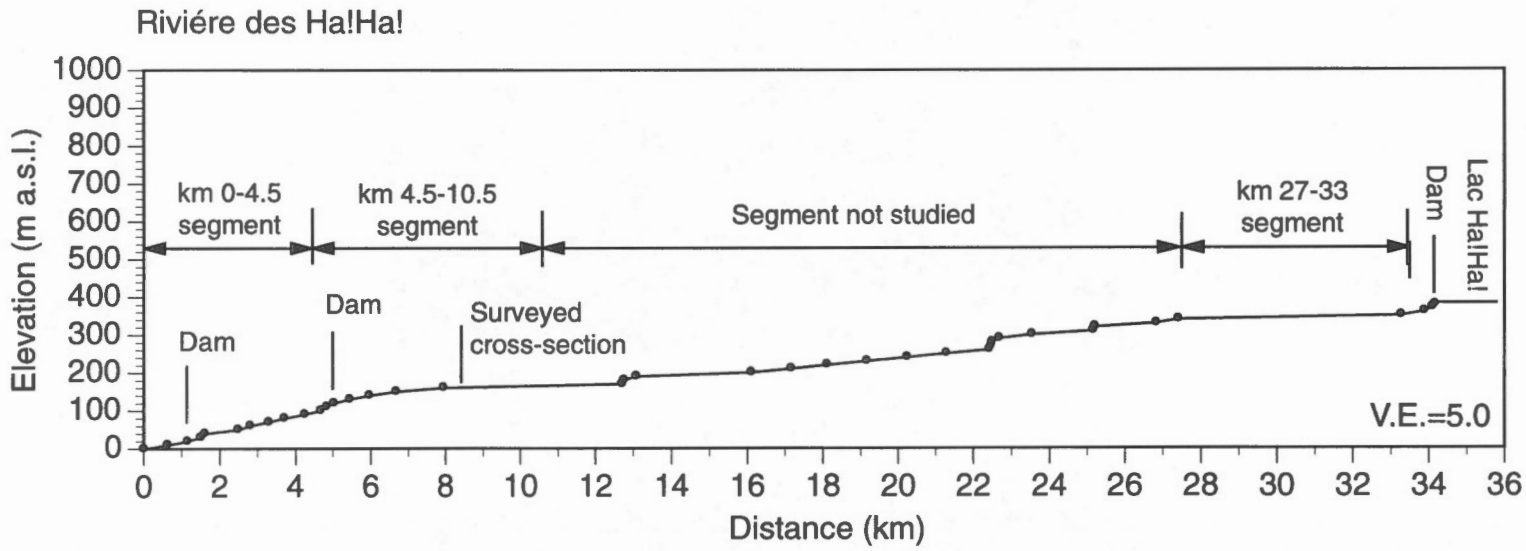
Riviére des Ha!Ha!
Elevation (m a.s.l.)
1000
900
800
700
600
500
400
300
200
100
0
km 0-4.5 segment
km 4.5-10.5 segment
Segment not studied
km 27-33 segment
Dam
Lac Ha!Ha!
Dam
Dam
Surveyed cross-section
V.E.=5.0
0
2
4
6
8
10
12
14
16
18
20
22
24
26
28
30
32
34
36
Distance (km)

Fig. 9.2

Fig. 9.3a

Fig. 9.3b

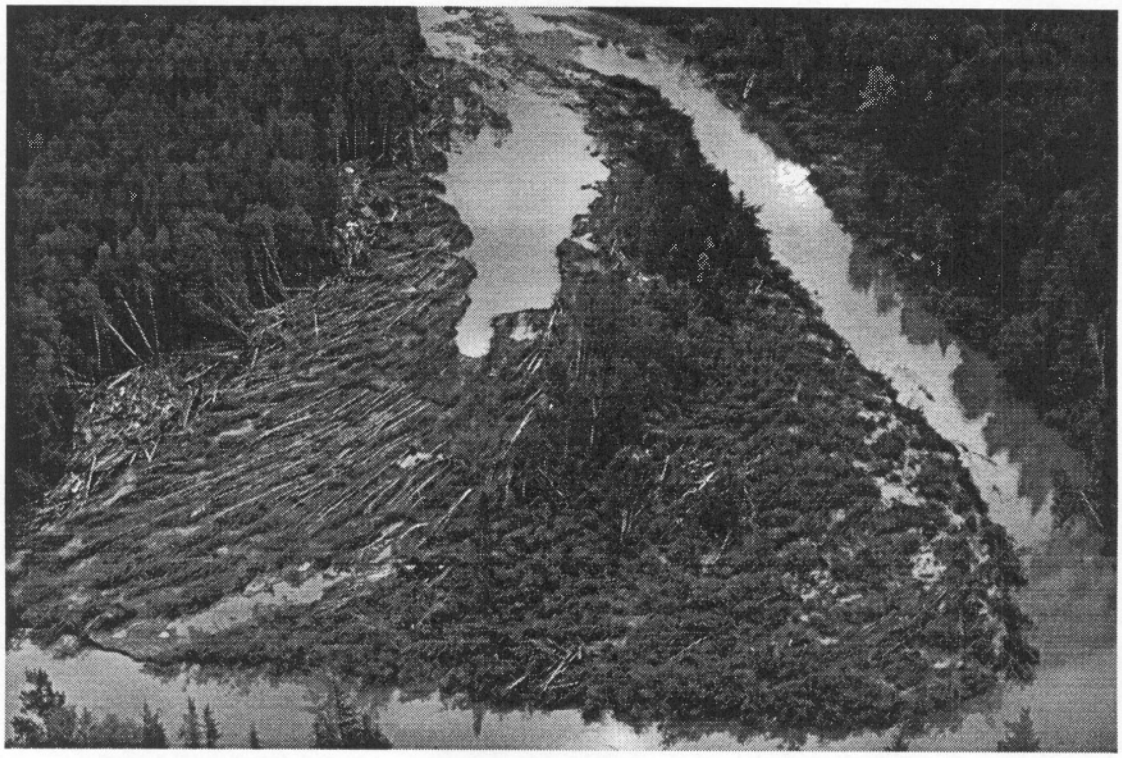

Fig. 9.4

Fig. 9.5a

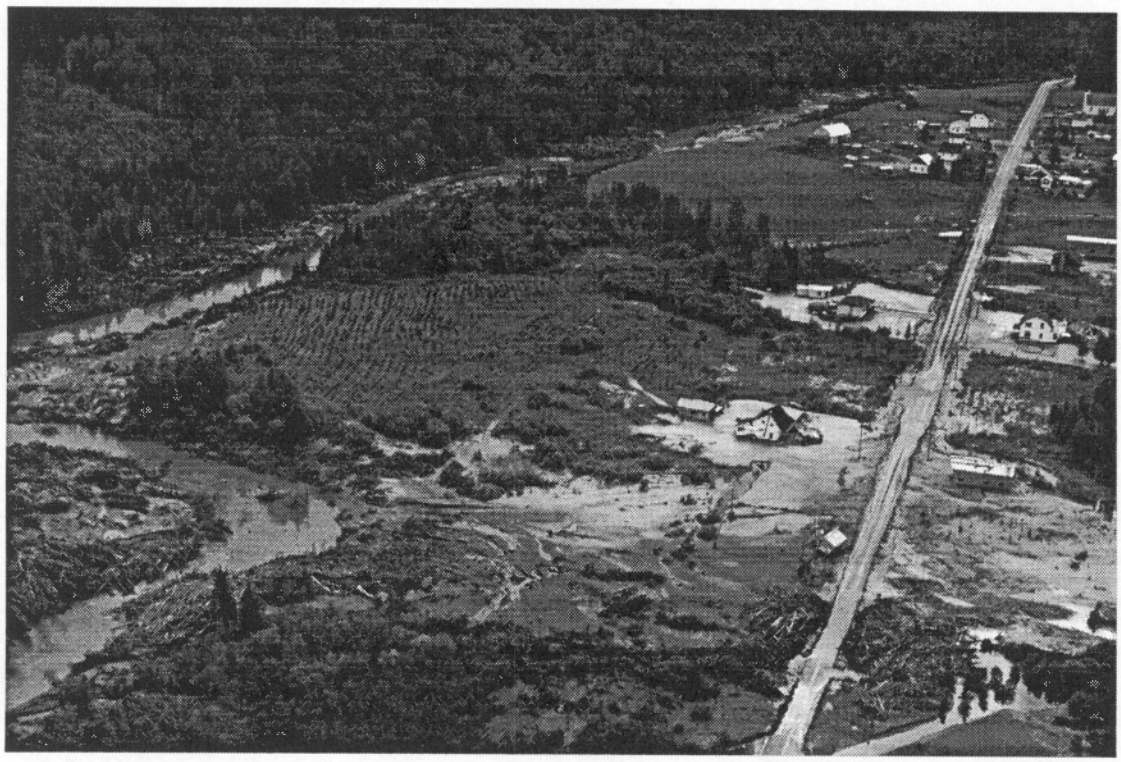

Fig. 9.5b

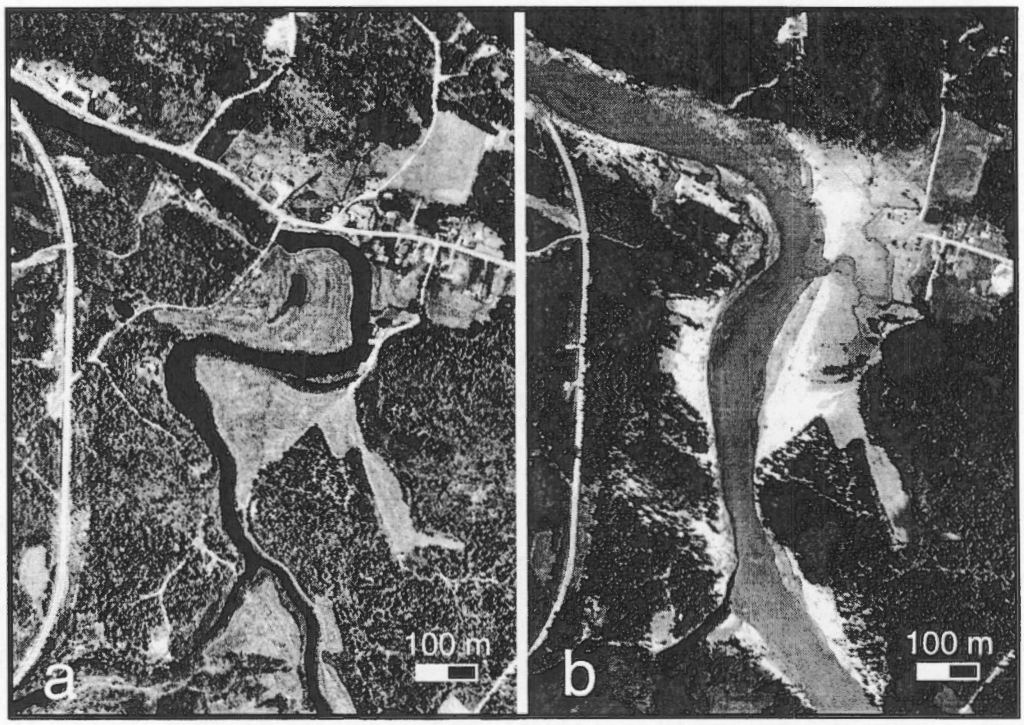

Fig. 9.6

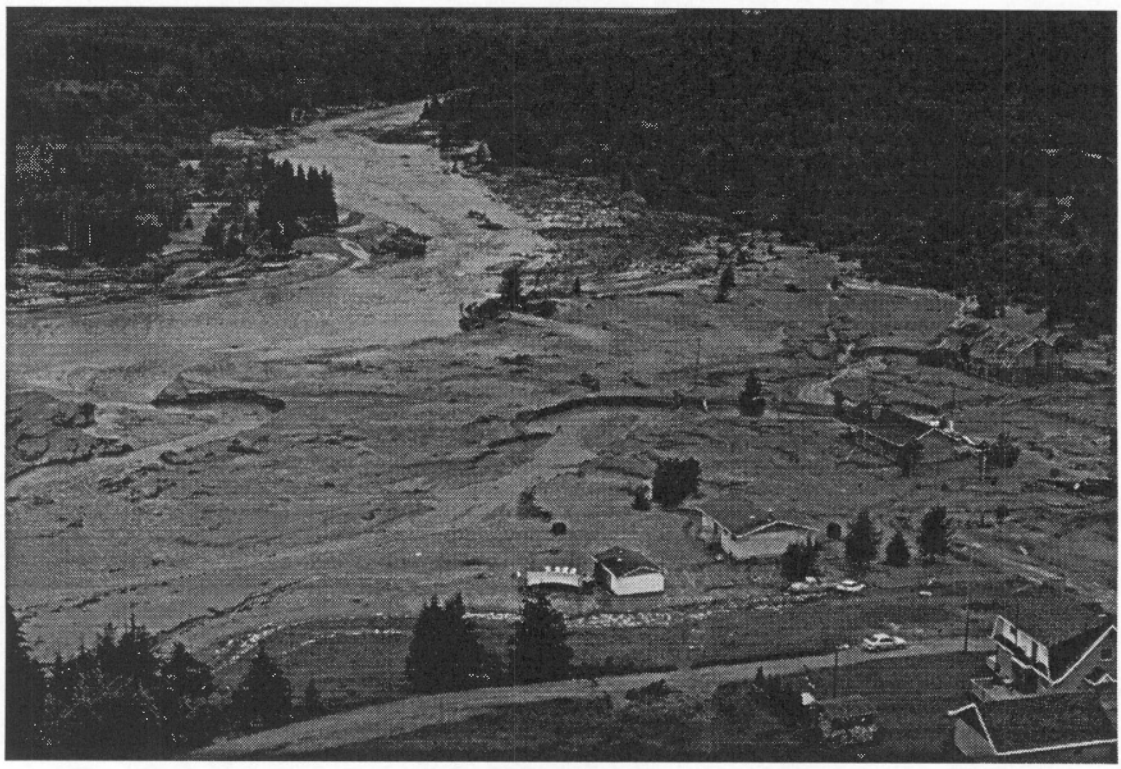

Fig. 9.7

Fig. 9.8

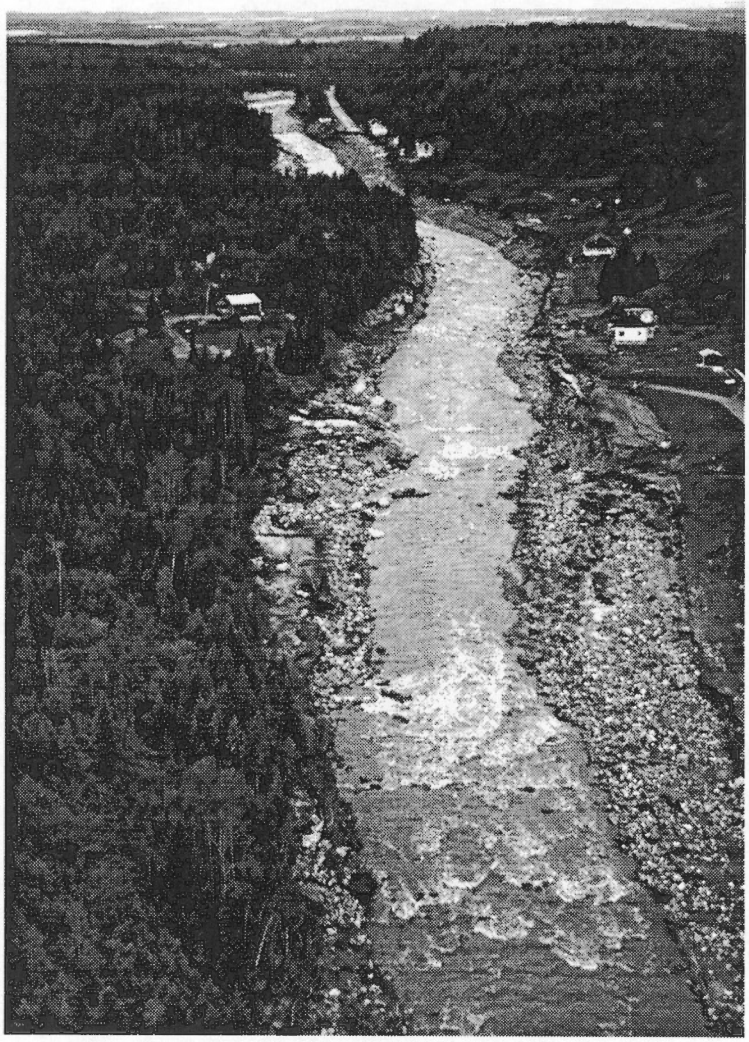

Fig. 9.9

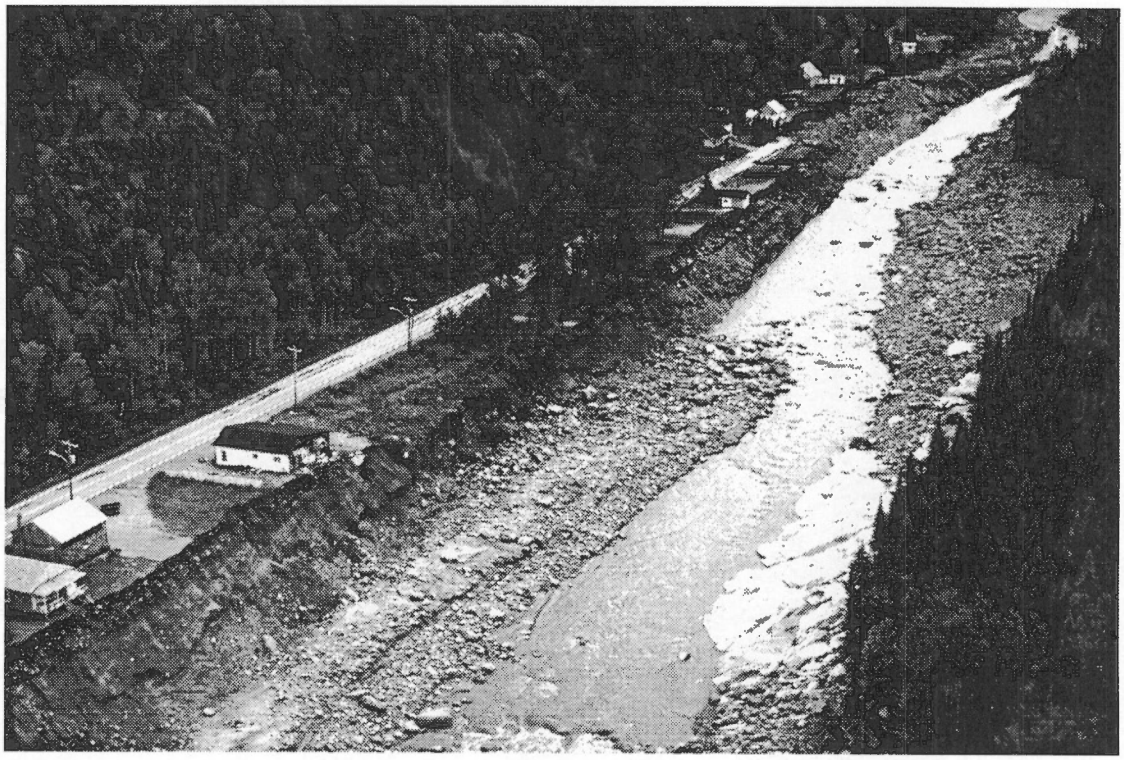

Fig. 9.10

Fig. 9.11

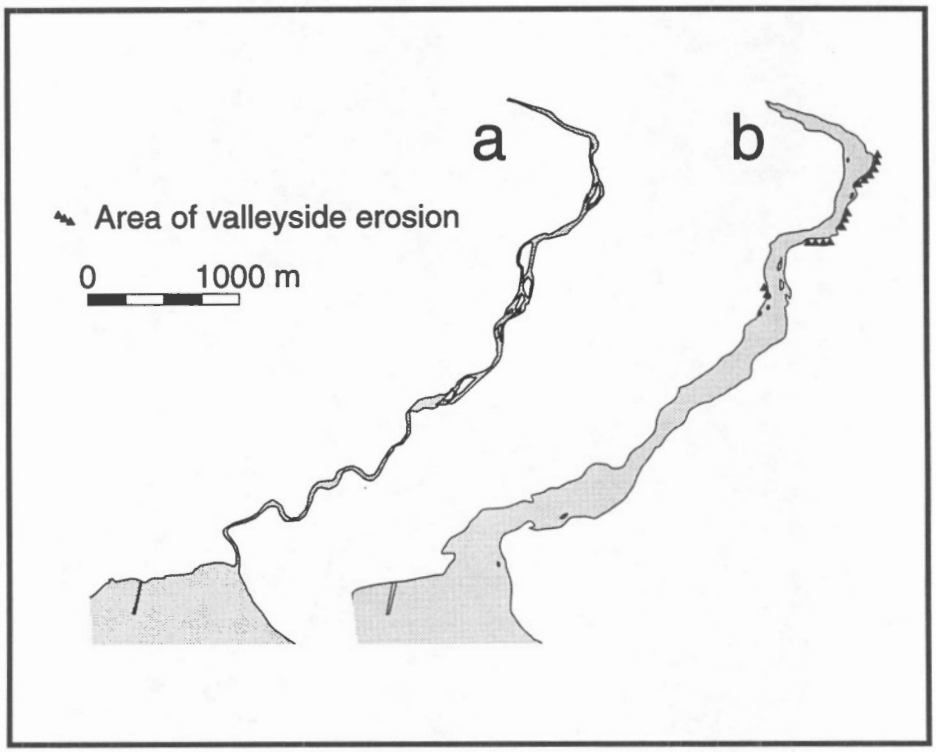

Fig. 9.12

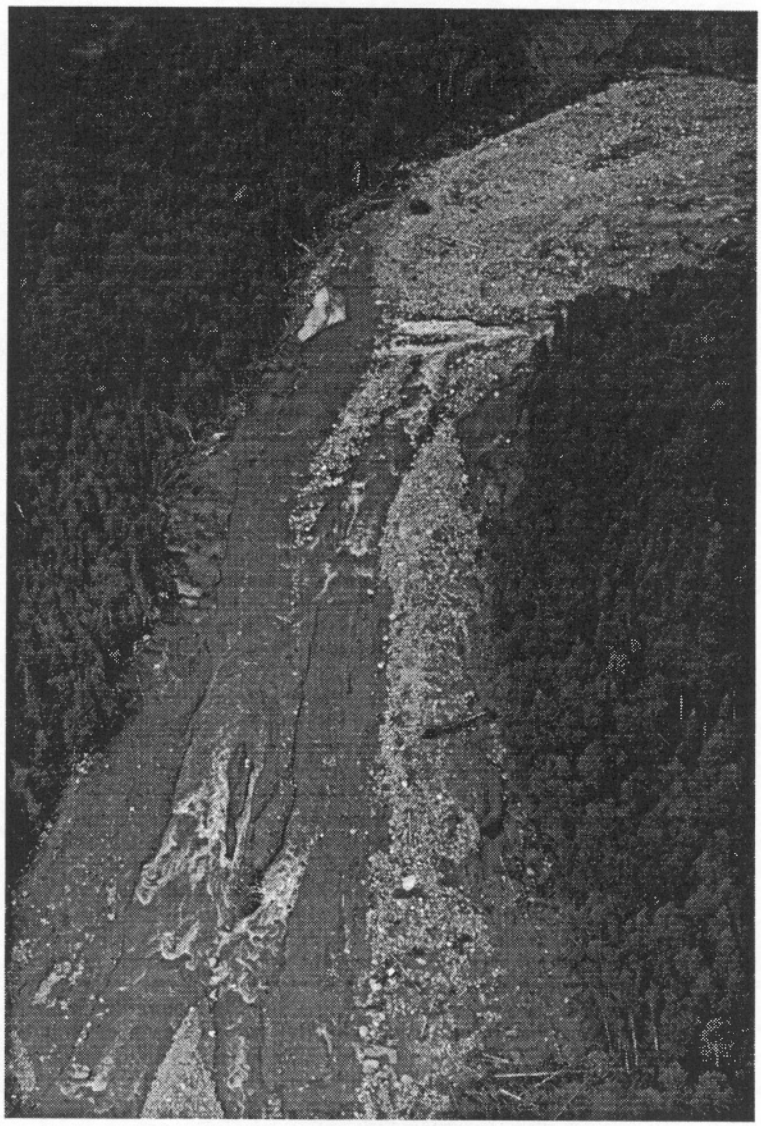

Fig. 9.13

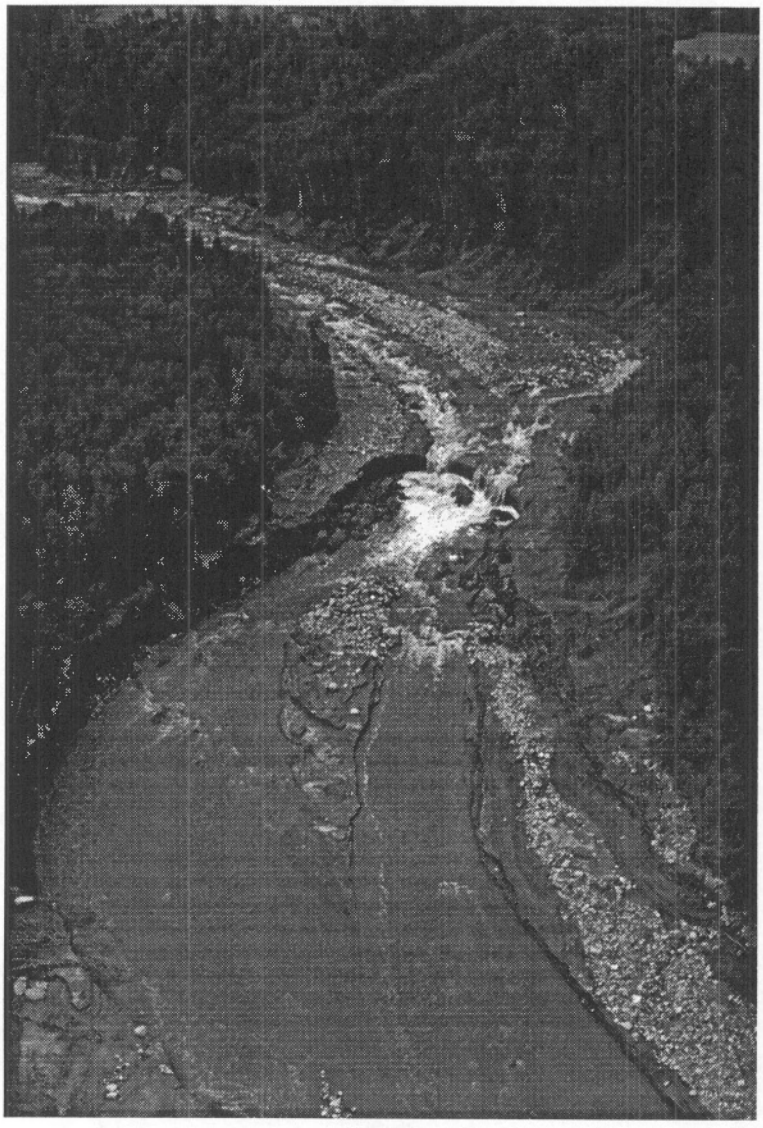

Fig. 9.14

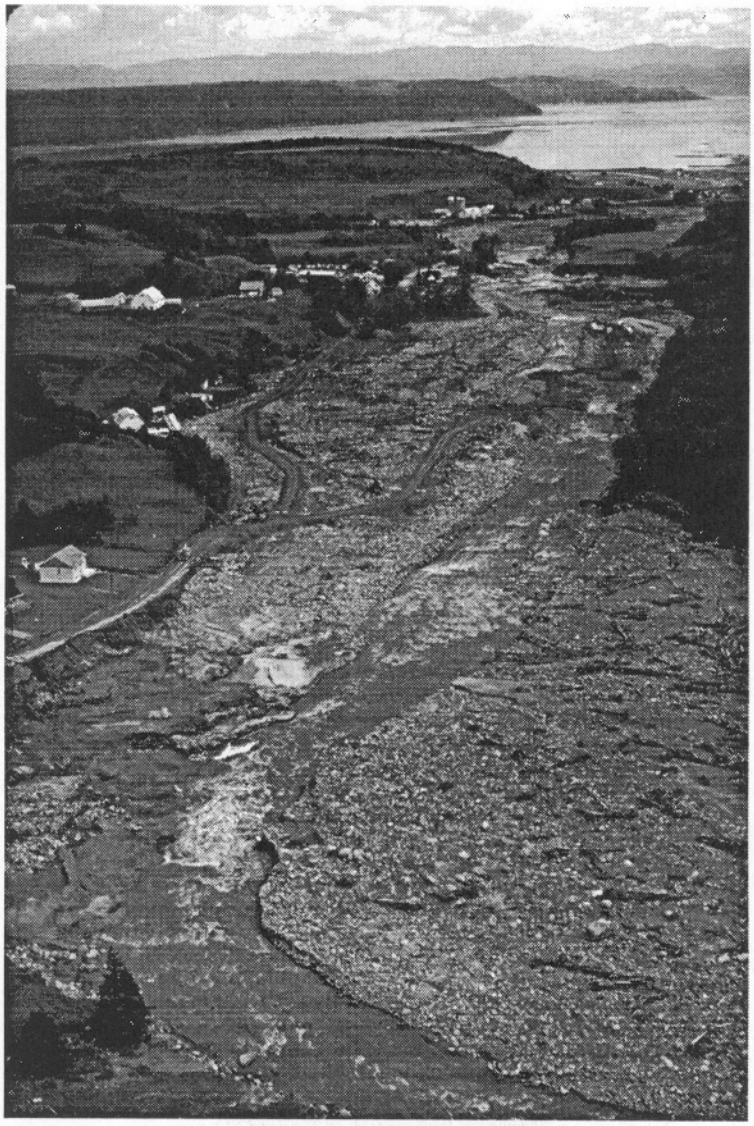

Fig. 9.15

Fig. 9.16

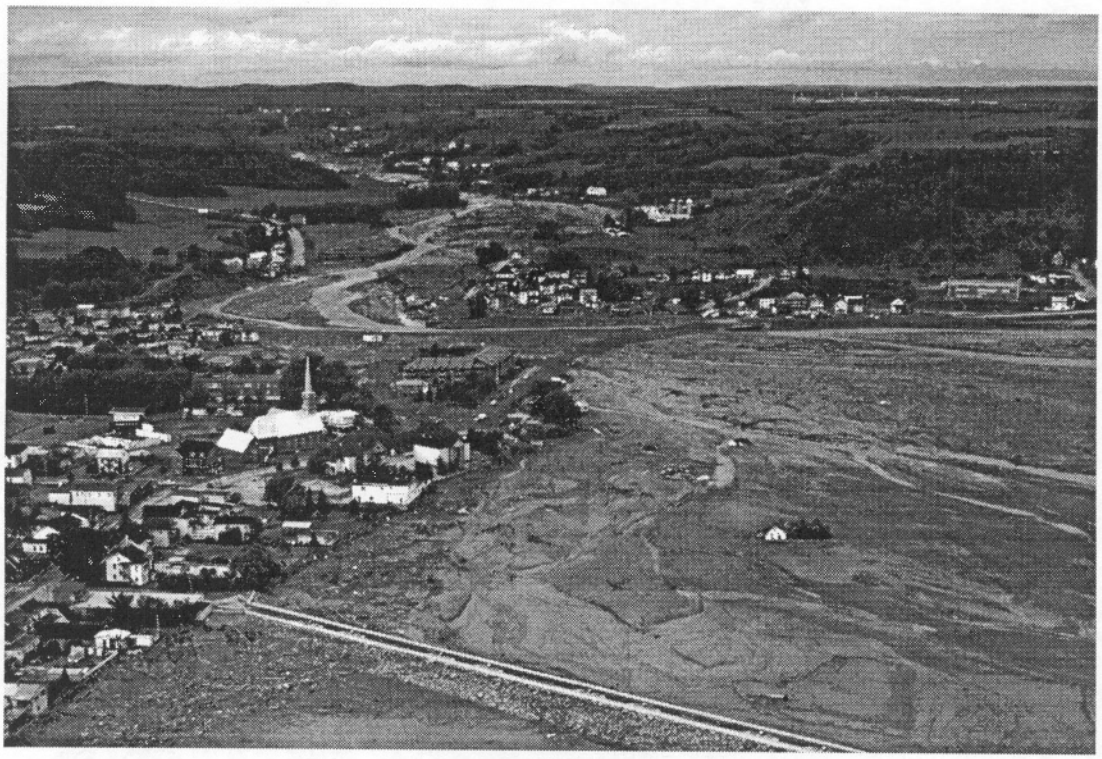

Fig. 9.17

10. RIVIÈRE DU MOULIN

General

The study reach along Rivière du Moulin constitutes the lower 17 km of the river and is situated entirely upon the lowland surface of the Saguenay Valley (Fig. 2.1). From km 17 to roughly 9.5, the river is incised into deltaic deposits and then into marine sediment from km 14.5 to the river mouth. Along much of the study reach, Rivière du Moulin occupies a shallow streamcut valley incised up to 10 m into the lowland surface (Fig. 10.1). However, beginning at about km 3, the channel gradient steepens markedly as the river descends the side of the valley occupied by Rivière Saguenay (Fig. 10.2). In conjunction with this descent, the river is contained within a well-defined valley up to 70 m deep. Numerous large Holocene landslide scars and extensive gullies are present within the marine sediment forming the sides of this deep valley (Fig. 2.1).

Along the study reach, the river character changes downstream gradually, yet significantly. At km 17-16, the river is incised to bedrock and flows across a short rapids. Downstream of km 16 to 12.5, the river is alluvial and exhibits a regular meandering planform. The valley bottom consists of a continuous floodplain up to 400 m wide with the outer banks of the meanders commonly being confined against the valleysides. The channel sinuosity is 1.6 and the channel ranges from 20-30 m wide. The channel is laterally stable, there being no obvious evidence of contemporary lateral channel instability. However, several ox bow lakes and channel scars are present, indicative of past channel migration. The floodplain and the river banks are heavily vegetated (Fig. 10.1).

Between km 12.5 and 3 , the channel alternates from alluvial and non-alluvial (confined by the valleysides) reaches, and follows an irregular meandering course. The channel sinuosity is 1.5 with the channel ranges from 20-30 m wide. Like the upstream reach, the channel here is also laterally stable. A narrow, fragmented, floodplain is present in places, but below km 5.5 the meanders generally are entrenched with only very isolated floodplain fragments occurring. Bedrock outcrops along the river at km 7-6.5, 5.5, and 4.5-4. At these locations, the channel locally steepens and short rapids are present (these rapids are not apparent in Fig. 10.2 because of the 10 m wide contour line interval on the base map).

From km 3 to the river mouth, the Rivière du Moulin flows primarily upon bedrock and several well-defined steps are present in the longitudinal profile (Fig. 10.2). The channel character consists of an alternating chutes and pools. The channel width is variable ranging from 20 to 60 m, the wider areas being the pool. At the river mouth, the channel is up to 100 m wide reflecting a tidal influence.

Below the village of Laterrière from km 16 to 3, Rivière du Moulin flows through an agricultural area while from km 3 extending to the community of Rivière-du-Moulin (suburb of Chicoutimi) at the river mouth (Fig. 10.3), the area adjacent to the river is forested. Many homes are present along the river, most prominently in Laterrière and Rivière-du-Moulin. Within these two centres, a number of homes are situated on the floodplain or low areas of the valleysides. Between Laterrière and km 6.5, homes adjacent to the river valley generally follow a major road along the westside of the river valley. The area adjacent to the river is uninhabited from km 6.5 and 0.8. The river is crossed by six road bridges and one railway bridge. The remnant of a small dam is present at km 4.2.

Geomorphic effects of the flood

Overall, the geomorphic effects of the flooding from the July 18-21, 1996 rainstorm were much less severe along Rivière du Moulin than along the other four rivers. Between km 17 and 5, the most significant erosion problems within the village of Laterrière occurred at km 16.6-16 and at km 14.2-14, and km 6.8 (Fig. 10.3). Within Laterrière, flood waters overtopped the banks and flowed across lowlying areas of the valley bottom causing erosion at some locations. Along the right bank at km 16.2, overflow and bank erosion removed several tens of square metres of thin overburden exposing the underlying bedrock (Fig. 10.3 and 10.4). The occurrence of this erosion relates to the relatively steep local gradient formed by the presence of the bedrock in the valley bottom which the river crosses and forms a short rapids (see *General* section, above). At km 16.6, bank erosion occurred adjacent to a road bridge (Fig. 10.5) which likely caused both a local constriction that accelerated the flood flow and an obstruction which diverted flow onto an adjacent road surface. Downstream at km 14.2, the road approach to a bridge was washed out and several homes located immediately downstream were damaged or destroyed (Fig. 10.6). Evidently, the flood flow was partially dammed behind the bridge and eventually spilled over the road. Similarly at km 6.8 (a location known as Chutes à Martel), the obstruction of the flood flow by a road bridge resulted in the road being washed out and a couple of homes immediately adjacent to both the river and bridge being either damaged or destroyed (Fig. 10.7).

Along most of the km 17 to 5 reach, negligible erosion and deposition occurred (Fig. 10.3); there being little geomorphic evidence of the flood (Fig. 10.3). Minor deposition occurred locally on the valley bottom between km 10 to 9 and 6 to 5, marking a high water line (Fig. 10.8). The lack of geomorphic effects along this reach undoubtedly reflects the generally low valley gradient (which translates into low erosive power for the flow), low suspended sediment concentrations in the flood water, and a relatively high resistance to erosion imparted by the combination of bank material and riverine vegetative cover. Isolated, small, shallow valleyside failures and sporadic areas of concave bank erosion occurred along the river where the channel was confined directly against a valleyside (Fig. 10.3).

Downstream between km 5 and 3, more extensive erosion occurred where the valley gradient steepens and the river is confined within entrenched meanders eroded into resistant fine-grained marine sediments (Figs. 10.2 and 10.3). Bank and channel bed erosion occurred discontinuously and there were several small, shallow bank failures (Fig. 10.3). Most significantly, a sharp meander located at about km 4 was completely cut-off during the flood when flow overtopped and eroded through the narrow 'gooseneck' between the entrance and exit channels of the meander (Fig. 10.3 and 10.9). Downstream at km 3.2, several small sand sheets forming overbank deposits are present on an isolated floodplain fragment (Fig. 10.10).

Below km 3 to the river mouth, the flood primarily scoured the vegetation cover from the bedrock surface immediately adjacent to the pre-flood river surface. Marine sediment was eroded at isolated locations where flood waters came in contact with it. At the river mouth, marine sediment along the valleysides and the bank of a paired alluvial surface were eroded over a distance of several hundred metres (Figs. 10.3 and 10.11). The upstream end of the right terrace surface was inundated and a thin veneer of silt and sand was deposited discontinuously over roughly a one hundred metre distance.

Because much of the valley bottom and valleysides along Rivière du Moulin are sparsely populated, damage to homes occurred primarily within or near Laterrière, and within Rivière-du-Moulin. At both locations, a number of homes were inundated and, damaged or destroyed. Notable damage elsewhere occurred to homes at Chutes à Martel (km 6.8) and at km 14.2-14, as described above. The flood damaged four bridges at km 16.5 14.2, 6.7 and 0.2.

Fig. 10.1 Photograph of Rivière du Moulin looking upvalley from km 13.5. Note the shallow river valley and thick vegetation along the valley bottom. This section of the river experienced negligible geomorphic change during the flood. Photograph taken on July 27, 1996 (GSC photograph 1997-42UU).

Fig. 10.2 Longitudinal profile of Rivière du Moulin study reach (data from 10 m contour lines on Québec Ministère de L'Energie et des Ressources maps 'Chicoutimi' (22D06-200-0202), and Laterrière (22D06-200-0102), 1:20 000 scale).

Fig. 10.3 (see POCKET) Map of the lower 17 km of Rivière du Moulin showing the locations of major communities, roads, and bridges. The locations of erosion and failures resulting from the flood are also shown. The scale (in blue) following the river marks kilometer distance allowing locations mentioned in the text to be keyed to the map. The yellow zones follow Dion (1986b) and designate areas having a medium to low potential for landsliding. Here, slopes are greater than 25% (14°), but there was no erosion at the toe of the slopes or evidence of major instability at the time of the original mapping. See Fig. 1.2 for the location of the map.

Fig. 10.4 Eroded area within Laterrière along the right bank at km 16.2 where much of the overburden has been stripped from the bedrock. A number of homes in this general area were damaged during the flood. Rivière du Moulin is in the foreground, flowing from right to left. Photograph taken on July 27, 1996 (GSC photograph 1997-41B).

Fig. 10.5 Eroded river banks at km 16.6 adjacent to a road bridge. Photograph taken on July 27, 1996 (GSC photograph 1997-41C).

Fig. 10.6 Washed-out road beside the bridge at km 14.2. Note the foundation marking the former location of a house that was swept downstream. The river flows from the top to bottom of the picture. Photograph taken on July 27, 1996 (GSC photograph 1997-42VV).

Fig. 10.7 Damaged and destroyed homes, and washed-out road at Chutes à Martel (km 6.8). Photograph taken on July 27, 1996 (GSC photograph 1997-42WW).

Fig. 10.8 Minor deposition on the floodplain and lower valleyside at km 6. Photograph taken on July 27, 1996 (GSC photograph 1997-42XX).

Fig. 10.9 Vertical multi-spectral video image of meander at km 4 which was completely cut-off during the flood, taken August 6, 1996 (courtesy of Canada Centre of Remote Sensing). The river flows from the bottom left corner of the picture. Image acquired on July 27, 1996.

Fig. 10.10 Discontinuous sand sheets forming overbank depositions on floodplain at km 3.2. Flow is from top to bottom of picture. Photograph taken on July 27, 1996 (GSC photograph 1997-42YY).

Fig. 10.11 Bank erosion along the right bank of Rivière du Moulin just above the river mouth. The river is flowing towards the bottom of the photograph. Photograph taken on July 27, 1996 (GSC photograph 1997-42ZZ).

Fig. 10.1

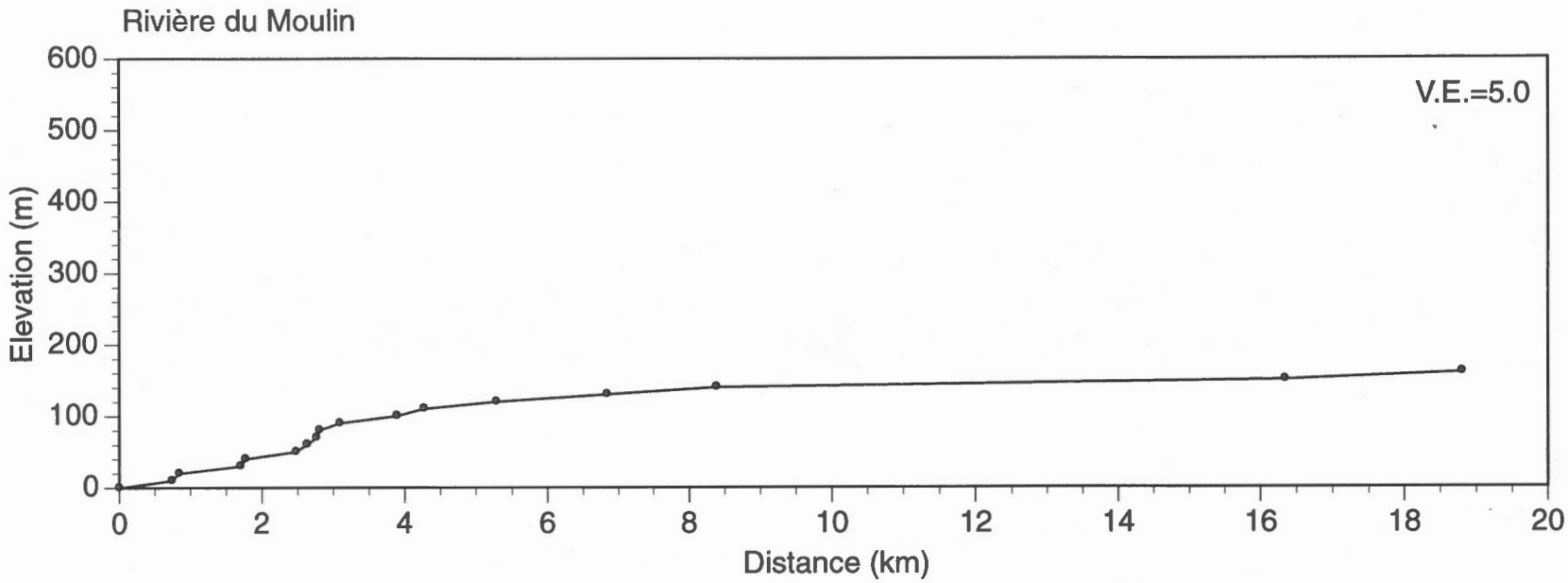
Rivière du Moulin
V.E.=5.0
Elevation (m)
600
500
400
300
200
100
0
0
2
4
6
8
10
12
14
16
18
20
Distance (km)

Fig. 10.2

Fig. 10.3 see POCKET

Fig. 10.4

Fig.10.5

Fig.10.6

Fig. 10.7

Fig.10.8

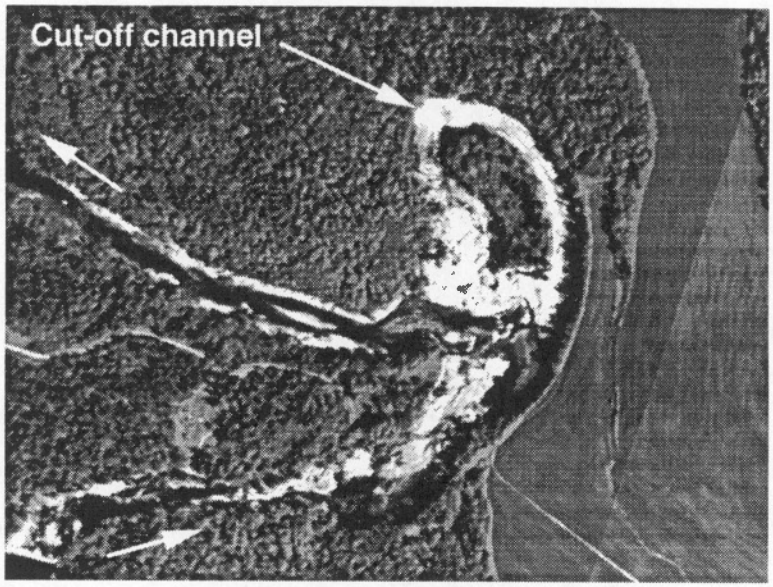

Fig. 10.9

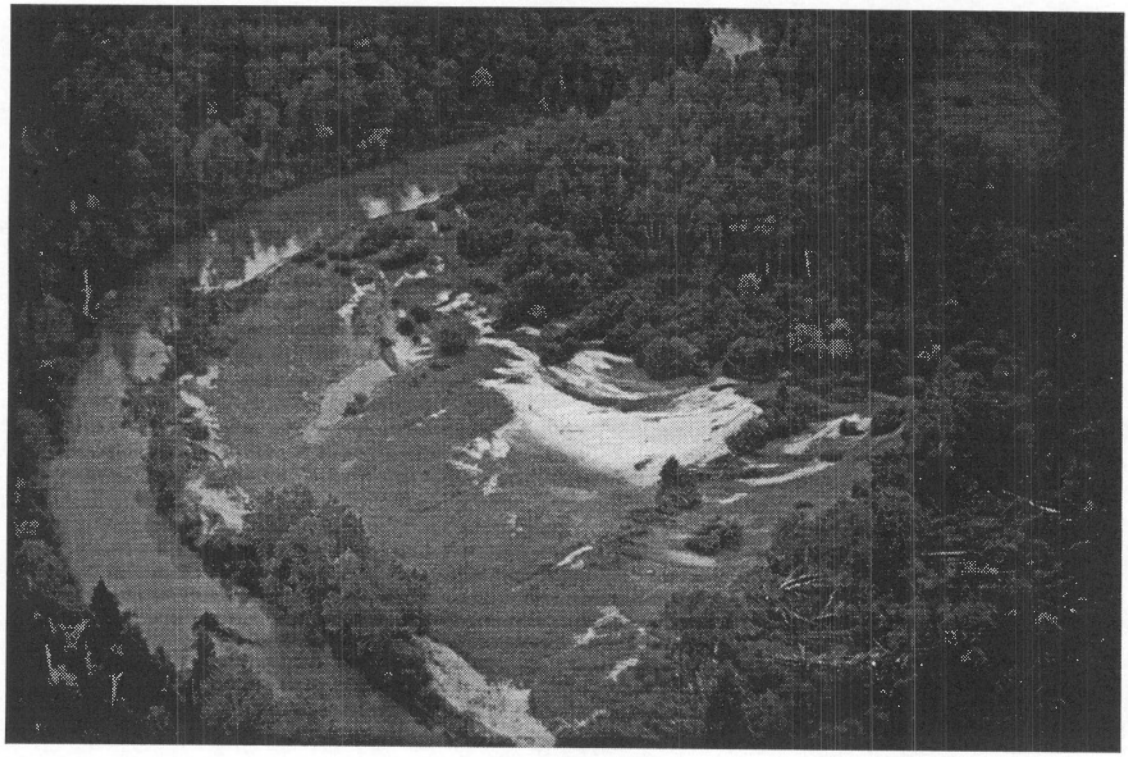

Fig. 10.10

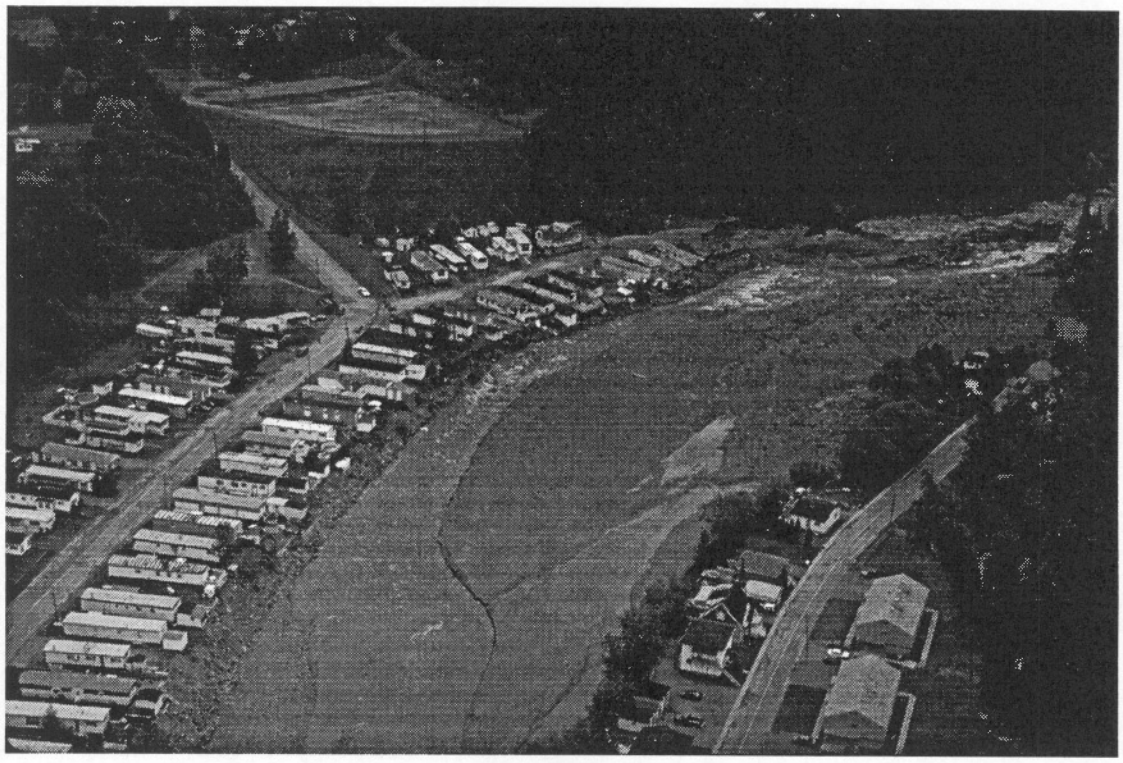

Fig.10.11

11. LANDSLIDING AND BANK INSTABILITY

Introduction

Slope stability concerns related to the flooding from the July 18-21, 1996 rainstorm were caused by bank erosion and oversteepening along the rivers, saturation of soils and, drawdown due to the rapid draining of reservoirs and the recession of flood levels. Depending upon local soil, slope, and groundwater conditions, one or a combination of these factors could contribute to slope instability or cause slope failures, as described below.

Bank erosion and oversteepening

Along the study rivers, erosion by the flood waters has undermined, scoured and otherwise modified river banks, as described in the previous five chapters. Bank erosion occurred locally along reaches of Rivière aux Sables, Rivière Chicoutimi and Rivière du Moulin, and along many kilometres of Rivière des Ha!Ha! and Rivière à Mars. There is potential for slope instability and slumping where banks have been steepened or where toe erosion has removed support from the lower portion of slopes, regardless of the actual amount of bank retreat. In some locations, vertical or near-vertical slopes have been formed in marine, glacial or alluvial deposits.

Slope stability at any given location is dependent primarily on sediment type, geotechnical properties, groundwater conditions, stratigraphy and bank height. However, at locations where banks have been oversteepened, there is a potential for further bank failure and collapse as these slopes likely will adjust to attain a new equilibrium form. Under certain circumstances, there may be a potential for retrogressive landsliding which could effect terrain for a considerable distance behind the slope.

Saturation of soils

A soil becomes saturated when the pores between soil particles are filled with water. In the summer, this occurs generally through the infiltration of rainfall into the ground, but locally by the inundation of the ground by floodwaters, or the vertical and/or lateral movement of groundwater through a soil. The rate of infiltration and subsequent movement through the ground depends upon the hydraulic conductivity of the soil which in turn is contingent upon soil texture and structure. The rate of infiltration for fine-grained soils is normally low, but may be increased where the soil substrate is broken-up by, for example, chemical and mechanical weathering, cracks and fractures, root penetrations and, animal and insect burrows. Whether a soil becomes saturated from a given rainstorm depends upon antecedent soil moisture conditions, the duration and intensity of the rainfall, the soil thickness, and the hydraulic conductivity of the material immediately underlying the soil unit.

The abnormally high rainfall in the few weeks prior to July 18 and the intensity and duration of the July 18-21, 1996 storm produced very wet or saturated soil conditions on slopes throughout most of the Saguenay region. These saturated soils because of their increased weight and locally high pore water pressures, had a greater potential for failure than prior to the storm event.

Drawdown and flood wave recession

Slope failures can be precipitated in a variety of sediment types along river banks and shorelines by the rapid lowering of water levels. The high pore water pressure generated by this change in water level is the principal mechanism for these failures, known as drawdown failures.

Generally, drawdown failures are associated with reservoirs where the water levels have been lowered quickly to prevent overtopping of a dam or dyke or in instances where dams or dykes have failed catastrophically. They could also occur by the lowering of the river level following the recession of a flood wave provided that there was sufficient infiltration of water into the river banks.

The potential for this type of failure is usually greatest immediately following the drop in water level when pore water pressures within the banks are highest. Since pore water pressures dissipate over time as water drains from the slope, the risk of failure will diminish.

As described in the chapters 6, 7 and 9, severe abutment erosion resulting from the overtopping of dams or dykes caused the total or partial drainage of eight reservoirs within a very short time. All five study rivers experienced very high levels of flooding which were maintained for a several days creating conditions favourable for drawdown failures.

Landsliding and bank instability

The landslide activity and potential slope stability problems caused by the flooding are generalized for each of the five study rivers in the sections below. In particular, those areas deemed likely to represent a future hazard from continued instability on slopes that were oversteepened or otherwise modified by fluvial erosion, are discussed. For Rivière aux Sables, Rivière Chicoutimi and Rivière du Moulin, the location of the flood triggered failures are depicted on maps which also show Dion's (1986b) zones of medium to low landslide risk; the only designation that is located along the rivers. For Rivière aux Sables and Rivière Chicoutimi, where many of the flood-triggered landslides occurred, the failure attributes are summarized in tables, including, where available, general information on material, size, type, cause, and damage. Landslide terminology follows Varnes (1978). On the maps and tables, each failure or group of small closely-spaced failures is assigned an individual alpha-numerical code.

The description of landslide morphology and interpretation of landslide causes and inferred mechanisms, are based solely on reconnaissance observations from the air and the interpretation of aerial photographs. This data, therefore, must be considered preliminary in nature.

Geotechnical data would be required in order to accurately evaluate the stability conditions for any given site. Engineering designs based on site specific geotechnical information would have to be developed in order to properly and safely reconstruct infrastructure elements, rehabilitate land or, re-develop and re-occupy property adjacent to river banks oversteepened by fluvial erosion or subject to failure. In some cases, should investigation indicate that the ground at a given site is potentially unstable, it may be more appropriate to re-locate infrastructure and buildings to a safe location rather than re-develop the potentially unstable location. These types of decisions can only be made with the support of complete geotechnical and land use evaluations.

Rivière aux Sables

Along Rivière aux Sables, a number of small, shallow landslides occurred along the river banks between km 7 and 2 (Fig. 6.1 and Table 11.1). Of these, failure S12 is located on the left bank at about km 6.9 just downstream of the mouth of Ruisseau Desgagné while two others (grouped as failure S11) are located just downstream at km 6.8 (Fig. 6.1 and Table 11.1). Failures S10, S9 and S8 (Figs. 6.1, 6.3c and 11.1; Table 11.1) are located between km 5.7 and 5.2. None of these slumps are close to residences or other buildings.

Two slumps (failures S6 and S7; Fig. 6.1 and Table 11.1) are located at km 4.9 along the left bank of Ruisseau des Chasseurs near its confluence with Rivière aux Sables. Each of these occurred within marine sediment and were initiated by elevated pore water pressures generated by the drainage of the Abitibi power station reservoir. Failure S6 incorporated part of the left abutment of a stream crossing while failure S7 consumed a considerable portion of the backyard of a residential property (Fig. 11.2). It does not appear that any buildings were lost or threatened by either failure, however, the crossing of Ruisseau des Chasseurs was completely washed-out due to the effects of the landslide and flooding. New culverts were required and the stream crossing was under construction within days of the event. The residential property will require a designed backfill, regrading and landscaping.

Failure S5 was the largest to occur along Rivière aux Sables and is located at km 3.6 immediately upstream of the railway bridge (Fig. 6.1 and Table 11.1). This shallow slump, about 55 m wide, involved several retrogressive slips of marine sediment (Figs. 6.7 and 11.3). The failure occurred along the banks of the Abitibi power station reservoir (dam located at km 3.2; Fig. 6.1) which was drained during the flood (see *Chapter 6 Rivière aux Sables - Geomorphic effects of the flood* section). Rapid drawdown of the reservoir was undoubtedly the major contributing factor for this failure. Although backfilling and reconstruction of the left railway bridge approach complicates the

interpretation, this landslide may have contributed to the damage of the railway bridge abutment and left bridge support. Fluvial scouring of the river bank and left bridge support foundation, however, also contributed to the damage to the bridge and abutment. Repair to the bridge will require new approach fill, the construction of a left bridge support, and replacement of the bridge deck and tracks. This work was underway immediately following the flood.

From km 3.5 to the confluence with the Rivière Saguenay, significant sections of valleyside were laterally eroded in the immediate vicinity of the Abitibi power station dam (km 3.2), Jonquière power station dam (km 2.6) and the Abitibi paper mill dam (km 1) because of overtopping and erosion of the abutting valleysides (Fig. 6.1; see *Chapter 6 Rivière aux Sables - Geomorphic effects of the flood* section). This erosion resulted in the formation of high near-vertical faces of marine sediment, particularly at the two Abitibi dams (Figs. 6.4b and 6.5). These oversteepened banks have a high potential for instability especially if they become saturated during the 1997 spring melt. Geotechnical evaluation of these slopes will be required prior any re-development in the vicinity. It should be noted, however, that the slope adjacent to the Abitibi power station dam had been regraded by November 1996 which would minimize any post-flood slope instability at this site. Also, considerable reconstruction has occurred at the Abitibi paper mill dam site which presumably included regrading of these slopes.

Failure S2 occurred along the left bank adjacent to the Jonquière power station dam (Fig. 6.1 and 6.6; Table 11.1). The failure likely was initiated by toe erosion when the dam was overtopped by floodwater and the left abutment was scoured. Failure S1 is located at km 1.8 (Fig. 6.1) and also likely was initiated by toe erosion.

Several small bank slides and flows (grouped under failures S3 and S4; Table 11.1) occurred along the right bank within the partially drained reservoir of Jonquière power station dam at km 2.6. These failures probably in part relate to drawdown of the reservoir caused by a shallow breach in the right concrete wing of the dam (see *Chapter 6 Rivière aux Sables - Geomorphic effects of the flood* section).

It should be noted that the area behind the right bank, adjacent to and immediately downstream of the Abitibi paper mill dam, was the site of the October 1924 Kénogami flowslide (Brzezinski, 1971), referred to previously. It involved about 2.0×10^6 m^3 of overconsolidated sensitive marine sediment and was responsible for damage to facilities at the (then) Price Brothers paper mill and for the death of Sir William Price the owner of the company. The regraded fill which now occupies the old landslide scar was partially eroded by flood waters spilling over the right wing wall of the dam prior to the breaching of the left abutment.

Of the failures (including groupings of failures) listed in Table 11.1, seven occurred within zones along the river mapped by Dion (1986b) as having a medium to low risk for

landsliding[1] (Fig. 6.1). Only one failure was retrogressive; the others were shallow slumps, flows or slides. Eight failures occurred along the banks of reservoirs which experienced drawdown. All of the other failures occurred along banks that were not visibly eroded during the flood and probably related to the elevation of pore water pressures generated by recession of the flood wave and saturation due to the high rainfall.

Rivière Chicoutimi

Along Rivière Chicoutimi, no failures or significant bank erosion which could cause instability problems, occurred between km 23.5 to 16 (Fig. 7.1). Erosion here was limited because of the low-angled banks that are formed to a large extent by bedrock or thin substrate covering bedrock.

Downstream of km 16, the river flows within a shallow, narrow valley incised within deltaic sand deposits and/or marine sediments, thus landsliding was more pervasive. Failure C16 (km 15.6) is the upstream-most landslide and consists of several small, shallow, coalesced slumps (Figs. 7.1 and 11.4; Table 11.2). It is situated along the outer bank of a tight meander bend where the river current during the flood was directed against the bank. Another group of coalesced, shallow slumps (failure C15) occurs at km 15. A number of isolated, small, shallow bank failures occur between km 14.5 and 10 (C14, C13, C12, C11, C10, C9 and C8; Fig. 7.1 and Table 11.2); most being located along the concave banks of river meanders. All of these failures have developed in fine-grained marine sediment possibly due to localized toe erosion in combination with the recession of the flood wave. None of the failures posed a threat to infrastructure or buildings.

A cluster of failures occurred within the reservoir of the Pont-Arnaud dam which was drained during the flood because of overtopping and erosion of the valleyside (Fig. 7.1; see *Chapter 6 Rivière Chicoutimi - Geomorphic effects of the flood* section). Failure C7 , 70 m wide with 30 m of setback, is a retrogressive slide that occurred within marine sediment along the left bank (Figs. 7.1, 7.6, and 11.5; Table 11.2). The failure was probably triggered by the combination of drawdown of the reservoir and, the increase in bank height and oversteepening caused by deep channel incision (Figs. 7.1 and 7.5). This failure was the largest to occur along the banks of the five study rivers; it resulted in damage to buildings on an industrial property.

Opposite failure C7, several small flows (grouped as failure C6) occurred along the right bank following the drainage of the Pont-Arnaud reservoir (Figs. 7.1, 7.6 and 11.6; Table 11.2). These flows appear to have occurred within saturated alluvial and organic-rich sediment rather than marine sediment. They undoubted relate to the drawdown of the reservoir and the oversteepening and increase in bank height caused by deep channel incision.

---

[1] Dion (1986b) defines the medium to low risk zone as having a potential for failure, however, no evidence of major instability was recognized at the time of mapping. Slopes in this unit are greater than 25% (14°), but generally there was no erosion at the slope toe (at the time of mapping).

A number of smaller slides (C5, C4, C3 and C2) occurred along both banks of the reservoir above the Elkem dam (km 4.0-4.5; Fig. 7.1). Although the Elkem reservoir was not drained during the flood, the initiation of these failures may have occurred due to the combination of recession of the flood waters and local bank erosion. Failure C1 located at km 2 well below the Elkem dam, possibly was triggered by rainfall rather than fluvial processes since it is located well back from the river.

Of the sixteen failures (or groupings of failures) mapped along Rivière Chicoutimi, fourteen were located within zones mapped by Dion (1986b) as having a medium to low risk of landsliding (see previous section for definition). Two of the three outside these zones occurred within a reservoir where draw down occurred, but specifically at locations where deep channel incision increased the height of the bank. The third failure, as mentioned, may not be related to fluvial processes.

It is interesting to note that despite the drainage of the Chute-Garneau reservoir and the extensive bank erosion which occurred adjacent to and immediate upstream of the Chute-Garneau dam, no landslides were triggered in this general area. Following the flood, the eroded left bank near the dam had near-vertical slopes formed from marine sediments (Fig. 7.3a). These slopes will be unstable until a new equilibrium form is obtained. This problem has been recognized by local authorities, and by November 1996 following the construction of a dyke across the channel eroded adjacent to the dam, a large quantity of fill had been placed along the toe of the banks to improve local stability.

Rivière à Mars

Flood effects along the lower 10 km of Rivière à Mars caused major widening of the river channel and erosion of literally kilometers of bank by the combination of lateral channel erosion, channel avulsions and the creation/re-activation of channels (see *Chapter 8 Rivière à Mars - Geomorphic effects of the flooding* section). This erosion has oversteepened banks primarily along floodplain and terrace surfaces. The stability of these oversteepened banks was not evaluated in this investigation, however, the banks should be considered as potentially unstable until evaluated or remedial work has been undertaken. At many localities, especially on the left bank along the lower 2 km of the river, extensive rehabilitation work was in progress or already been completed by November 1996.

From the perspective of slope stability, the most spectacular failure occurred at km 7.5 which was one of only two locations where the river erosion actually eroded the margin of the valleysides (up to 60 m high) rather than a floodplain or terrace surface (Fig. 8.4). Here, fluvial erosion in marine sediment at the toe of the valleyside has produced a major cutbank, at least 200 m long (Fig. 11.7 and 11.8). This toe erosion has resulted in the collapse of up to about 25-35 m of overlying sediment (marine sediment, deltaic sand and gravel) much of which has been washed away by the river (Fig. 11.7). This collapse undermined about 125 m of railway right-of-way located partway up the slope, leaving

the tracks and ties suspended above the failure (Fig. 8.6). By November 1996, the failed bank had been entirely regraded and the damage to the railway line repaired.

Rivière des Ha!Ha!

Extensive erosion occurred along many reaches of Rivière des Ha!Ha! because of the large flood discharge (see *Chapter 5 Hydrology - Drainage of Lac Ha!Ha! reservoir* section). The majority of the 34 km long river is above the marine limit of 165 m a.s.l. (see *Chapter 2 Background - Study area* section) and does not flow within the areas of fine-grained sensitive marine sediments; Dion (1986a) shows fine-grained marine sediment only downstream of km 6. Nonetheless, significant slope instability occurred along some upstream parts of the river and within the drained basin of Lac Ha!Ha!.

Most significant from the slope instability perspective was the erosion that occurred along the lower 8 km of the river where the river margins are settled. As described above (see *Chapter 9 Rivière des Ha!Ha!- km 4.5 to the river mouth segment* section), the lower 4.5 km of Rivière des Ha!Ha! flows within a deep valley that gradually widens toward the river mouth. Along this reach, extensive channel widening occurred, similar to that along the lower 10 km of Rivière à Mars. This widening resulted in lateral erosion along the margins of the floodplain, terraces, and valleysides, particularly below km 4. It caused widespread undermining and destruction of infrastructure and buildings although very little of this impact can be attributed to landsliding. The oversteepened terrace banks are up to about 20 m high and generally consist of interbedded units of landslide debris and alluvial sand/gravel. These slopes have the potential for failure. Prior to re-occupation or re-development of land adjacent to these slopes, a geotechnical evaluation would be required in order to assess the bank stability and design remedial measures.

Erosion of the valleysides exposed marine sediments between km 4.1 and 3 (Fig. 9.12). While all of these areas may experience future instability, particularly notable is the left bank of the river where it forms a concave bank of a tight bend at about km 4 (Fig. 11.9). Here, toe erosion is the underlying mechanism for the initiation of slides in along the overlying steep bank, about 20 m high. Examination of pre-flood aerial photographs indicate that this bank had been subjected to ongoing slope instability prior to the July 1996 flood. In addition, on the right bank about km 4.3, below a bedrock canyon, a new post-flood slump occurred in marine sediment.

It also should be noted that there were a number of small, shallow flows and slides which occurred within marine sediment on steep slopes of the valleysides, far above and completely unrelated to the flooding and erosion along the valley bottom. One of these failures on the southeast outskirts of Grande Baie, engulfed a residence and displaced it from its foundation; mud flowed into the basement and killed two children. As a result of this event, a number of other homes in the immediate vicinity were determined to be at risk of future landsliding and were condemned.

Between km 7.8 and 5, Rivière des Ha!Ha! experienced incision up to 15-20 m and moderate channel widening which oversteepened the river banks formed of alluvium and/or glacigenic diamicton (till?, marine sediment?) (Fig. 9.10). No failures occurred along this reach, but the oversteepened banks must be regarded as unstable and subject to post-flood adjustment until an equilibrium form is obtained. The road and many homes along this reach were damaged or destroyed by undermining due to the bank erosion. Many of the undamaged homes that remain are situated close to the banks and could be vulnerable to damage from future slope instability. However, since the flood all of the homeowners have been bought out and the homes condemned.

Upstream between km 13.7 and 12.5 (Fig. 9.1), an area of extensive landsliding consisting of numerous flows occurred along freshly eroded valleysides. The cause of this landslide activity relates to a change in the river course and deep erosion along a new channel. Flood waters at about km 13 overtopped a low divide and flowed into a ravine which provided an alternative route that re-joins the river at km 12.5. Subsequent incision and lateral erosion along the new course created a wide, deep channel. The incision along the new channel course propagated upstream and eventually left the entrance to the original channel hanging on the valleyside. Subsequently, the entire flow was carried down the new channel. The combination of lateral erosion and downcutting between km 13.7 and 12.5 removed a considerable amount of material from the valley bottom which was transported downvalley.

The sediments forming the newly eroded valleysides, now 15-25 m high, were probably saturated prior to the flood. As the flood level waned and the river bed physically lowered by channel incision, seepage of groundwater from both a sand unit (5-10 m thick) and underlying cohesive fine-grained unit (10-15 m thick), likely caused saturated valleyside material to fail creating numerous slides, slumps and flows along the banks (Fig. 11.10). These failures can be considered as drawdown related in a situation similar to those which occurred along several of the drained reservoirs of Rivière aux Sables and Rivière Chicoutimi, however, the cause of drawdown is very different (deep channel erosion into saturated sediment rather than reservoir drainage). Although the geomorphic changes at this reach are extensive and further slope adjustment and erosion are likely, the impact will be minimal because this is an uninhabited part of Rivière des Ha!Ha!.

At Lac Ha!Ha!, numerous small flows were observed within the lake bottom sediments of the drained basin. Some failures display retrogressive characteristics (Figs. 11.11 and 11.12). The occurrence of the failures can be attributed to high pore water pressures developed because of the rapid drawdown of the lake following the erosion of the saddle dyke (see *Chapter 5 Hydrology - Drainage of Lac Ha!Ha! reservoir* section). None of these failures affected infrastructure or buildings because they were confined to the lake bottom sediments.

Rivière du Moulin

Along Rivière du Moulin, the geomorphic effects of the flooding were much less severe than those observed along the other four rivers. Of the slumps mapped, seven are present between km 5.5 and 3 where the river is confined within entrenched meanders and the gradient is relatively steep (Figs. 10.2 and 10.3). All of these occurred along or immediately downstream of the outer banks of river meanders at locations where the river is confined directly against the valleyside. The remaining four slumps occurred between km 10.5 and 9 (Fig. 10.3).

All of the failures along the river are small and shallow. Likely failure mechanisms include local bank erosion and recession of the flood wave. The failures occurred along unpopulated sections of the river and caused minimal property damage because they were so shallow.

Table 11.1 Bank failures along Rivière aux Sables (refer to Fig. 6.1 for locations)

Failure	Class	Material	Width (m)	Type	Cause	Damage
S1	S	M	~85	Sd	E	F
S2	S	M	~30	Sp	E	U
S3	G	F/M	10-15[a]	Sd	D, E	U
S4	G	F/M	10-15[a]	Sd, F	D, E	U
S5	S	M/A	~55	Rs	D	U, I?, B?
S6	S	M	~15	Sp	D	U, I
S7	S	M	~15	Sp	D	U
S8	S	M	~15	Sp	D, F	F
S9	S	M	~20	Sp	D, F	F
S10	G	M	15-20[a]	Sp	D, F	F
S11	G	M	~10[a]	Sp	F, E?	F
S12	S	M	5-10	Sp	F, E?	F

Class: S - single failure, G - group of coalesced or closely-spaced failures

Materials: A - alluvium, M - marine silt and clay, F - fill

Width: [a] - width of individual failures within group

Type: Sp - slump, Rs - retrogressive slide, Sd - slide, F - flow

Cause: E - bank erosion, D - drawdown from the drainage of a reservoir, F - drawdown from recession of the flood wave

Damage: U - urban & industrial property, F - field or forest, I - infrastructure: road or railway, B - bridge

Table 11.2 Bank failures along Rivière Chicoutimi (refer to Fig. 7.1 for locations)

Failure	Class	Material	Width (m)	Type	Cause	Damage
C1	S	?	30-35	Sd	O	F
C2	S	M	~30	Sp	E	F
C3	S	M	~25	Sp	E	F
C4	S	M	~30	Sp	E	F
C5	S	M	~15	Sp	E	F
C6	G	A/S	~40[a]	F	D, E	U
C7	S	M	~70	Rs	D, E	U, H
C8	G	M	~95[a]	Sp	E	F
C9	G	M	20-25[b]	Sp	E	F
C10	S	?	~10	Sp	E	F
C11	S	?	~20	Sp	E	F
C12	S	S/M	~20	Sp	E	F
C13	S	S/M	~30	Sp	E	F
C14	G	S/M	20-25[b]	Sp?	E	F
C15	G	S/M	~90[a]	Sp	E	F
C16	G	S/M	~125[a]	Sp	E	F

Class: S - single failure, G - group of coalesced or closely-spaced failures

Materials: A - alluvium, M - marine silt and clay, S - sand

Width: [a] - total width of failing bank

[b] - width of individual failures within group

Type: Sp - slump, F- flow, Sd - Slide, Rs - retrogressive slide

Cause: E - bank erosion, D - drawdown from the drainage of a reservoir, F - drawdown from recession of the flood wave

Damage: H - houses & buildings, U - urban & industrial property, F - field or forest

Fig. 11.1 The location of three slumps along the right bank of Rivière aux Sables in fine-grained marine sediment (marked by arrows). The two slumps are grouped as the failure S10, the other is failure S9. The river flows from left to right. Photograph taken on July 26, 1996 (GSC photograph 1997-41D).

Fig. 11.2 Failures S7 and S6 along Ruis des Chasseurs immediately above its confluence with Rivière aux Sables. Note backfilling of the S7 is underway and the reconstruction of the stream crossing on the left has already begun. Photograph taken on July 26, 1996 (GSC photograph 1997-41E).

Fig. 11.3 The failure S5 along the left bank just upstream of a railway bridge (between the arrows). Most of the left bank in the photograph has been affected by either failure or bank erosion. At the bridge, the left bridge support has partially toppled because of foundation scouring and left approach was eroded away. Remedial work at the site is underway and involves the placement of geotextile and coarse fill. Photograph taken on July 26, 1996 (GSC photograph 1997-41F).

Fig. 11.4 Failure C16 within fine-grained marine sediment along the right bank of Rivière Chicoutimi. The failure consists of several coalesced slumps along Rivière Chicoutimi. Photograph taken on July 26, 1996 (GSC photograph 1997-41G).

Fig. 11.5 Failure C7 along the left bank Rivière Chicoutimi within the area formerly inundated by the Pont-Arnaud reservoir. This retrogressive slide was caused by the rapid drawdown of the reservoir and erosion of the bank. Photograph taken on July 26, 1996 (GSC photograph 1997-41H).

Fig. 11.6 Shallow flows of failure C6 within alluvium and organic-rich sediment along an eroded bank of the drained Pont-Arnaud reservoir. Photograph taken on July 26, 1996 (GSC photograph 1997-41I).

Fig. 11.7 Large bank failure along the valleyside of Rivière à Mars at km 7.5 where fine-grained marine sediments are overlain by deltaic sand and gravel. Cutbank erosion of the toe of the slope has initiated the failure. Sand and gravel are now draped over parts of the lower portion of the failure. The erosion has undermined a railway right-of-way leaving the tracks suspended over much of the failed area. Photograph taken on July 27, 1996 (GSC photograph 1997-41J).

Fig. 11.8 Close up of the bank failure in Fig. 11.7. Photograph taken on July 27, 1996 (GSC photograph 1997-41K).

Fig. 11.9 High cutbank exposing fine-grained marine sediment at km 4, Rivière des Ha!Ha!. Photograph taken on July 28, 1996 (GSC photograph 1997-41L).

Fig. 11.10 Bank failures within sand and gravel, and cohesive fine-grained sediments along an eroded section of valley along Rivière des Ha!Ha! between km 12.5 and 13.7. Failures of this type occurred along an approx. 1.2 km reach where a new channel was deeply incised initiating de-watering of the saturated banks. Photograph taken on July 28, 1996 (GSC photograph 1997-41M).

Fig. 11.11 Multiple drawdown slumps and flows within the drained Lac Ha!Ha! basin; all within soft organic-rich lacustrine sediment. Photograph taken on July 28, 1996 (GSC photograph 1997-41N).

Fig. 11.12 Retrogressive flow slide within exposed lake bottom sediments of Lac Ha!Ha!. Photograph taken on July 28, 1996 (GSC photograph 1997-41O).

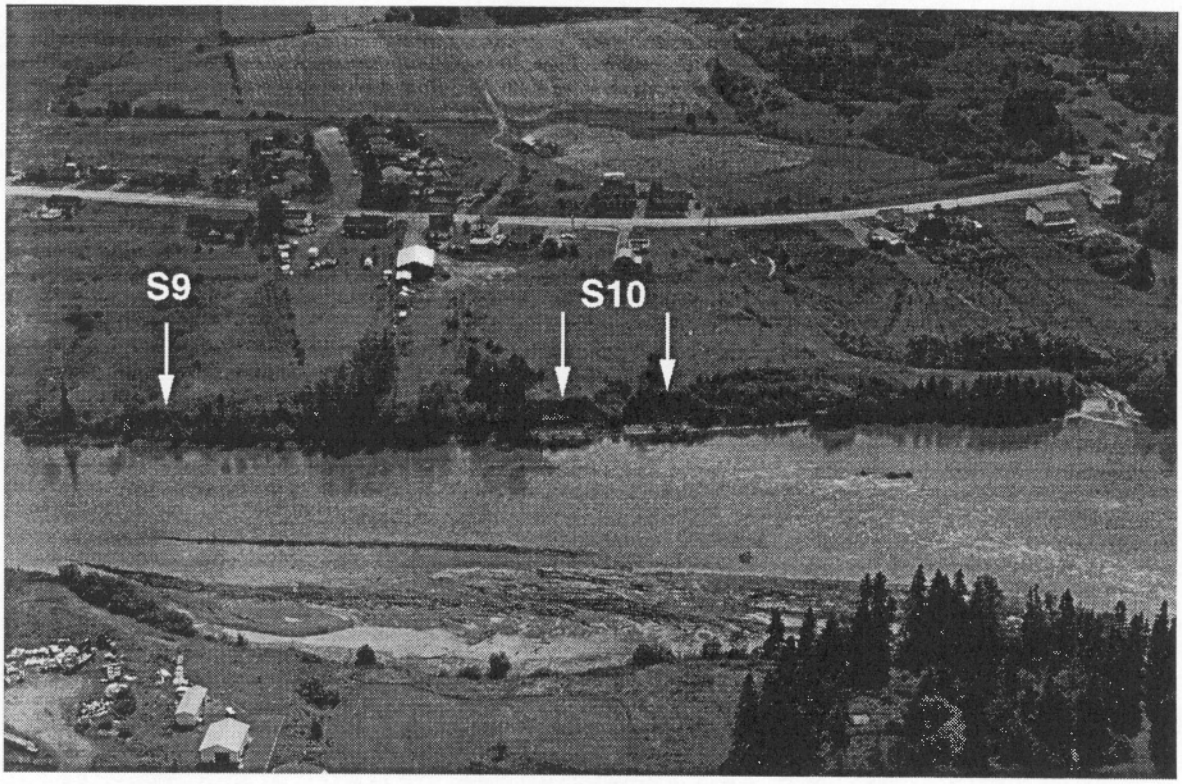

Fig. 11.1

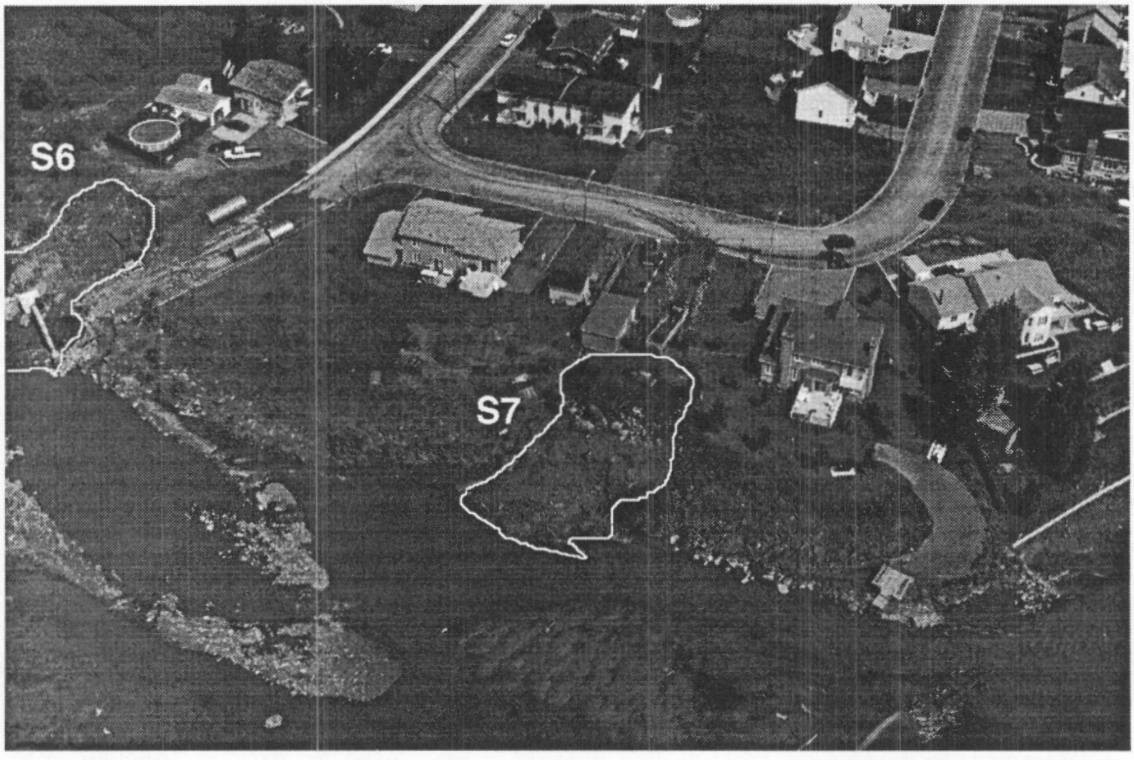

Fig. 11.2

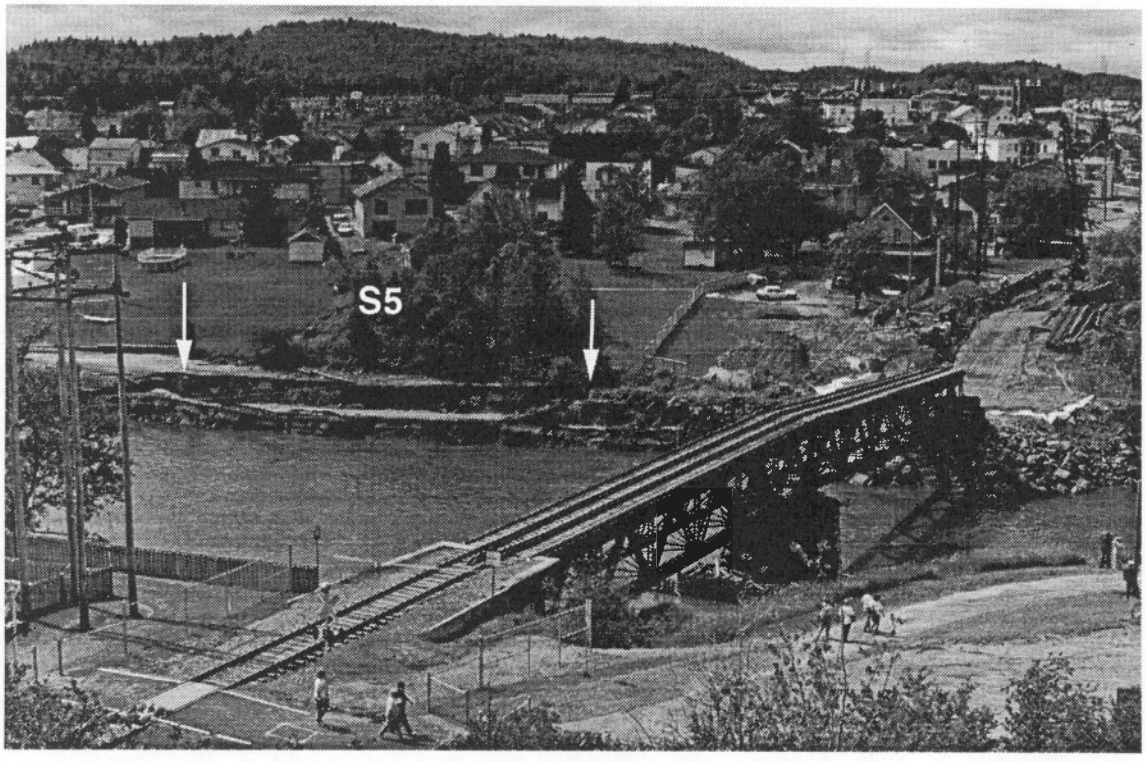

Fig. 11.3

Fig. 11.4

Fig. 11.5

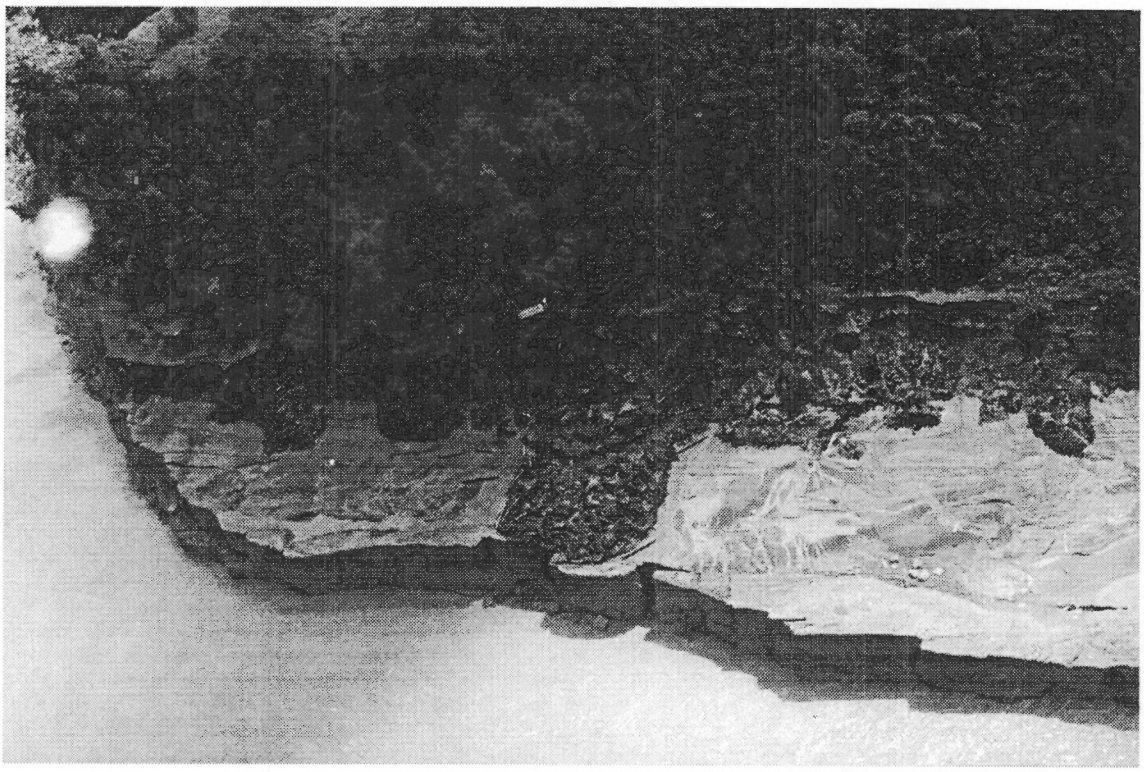

Fig. 11.6

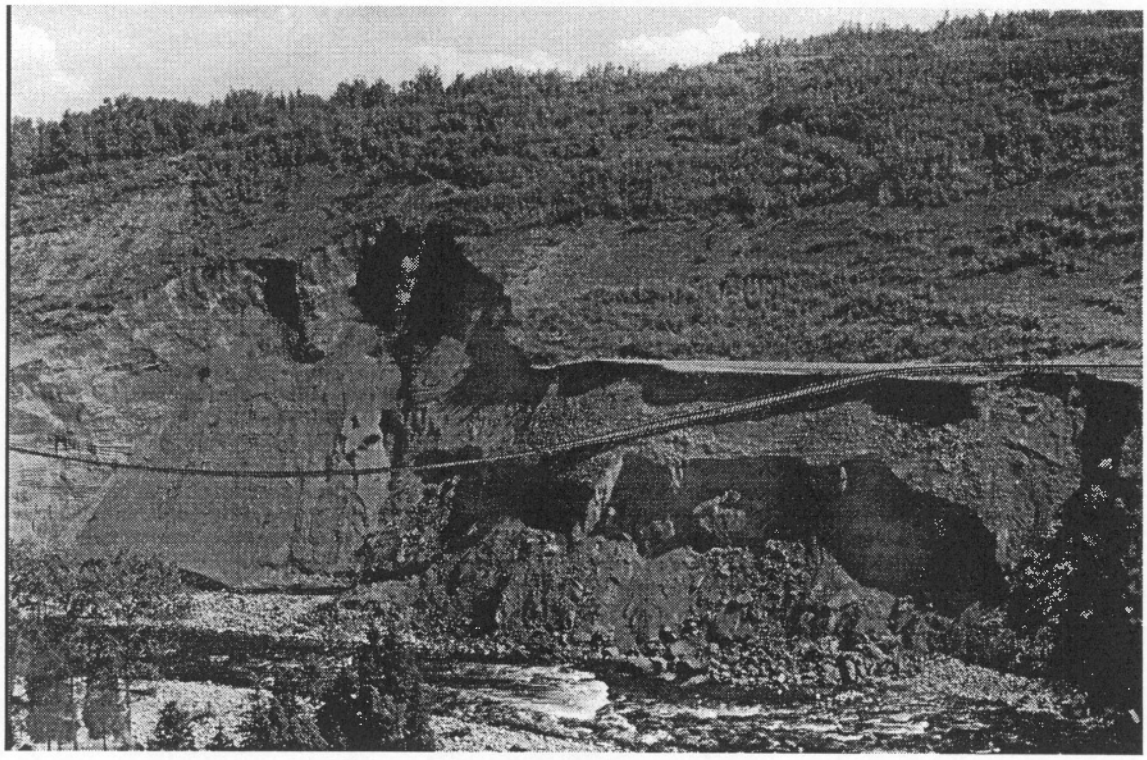

Fig. 11.7

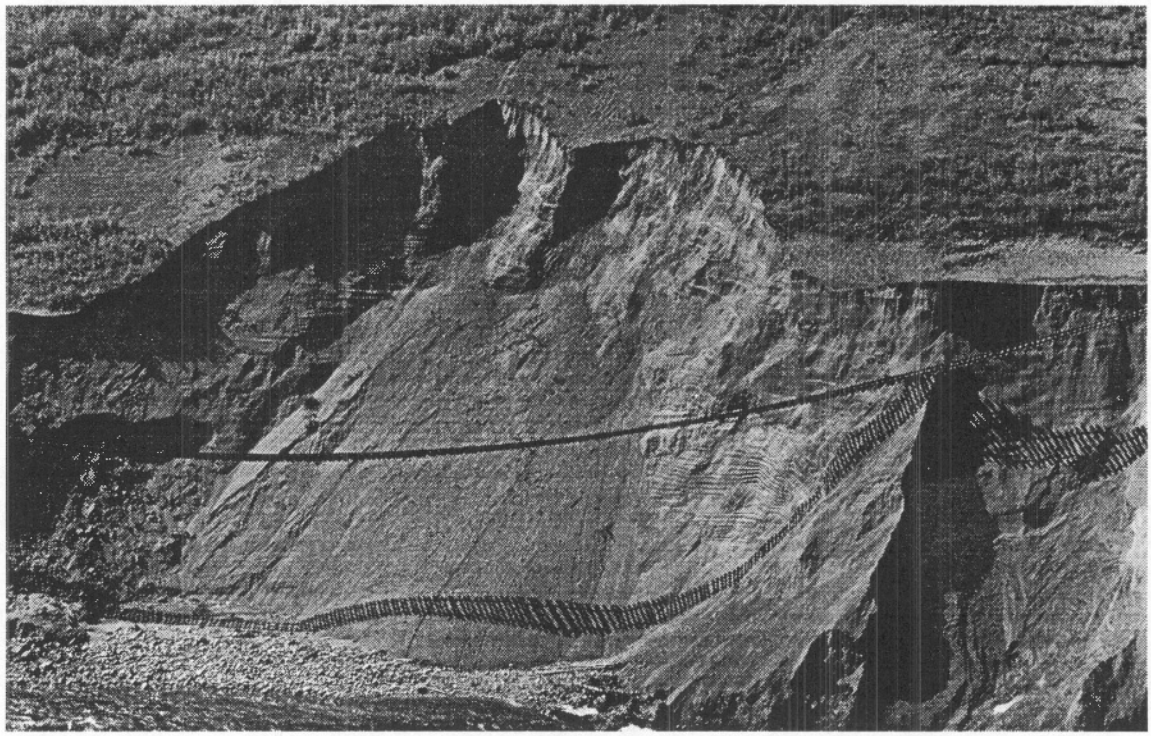

Fig. 11.8

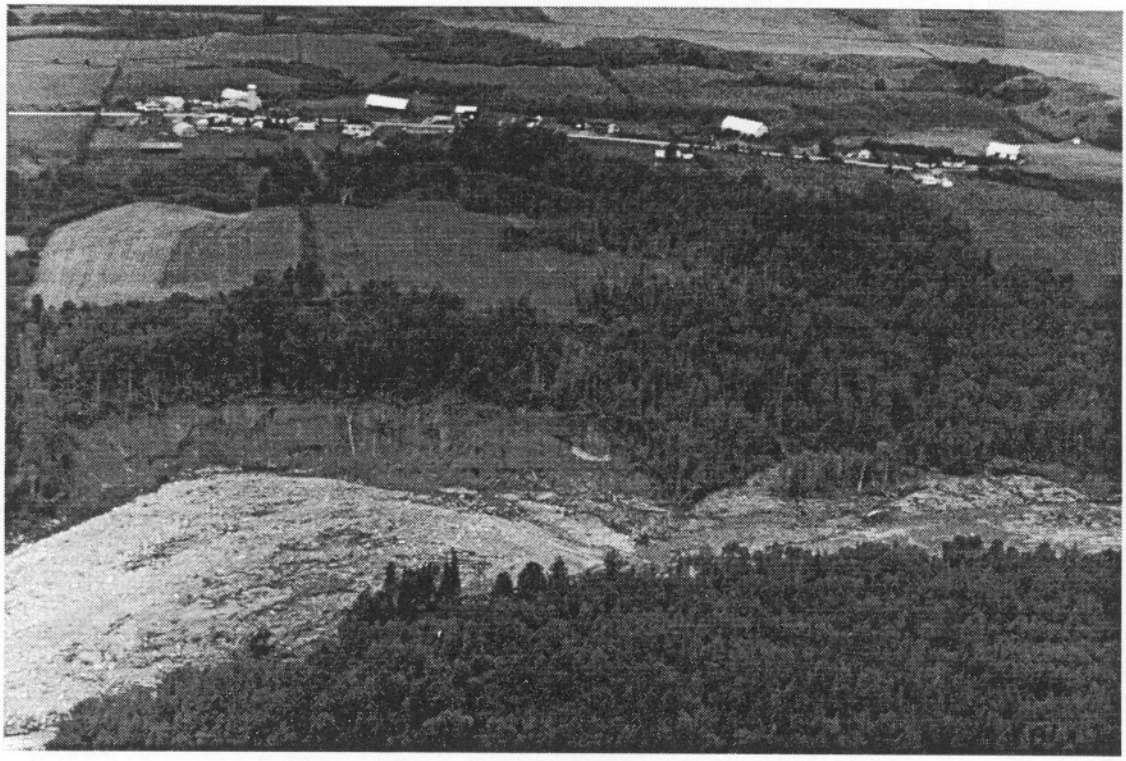

Fig. 11.9

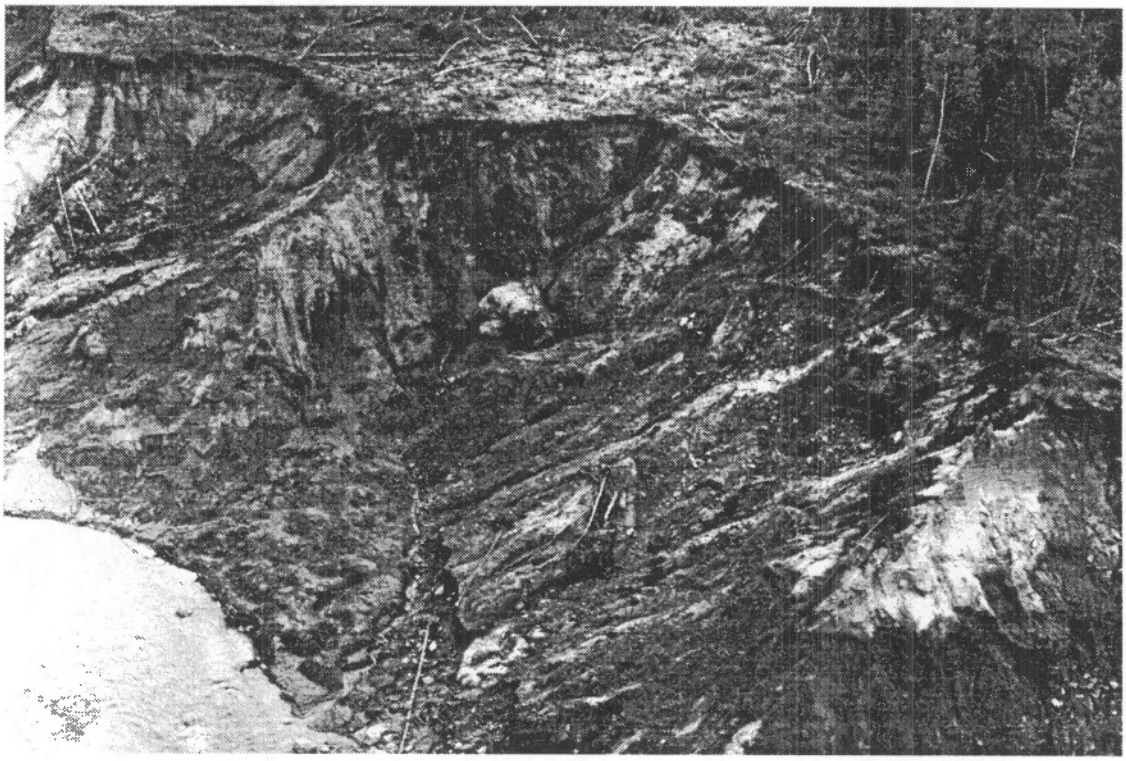

Fig. 11.10

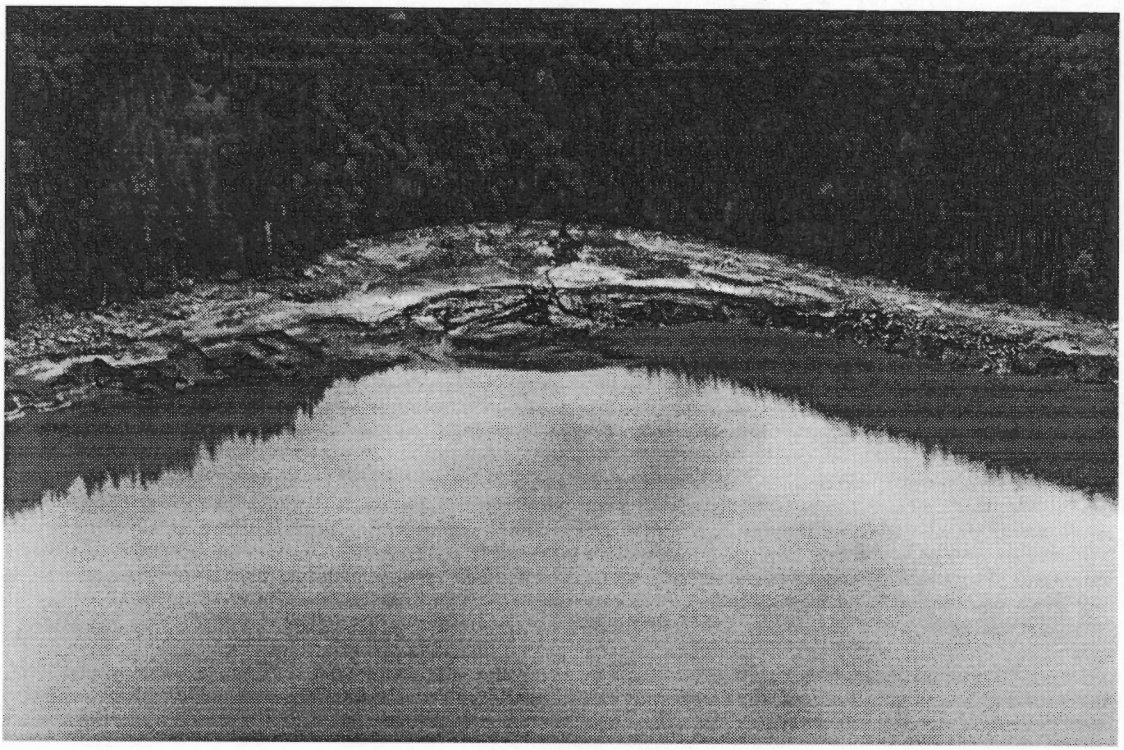

Fig.11.11

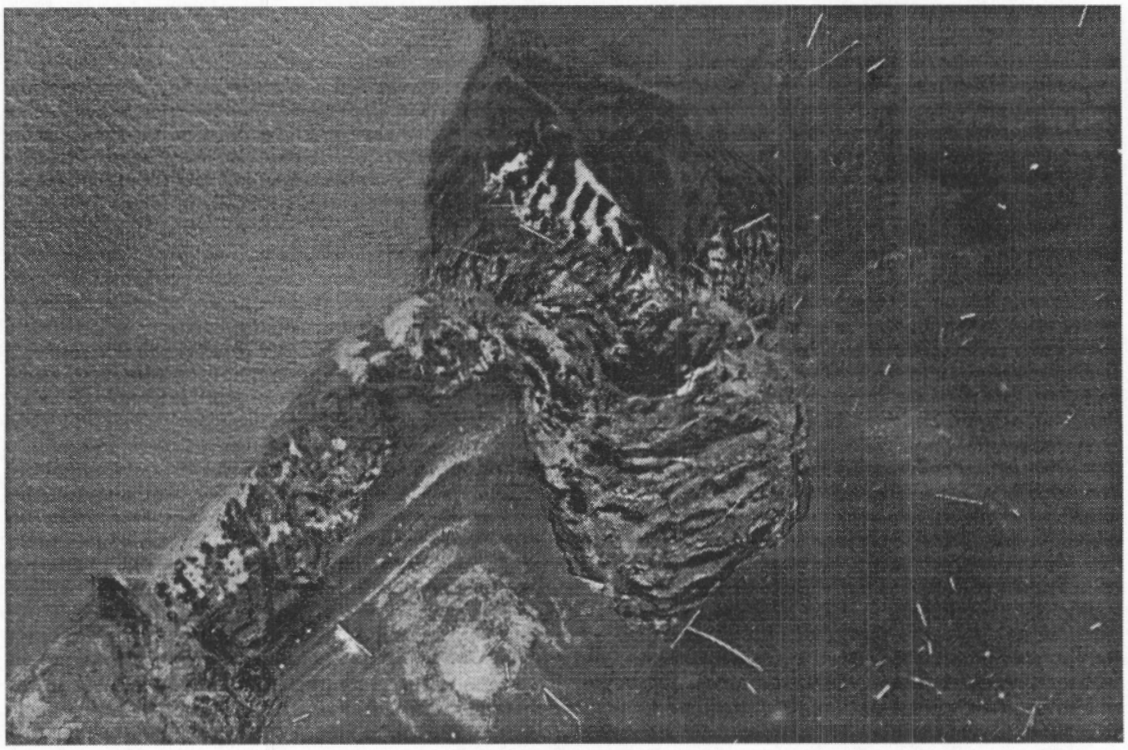

Fig. 11.12

12. SUMMARY

The flooding along Rivière aux Sables, Rivière Chicoutimi, Rivière du Moulin, Rivière à Mars, and Rivière des Ha!Ha! was caused by high rainfall associated with a major storm which occurred between July 18-21, 1996. In excess of 200 mm of rain fell within the watersheds of these five rivers, the majority within a 36 hr period.

Flood discharges of about 660 and 1200 m^3s^{-1} along Rivière aux Sables and Rivière Chicoutimi, respectively, were over twice the previously recorded maximum daily flows. The flood discharge along the lower part of Rivière des Ha!Ha! is estimated to have reached between 1080-1260 m^3s^{-1}, a full order-of-magnitude greater than the previously recorded maximum daily flow. Rivière des Ha!Ha! experienced the highest discharge of any river in the region relative to the size of the drainage basin because of additional outflow from the rapid drainage of Lac Ha!Ha!. Because of this extraordinary combination of high rainfall and lake drainage, the flood discharge along Rivière des Ha!Ha! seems unlikely to be surpassed in the future by a strictly natural occurrence (i.e., rainfall and/or snowmelt event).

The most significant geomorphic effects along Rivière aux Sables and Rivière Chicoutimi occurred at four dam sites where unconsolidated sediments abutting the dams were overtopped and eroded by the rivers. At each site, this resulted in the formation of a new channel adjacent to the dam, the erosion of many tens of metres of valleyside, and the drainage of the reservoir. Extensive fluvial incision into the bed of the drained reservoir occurred upstream of one dam. The post-flood river flow within these new channels by-passed the dams leaving the structures intact, but non-functional. At a dam site within the City of Chicoutimi, flood waters spilled over the concrete wing of the dam (which remained intact) and flowed through a residential-commercial area causing extensive erosion and flood damage. Elsewhere along the two rivers, the geomorphic effects ranged from negligible to moderate, with the most significant effects being the formation of scour pits at isolated floodplain locations along Rivière Chicoutimi, and bank erosion and channel scouring at some bridge crossings along both rivers.

Extensive erosion of the floodplain and terrace margins along the lower 10 km of Rivière à Mars occurred through extensive lateral bank erosion, avulsions, and channel reactivation/creation. This produced a flood channel, 50-380 m wide, that locally was up to 19 times wider than the pre-flood channel. Within the flood channel, the immediate post-flood river exhibited a braided planform, in contrast to the pre-flood meander or transitional planform.

Flooding resulted in extensive geomorphic changes along Rivière des Ha!Ha!. At Lac Ha!Ha!, a new channel, 2 km long, was formed beginning at the location of a saddle dyke that was overtopped and eroded during the rainstorm. This new channel carried escaping Lac Ha!Ha! waters downvalley to joining the pre-flood river channel and greatly

accentuated the storm runoff. Along the pre-flood channel, the geomorphic effects of the flooding varied along the alluvial sections of the river. In general, wide, relatively gently-sloped reaches of valley bottom experienced considerable accretion of sand and silt (up to several metres) and negligible to minor erosion. Major channel incision and moderate channel widening occurred along confined, relatively steeply-sloped sections of valley. Along similarly sloped, but much wider reaches of valley, major channel widening with minor to negligible incision occurred, resulting in the reworking of large areas of the floodplain and erosion of terraces along the valley bottom. Sediment and debris eroded from upstream aggraded the tidal flats at the river mouth.

Negligible to minor geomorphic changes occurred along the lower 17 km of Rivière du Moulin; there being little evidence of the recent flood along long reaches of the river valley. The most significant effect was the cut-off of an entrenched, tight meander and bank erosion at the river mouth.

Along all five of the study rivers, flooding caused extensive economic and human impacts. Numerous homes built on lowlying areas were damaged or destroyed by inundation and/or bank erosion. Particularly notable was the loss of homes situated above the flood levels by undermining due to major terrace or valleyside erosion. Infrastructure and industry were significantly affected by the damage or destruction of road and railway bridges, the washing-out of roads, and damage or loss of function of dams.

Numerous landslides occurred along the five study rivers. Although two retrogressive slides caused damage to infrastructure and buildings, most failures were shallow and of limited extent. Triggering mechanisms included bank erosion, saturation of the ground from the rainfall, drawdown of reservoirs and recession of flood waves; or a combination of the above. Most of the failures occurred within fine-grained marine sediments, but those within the drained Lac Ha!Ha! basin and along a newly eroded reach of Rivière des Ha!Ha! are notable exceptions occurring in glacial and lacustrine sediments, respectively. Overall, landsliding along the river banks was a relative minor part of the flood impacts.

Fluvial erosion resulted in the oversteepening of numerous river banks, some composed of fine-grained marine sediment. These slopes may be unstable and have the potential for future failure. Prior to re-development adjacent to landslides or areas of oversteepened banks, geotechnical evaluations on a site-by-site basis are required to ensure that adequate plans, designs and mitigative measures are implemented.

ADDENDUM

Readers interested in more information about the Saguenay flooding will find the following reports of interest. These were not available at the time of writing and for some aspects of the flood event they contain more update and detailed information.

Commission scientifique et technique sur la gestion des barrages

1997: Rapport: Commission scientifique et technique sur la gestion des barrages; unpublished report, Quebec, Janvier 1997, 241 p. + annexes.

The official report of the Nicolet Commission. It contains a broad range of information about the flooding including, an overview of the flood effects on a large number of rivers systems in Saguenay area, estimates of peak flows, and information on many of the dams.

INRS-Eau

1997: Simulation hydrodynamique et bilan sédimentaire des rivières Chicoutimi et des Ha!Ha! lors des crues exceptionnelles de juillet 1996; Rapport INRS-Eau No. R487, Traveaux réalisés pour le compte de la Commission scientifique et technique sur la gestion des barrages, 207 p.

A report based upon work completed for the Nicolet Commission and includes, modelling of flood levels along Rivière Chicoutimi and Rivière des Ha!Ha!, details of the incision at the Chute-Garneau and Pont Arnaud dams along Rivière Chicoutimi, and the change in topography and the volume of erosion/deposition along the Rivière des Ha!Ha!.

REFERENCES

Baker, V.R. and Costa, J.E.

1987: Flood power; in Catastrophic flooding; (ed.) Mayer, L. and Nash, D., Allen and Unwin, London, p. 1-21.

Barnes, H.H. Jr.

1967: Roughness characteristics of natural channels; U.S. Geological Survey Water-Supply Paper 1849, 213 p.

Bentley, S.P. and Smalley, I.J.

1979: Mineralogy of a Leda/Champlain clay from Gloucester (Ottawa, Ontario); Engineering Geology, v. 14, p. 209-217.

Bjerrum, L., Loken, T., Heiberg, S., and Foster, R.

1969: A field study of factors responsible for quick clay slides; in Seventh International Conference on Soil Mechanics and Foundation Engineering Proceedings, Mexico, v. 2, p. 531-540.

Brzezinski, L.S.

1971: A review of the 1924 Kénogami landslide; Canadian Geotechnical Journal, v. 8, p. 16.

Carpentier, A.

1996: Flood of July 19-20-21, 1996 north region of St. Lawrence River, Quebec; Water News, Newsletter of the Canadian Water Resources Association, v. 15, no. 3, p. 1-3.

Costa, J.E.

1987: A comparison of the largest rainfall-runoff floods in the United States with those of the People's Republic of China and the world; Journal of Hydrology, v. 96. p. 101-115.

Costa, J.E.

1988: Floods from dam failures; in Flood Geomorphology; (ed.) Baker V.R., Kochel R.C. and Patton P.C; J. Wiley and Sons, p. 439-463.

Desloges, J.R., Jones, D.P., and Ricker, K.E.

1989: Estimates of peak discharge from the drainage of ice-dammed Ape lake, British Columbia, Canada; Journal of Glaciology, v. 35, p. 349-354.

Dion, D.J.

1986a: Carte d'aptitude region de Jonquière-Chicoutimi-La Baie; Ministère des Richesses Naturelles du Québec, carte no: 1998 du DV 83-15, scale 1:50 000.

Dion, D.J.
1986b: Levé geotechnique de la region de Jonquière - Chicoutimi - La Baie Québec; Ministère des Richesses Naturelles du Québec; Série des manuscrits bruts, MB 86-51.

Emergency Preparedness Digest
1997: When nature runs wild; Emergency Preparedness Digest, Emergency Preparedness Canada, v. 24, no. 1, p. 8.

Environment Canada
1996: Canadian climate summary; Environment Canada, July 1996, v. 1, 10 p.

Environnement et Faune Québec
1996a: Gestion du Lac Kénogami et des autres lacs-réservoirs; Direction de l'hydraulique, Le 17 août 1996, 80 p. + annexes.

Environnement et Faune Québec
1996b: Gestion du Lac Kénogami; unpublished manuscript.

Ferguson, R.I.
1986: River loads underestimated by rating curves; Water Resources Research, v. 22, p. 74-76.

Fisheries and Environment Canada
1978: Hydrological atlas of Canada; Fisheries and Environment Canada.

Fulton, R.J., compiler
1995: Surficial materials of Canada; Geological Survey of Canada, Map 1880A, scale 1: 5 000 000.

Gadd, N.R.
1986: Lithofacies of Leda Clay in the Ottawa Basin of the Champlain Sea; Geological Survey of Canada, Paper 85-21, 44 p.

Kellerhals, R., Church, M., and Bray, D.I.
1976: Classification and analysis of river processes; Journal of the Hydraulics Division, Proceeding of the American Society of Civil Engineers, v. 102, p. 813-829.

Kochel, R.C.
1988: Geomorphic impact of large floods: reviews and new perspectives on magnitude and frequency; in Flood Geomorphology; (ed.) Baker V.R., Kochel R.C. and Patton P.C; J. Wiley and Sons, New York, p. 169-187.

LaSalle, P. and Tremblay, G.
1978: Dépot meubles, Saguenay Lac Saint-Jean; Ministère des Richesses naturelles, Report géologique 191, 61p.

LaSalle, P. and Chagnon, J.-V.
1968: An ancient landslide along the Saguenay River, Quebec; Canadian Geotechnical Journal, v. 5, p. 548-549.

La Rochelle, P., Chagnon, J.Y., and Lefebvre, G.
1970: Regional geology and landslides in the marine clay deposits of eastern Canada; Canadian Geotechnical Journal, v. 7, p. 145-156.

Le Quotidien
1996: Stone décline toute responsabilité; Saturday, July 27, 1996.

Miller, D.M.
1984: Reducing transformation bias in curve fitting; The American Statistician, v. 38, p. 124-126.

Occhietti, S.
1989: Quaternary geology of St. Lawrence Valley and adjacent Appalachian sub region; in Chapter 4 of Quaternary Geology of Canada and Greenland, R.J. Fulton, (ed.); Geological Survey of Canada, Geology of Canada, no. 1, (also Geological Society of America, The Geology of North America, v. K-1), p. 350-389.

Parent, M., Dubois, J.-M.M., Bail, P., Larocque, A. and Larocque, G.
1985: Paléogéographie du Québec méridional entre 12 500 et 8000 ans BP; Recherches amérindiennes au Québec, v. 15, p. 17-37.

Progrès-dimanche
1996: Québec et Ottawa travaillent à l'unisson; Sunday, July 28, 1996.

Richards, K
1982: Rivers, form and process in alluvial channels; Methuen Inc., New York, 358 p.

Ottawa Citizen
1997: Water management system needs complete overhaul, report says; January 17, 1997.

Tavenas, F.
1984: Landslides in Canadian sensitive clays: a state-of-the-art; in Fourth International Symposium on Landslides, Toronto, Ont, University of Toronto, Downsview, Ont; vol. 1, p. 141-153.

Tavenas, F., Chagnon, J.Y., and La Rochelle, P.
1971: The Saint-Jean-Vianney landslides: observations and eyewitnesses accounts; Canadian Geotechnical Journal, v. 8, p. 463-478.

Varnes, D.J.
1978: Slope movement types and processes; in Landslides analysis and control, R.L. Schuster and Krizek, R.J. (eds.); National Academy of Sciences, Transportation Research Board Special Report 176, p. 11-33.

Vincent, J.-S.
1989: Quaternary geology of the southeastern Canadian Shield; in Chapter 3 of Quaternary Geology of Canada and Greenland, R.J. Fulton, (ed.); Geological Survey of Canada, Geology of Canada, no. 1, (also Geological Society of America, The Geology of North America, v. K-1), p. 249-317.

Water Survey of Canada
1992: Historical Streamflow summary to 1990 - Quebec; Inland Waters Directorate, Water Resources Branch, Environment Canada, 526 p.